



Technical University of Denmark (DTU)
DTU Chemical Engineering
German Aerospace Center (DLR)
Institute of Future Fuels

Techno-economic analysis of a solar ammonia and fertilizer production

Master Thesis



Techno-economic analysis of a solar ammonia and fertilizer production

Master Thesis
December, 2022

By
Pablo López Martínez

Copyright: Reproduction of this publication in whole or in part must include the customary bibliographic citation, including author attribution, report title, etc.

Cover photo: German Aerospace Center, 2018

Published by: German Aerospace center, Institute of Future Fuels, Linder Höhe, 51147 Cologne Germany

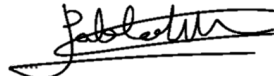
DTU, Process and Systems Engineering Centre, Søtofts Plads, Building 224, 2800 Kgs.Lyngby, Denmark

Approval

This Master's thesis has been performed over a period of six months at the Institute for Future Fuels, part of the German Aerospace Centre (DLR), in partial fulfillment for the degree Master of Science in Chemical & Biochemical Engineering, MSc Eng. This work has been supervised by Nicole Neumann and David Baumstark at DLR and by Gürkan Sin at DTU. The thesis is credited with 35 ECTS points.

It is assumed that the reader has a basic knowledge in the area of chemical process engineering.

Pablo López Martínez - s210292



.....
Signature

.....
30/11/2022

Date

Abstract

Due to rapid climate change, society and politics pushes the fertiliser industry to decarbonise and reduce its emissions, as it is responsible for 1.4% of annual CO₂ emissions. To avoid this environmental problematic, research and development in the chemical industry is currently focused on the search for the production of green ammonia and its integration into the production of nitric acid. This work aims to contribute to the quest of new sustainable processes that help the decarbonisation of the fertiliser industry.

The MSc thesis focus on the search of synergies between solar-powered nitrogen and hydrogen production technologies to provide green ammonia, and the subsequent nitric acid process. Specific attention is put on the effect of utilizing the oxygen by-product from solar-powered thermochemical air separation to produce nitrogen, and from water splitting to provide green hydrogen.

A techno-economic evaluation is performed for three different types of nitric acid plants: a conventional nitric plant (CONV-NA), i.e using fossil-based ammonia, a solar-based ammonia to nitric acid plant (SOL-NA) and a optimised solar-based ammonia to nitric acid plant (OXY-SOL-NA), in which surplus oxygen from green ammonia production is injected into SOL-NA. All the plants are simulated in Aspen Plus® and their economic analysis is performed by following the methodology of the book entitled: *Plant Design and Economics for Chemical Engineers*.

A reference case of a mono-pressure nitric acid production process is simulated for a plant capacity of 700 t/d (eq. 100%) at a concentration of 60 wt% (CONV-NA). The investigations of injecting pure oxygen at four different points of the plant show that daily nitric acid production can be boosted by 0.34% and final NO_x concentration of the absorption column can be reduced by up to 43.6% by enriching the main air pipeline with oxygen.

The capital costs for the OXY-SOL-NA plant are reduced by 0.65 M€ compared to the CONV-NA and SOL-NA plants. Nevertheless, the operating costs end up being more relevant in the final cash flow analysis. The CONV-NA plant has 17% lower operating costs compared to the two green ammonia plants which is explained by the fact that ammonia costs accounted for 52.65% of the total operating costs. For that reason, CONV-NA plant has an end-product price 14% lower than the other plants. Regardless of environmental considerations, such a significant difference in the final price may make your product unable to compete with other potential competitors.

Currently, green ammonia is mainly dependent on the price of green hydrogen production due to the high LCOE for solar energy and the lack of maturity of water splitting technologies. CO₂ pricing policies could make the implementation of green NH₃ in the nitric acid production process feasible in the near future.

Acknowledgements

First of all, I would like to thank my parents for all the support, effort and education they have given me, and clearly this would not have been possible without them. I cannot forget the motivation and help that my brothers, Marcos and Raul, offer me. But the most beautiful part of this two-year journey has been to meet Nuria who shows me her unconditional support and affection on a daily basis and who has helped me to overcome all the obstacles of this work.

I would also like to thank Nicole and David for this opportunity at the German aerospace center (DLR) and for their guidance and suggestions to improve my work. At the same time, I am grateful to my supervisor at Technical University of Denmark (DTU)- Prof. Gürkan Sin for showing keen interest about my work and also for helping me in the realization of this thesis.

Finally, I would like to highlight the many wonderful people I have met during these two years: especially at Basecamp in Denmark and during my last period in Germany with the European Space Agency (ESA) interns.

Contents

Preface	ii
Abstract	iii
Acknowledgements	iv
1 Introduction	1
1.1 Motivation	2
1.2 Thesis objectives	3
2 Theory and background	5
2.1 Conventional ammonia and nitric acid production	5
2.1.1 Haber-Bosch process	5
2.1.2 Ostwald process	7
2.2 Solar-based ammonia and nitric acid production	11
2.2.1 Solar energy production	11
2.2.2 Solar hydrogen production	13
2.2.3 Solar-driven air separation	15
2.2.4 Oxygen-enriched air into conventional nitric acid process	16
3 Methodology	17
3.1 Process simulation	17
3.1.1 Thermodynamic models	17
3.1.2 Implemented kinetics	18
3.1.3 Pinch analysis	21
3.1.4 Optimised nitric acid plant	22
3.2 Economic analysis	24
3.2.1 Capital expenses (CapEx)	24
3.2.2 Operational expenses (OpEx)	25
3.2.3 Profitability metrics	26
3.2.4 Sensitivity analysis	28
3.2.5 Assumptions	28
4 Results and discussion	31
4.1 Process simulation	31
4.1.1 Sensitivity analysis	36
4.1.2 Pinch analysis	38
4.1.3 Optimised nitric acid plant through oxygen injections	40
4.2 Economic analysis	43
4.2.1 Sensitivity analysis	44
5 Conclusions	47
Bibliography	49
A User kinetic subroutines in Aspen Plus	53
B Schematic configurations	60
C Summary of the patents studied	61

D	Simulation results	63
E	Pinch analysis calculations	65
F	Design of the combustion chamber (R-101)	66
G	Economic analysis	68

List of Figures

Figure 1.1	The industrial manufacturing of inorganic fertilisers [3]	1
Figure 1.2	Atmospheric carbon dioxide and annual emissions [11]	2
Figure 2.1	Flowsheet of a conventional ammonia and nitric acid production	5
Figure 2.2	Block chart of Haber-Bosch process	6
Figure 2.3	Block chart of the Ostwald Process	7
Figure 2.4	NO _x absorption mechanism	8
Figure 2.5	Simplified flowsheet of a medium-pressure process	9
Figure 2.6	Solar-based ammonia & nitric acid production	11
Figure 2.7	Schematic structure of the energy conversion in a CSP plant.	12
Figure 2.8	Types of receivers in CSP plants.	12
Figure 2.9	Comparison of core CSP technologies [19].	13
Figure 2.10	Electrolyser technologies	14
Figure 2.11	Solar thermochemical water-splitting cycle [30].	15
Figure 3.1	Simplified mechanism (Miller's approach) [40].	20
Figure 4.1	Conventional nitric acid plant flowsheet in Aspen Plus®	32
Figure 4.2	Heat-recovery unit: series of heat exchangers.	33
Figure 4.3	Nitrogen oxides oxidation results	34
Figure 4.4	Profiles along the absorption tower (I)	35
Figure 4.5	Profiles along the absorption tower (II)	36
Figure 4.6	Effect on the production of nitric acid.	37
Figure 4.7	Effect on the acid strength.	37
Figure 4.8	Effect on the NO _x composition.	38
Figure 4.9	Composite curves for the hot scale temperature	39
Figure 4.10	Shifted composite curves	39
Figure 4.11	Effect of pure-oxygen injections into different points	40
Figure 4.12	Effect of O ₂ injection on the NO _x concentration	41
Figure 4.13	Compressor characteristics (C-101)	42
Figure 4.14	Sensitivity analysis on the three main cost drivers	45
Figure 4.15	Response of the MSEP of nitric acid to changes in the m _{ar}	45
Figure 4.16	Sensitivity analysis on profitability metrics for OXY-SOL-NA	46
Figure 4.17	Sensitivity analysis on profitability metrics for OXY-SOL-NA	46
Figure A.1	Basic steps and required programs.	54
Figure A.2	Set compiler window	54
Figure A.3	.opt file creation in Notepad. a. Step 4 and b. Step 6.	55
Figure A.4	Customize Aspen Plus window.	55
Figure A.5	Linking fortran code compiled with Aspen Plus®.	56
Figure B.1	Schematic configurations.	60
Figure D.1	Profiles along the cooler/condenser (E-107)	64
Figure F.1	Sketch combustion chamber.	66
Figure F.2	R-101 specification sheet.	67

Figure G.1	Operating labor requirements in the chemical process industry [48]	68
Figure G.2	Price index of all countries assessed [59]	68
Figure G.3	MACRS depreciation rates [48]	69
Figure G.4	Purchased cost of fixed-tube sheet heat exchangers	69
Figure G.5	Purchased cost of shop-fabricated tanks	70
Figure G.6	Purchased cost of compressors	70
Figure G.7	Pie chart of the percentage of equipment cost unities	71
Figure G.8	Pie chart of the percentage of raw materials.	71
Figure G.9	Pie chart of the percentage of utilities for all the plants.	72
Figure G.10	Ammonia price for Western Europe in the last decade [12].	72
Figure G.11	Pie chart of the percentage of OpEx for CONV-NA plant.	72
Figure G.12	Pie chart of the percentage of OpEx for SOL-NA plant.	73
Figure G.13	Pie chart of the percentage of OpEx for OXY-SOL-NA plant.	73
Figure G.14	Profitability evaluation for CONV-NA.	74
Figure G.15	Profitability evaluation for SOL-NA.	75
Figure G.16	Profitability evaluation for OXY-SOL-NA.	76
Figure G.17	Sensitivity results CONV-NA.	77
Figure G.18	Sensitivity results SOL-NA.	77

List of Tables

Table 3.1	Thermodynamic model for each section of the nitric acid plant	18
Table 3.2	Summary of industry-approved patents.	22
Table 3.3	Estimation cost factor for a fluid processing plant [51]	25
Table 3.5	Market prices for raw materials and utilities	29
Table 4.1	Ammonia combustion chamber specifications (R-101)	33
Table 4.2	Reactive heat exchangers specifications	34
Table 4.3	Absorption and bleacher column specifications	35
Table 4.4	Summary of stream temperatures and heat duties	38
Table 4.5	Summary of the maximum percentage increase for the four cases.	42
Table 4.6	Equipment costs results for the investigated plants	43
Table 4.7	Summary economic results for the investigated plants.	44
Table 4.8	Feasibility metrics to ensure a $m_{ar} = 10\%$	44
Table D.1	Stream results of a monopressure nitric acid plant in Aspen Plus (1)	63
Table D.2	Stream results of a monopressure nitric acid plant in Aspen Plus (2)	63
Table E.1	Summary of the pinch calculations ($\Delta T_{min} = 10\text{ K}$)	65

List of abbreviations

AACE	Association for the Advancement of Cost Engineering
Al₂O₃	Aluminium oxide
Ar	Argon
CapEx	Capital Expenses
CEPCI	Chemical Engineering Plant Cost Index
CH₄	Methane
CO	Carbon monoxide
CO₂	Carbon dioxide
CPI	Commodity Price Index
CrO	Chromium oxide
CSP	Concentrated Solar Power
CuO	Cupric oxide
DCFR	Discounted Cash Flow Rate
EC	Equipment Cost
FCI	Fixed Capital Investment
Fe₃O₄	Ferric oxide
H₂	Hydrogen
H₂O	Water
H₃O⁺	Hydronium ion
HENS	Heat Exchanger Network Synthesis
HNO₂	Nitrous acid
HNO₃	Nitric acid
MACRS	Modified Accelerated Cost Recovery System
MO_{ox}	Metal oxide oxidation
MO_{red}	Metal oxide reduction
MSEP	Minimum SELLing Price
N₂	Nitrogen
N₂O₃	Dinitrogen trioxide

N_2O_4	Dinitrogen tetroxide
NH_3	Ammonia
NO	Nitric oxide
NO_2	Nitrogen dioxide
NO_3^-	Nitrate ion
NO_x	Nitrogen oxides
<i>NRTL</i>	Non-Random Two Liquids
O_2	Oxygen
<i>OpEx</i>	Operational Expenses
<i>PBP</i>	PayBack Period
<i>PEM</i>	Proton Exchange Membrane
<i>PSA</i>	Pressure Swing Adsorption
<i>Pt</i>	Platinum
<i>PTA</i>	Problem Table Algorithm
<i>PV</i>	PhotoVoltaic
<i>Rh</i>	Rhodium
<i>RK</i>	Redlich-Kwong
<i>ROI</i>	Return Of Investment
<i>SMR</i>	Steam Methane Reforming
SO_2	Sulfur dioxide
<i>SOEC</i>	Solid Oxide Electrolysis Cell
<i>TCI</i>	Total Capital Investment
<i>TSA</i>	Temperature Swing Adsorption
<i>ZnO</i>	Zinc oxide

List of symbols

ΔH	Enthalpy [kJ/mol]
ΔT	Difference of temperature [$^{\circ}C$]
€	Euro
π	Pi number
A	Interfacial area [m ²]
b	Backward reaction
C_p	Specific heat capacity [kJ/kg $^{\circ}C$]
d	Diameter [m]
f	Forward reaction
F	Flow rate [m ³]
g	Gas
h	Height [m]
J	Absorption rate [kmol · m ² · kPa ⁻¹ s ⁻¹]
k	Kinetic constant
K_{eq}	Equilibrium constant
l	Liquid
m_{ar}	Minimum Annual Return of investment
P	Pressure [bar]
Q	Heat duty [kW]
r	Reaction rate
R	Ideal gas constant
S_i	Equipment input variable
t	Time [s]
T	Temperature [$^{\circ}C$]
T_{in}	Inlet temperature [$^{\circ}C$]
T_{out}	Outlet temperature [$^{\circ}C$]
u_g	Gas velocity [m/s]
W	Weight fraction

1 Introduction

The world population growth from 1.6 billion people in 1900 to today's 8 billion would not have been possible without the development of the fertiliser industry [1]. One of the major inventions of the 20th century was the industrial synthesis of ammonia (NH_3) for the production of nitrogen-based fertilisers. In order to understand the importance of nitrogen for human beings, it is essential to mention that agricultural crops supply almost 90% of those essential amino acids needed for tissue growth and proper development of a human body [2]. They can be supplied directly by cereals and pulses or indirectly by foods of animal origin.

Fertilisers provide essential nutrients to improve the growth and fertility of agricultural crops. These can be classified as natural/organic or synthetic/inorganic depending on their origin.

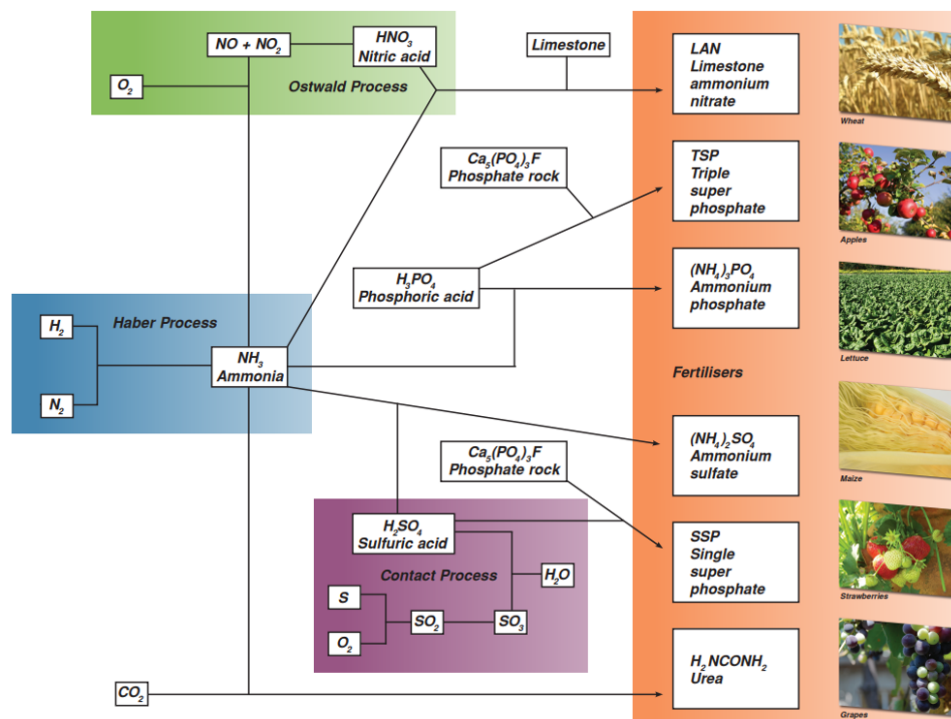


Figure 1.1: The industrial manufacturing of inorganic fertilisers [3]

Ammonia constitutes the main precursor for the production of mineral fertilisers such as urea, ammonium nitrate, calcium nitrate or ammonium sulphate among others. Figure 1.1 shows clearly how synthetic fertilisers have their origin in ammonia.

About 85% of the ammonia produced worldwide is used solely for fertiliser production [4]. Around 90% of the world's ammonia production is through what is known as the Haber-Bosch process, in which nitrogen (N_2) and hydrogen (H_2) react catalytically at high temperatures and pressures [5].

Nitric acid, along with ammonia, constitutes an important feedstock for the production of nitrates due to its high nitrogen content (15.5 - 34.5%) and its rapid release as a major

plant nutrient. Around the 80% of nitric acid global production is used to produce fertilisers [2]. The nitric acid synthesis process is known as the Ostwald process, in which ammonia is oxidised in the presence of a Pt-Rh-based catalyst to form different nitrogen oxide gases which are eventually absorbed by an aqueous solution [6].

Despite the importance of nitrogen-based fertilisers for modern society, their production and use have considerable impacts on the environment. The high energy consumption for production results in large amounts of CO₂ and other greenhouse gases such as nitrous oxide (N₂O). Moreover, emissions generated by the agriculture sector, together with impacts on ecosystems and air quality, must be taken into account [7].

1.1 Motivation

In the last century, population growth coupled with industrial development has led to an exponential increase in CO₂ emissions (Figure 1.2), to the point that in December 2016 a climate emergency was declared for the first time by a local government [8]. In this context, it is remarkable to note that the total amount of CO₂ equivalents released into the atmosphere due to ammonia production is about 400 Mt/ year, which corresponds to 1.5 % of all greenhouse gas (GHG) emissions [9].

This carbon footprint is mainly due to Haber-Bosch process, which is powered by the use of fossil fuels. 95% of the annual production of H₂ (grey hydrogen) comes from fossil gas, oil and coal [10]. In light of the environmental goals defined by the Paris Climate Agreement, the main feedstocks of ammonia synthesis must be obtained from renewable energies and sources to meet targets for the global decarbonisation.

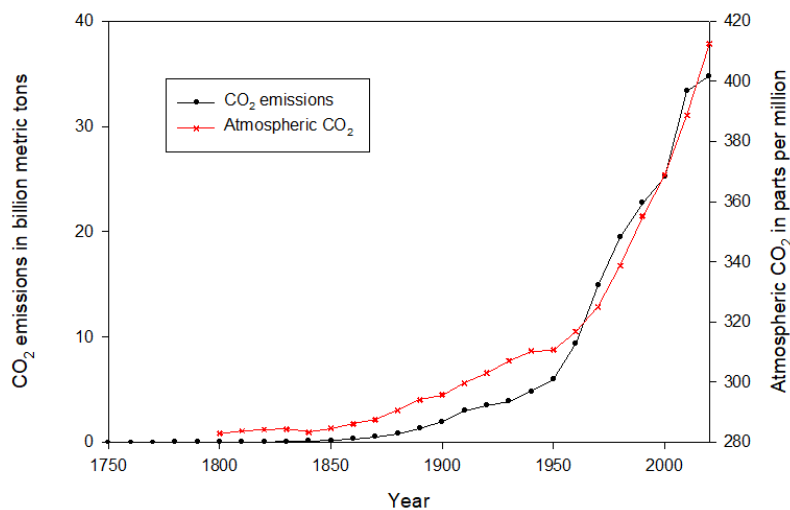


Figure 1.2: Atmospheric carbon dioxide and annual emissions [11]

While the environmental impact of ammonia production is mainly focused on CO₂ emissions, it is worth noting the wide range of negative impacts of mineral fertiliser production:

- High N₂O emissions from nitric acid manufacture are contributing significantly to rapid climate change.
- Large concentrations of NO_x gases together with pollutants emitted from production facilities cause air and soil pollution.

- Excess nitrogen in aquatic and terrestrial ecosystems is causing the progressive degradation of water and soil quality leading to a progressive loss of biodiversity.

To avoid this rapid destruction of the planet, there is a frenetic search for new technologies to help reduce the environmental impact of the fertiliser industry. Research and development in the chemical industry is currently focused on the search for green ammonia production. The use of wind, biomass and solar energy can play a key role in the transition from fossil fuels to renewable energies. Water electrolysis and air separation powered by renewable energy or heat can produce ammonia without emitting CO₂ into the atmosphere [12].

120 million tonnes (Mt) of grey hydrogen are produced every year for industrial purposes [9]. According to *IRENA'S World Energy Transitions Outlook*, 400 Mt of hydrogen would be needed by 2025, which translates into an increase of more than 230 % of current hydrogen demand [13]. This demand is expected to be supplied mainly by hydrogen from water electrolysis, which will mean an exponential increase in the production and availability of oxygen as a by-product of this process.

Surplus oxygen can be integrated into existing nitric acid plants to increase production and reduce NO_x emissions or allow a reduction in the capital cost of new nitric acid plants [14]. Within the next 5–10 years, stricter emission limits on nitrous oxide (N₂O) and NO_x emissions are expected to be imposed for the manufacture of nitric acid and pure oxygen can contribute to meeting future environmental regulations.

1.2 Thesis objectives

This work aims to contribute to the quest of new sustainable processes that help the decarbonisation of the fertiliser industry.

The investigations in this thesis focus on the search of synergies between solar-powered nitrogen and hydrogen production technologies to provide green ammonia, and the subsequent nitric acid process. Specific attention is put on the effect of utilizing the oxygen by-product from solar-powered thermochemical air separation to produce nitrogen, and from water splitting to provide green hydrogen.

The main objectives are to study the technological and economical feasibility of producing nitric acid using green ammonia powered by solar energy and how oxygen injection might influence the nitric acid plant design and economics. Within the main objectives, sub-objectives can be highlighted that lead to the final goals:

- Get familiarise with the ammonia (Haber-Bosch) and nitric acid (Ostwald) synthesis processes and identify the reactions and mechanism involved.
- Summarise the different technologies that make possible a solar-based ammonia production and its implementation into the Ostwald process.
- Literature review of the advantages and disadvantages of oxygen injection at different locations of existing nitric acid plants.
- Simulate the Ostwald process using Aspen Plus® V11 as a process simulation software.
- Compare the simulation results with open literature and discuss them with people from the industry.

- Perform sensitivity analysis on the more complex units of the process such as the cooler/condenser or the absorption column.
- Execute heat integration in the simulated plant by applying the pinch analysis methodology.
- Investigate how oxygen injections at different locations affect the final nitric acid production, the acid strength and the NO_x concentration at the top of the absorption column.
- Carry out an economic analysis of three different types of nitric acid plant based on the simulation results:
 1. **Conventional nitric acid plant (CON-NA):** Considering ammonia and electricity prices of fossil-based production
 2. **Solar-based nitric acid plant (SOL-NA):** Considering ammonia and electricity prices of solar-based production
 3. **Optimised solar-based nitric acid plant (OXY-SOL-NA):** Integrating the surplus oxygen from water electrolysis in the SOL-NA plant.
- Perform sensitivity analysis on profitability metrics such as return of investment (ROI), minimum selling price (MSEP) and payback period (PBP) among others.

2 Theory and background

2.1 Conventional ammonia and nitric acid production

Ammonia and nitric acid constitutes the basis for important fertilisers such as urea or ammonium nitrate. The synthesis of ammonia is well-known as the Haber-Bosch process and the nitric acid synthesis as the Ostwald process in reference of their inventors. Both processes were developed in the first decade of the 20th century and are still used today to produce these two valuable products.

Figure 2.1 shows the conventional pathway for ammonia and nitric acid production. The energy carrier for the processes is grid electricity, hydrogen production is obtained using natural gas by the process known as steam methane reforming (SMR) and nitrogen is generally separated from air by cryogenic air separation or pressure swing adsorption. At this point, ammonia production from the Haber-Bosch process is burned with air to form nitrogen oxides gases which will be absorbed with water to form nitric acid.

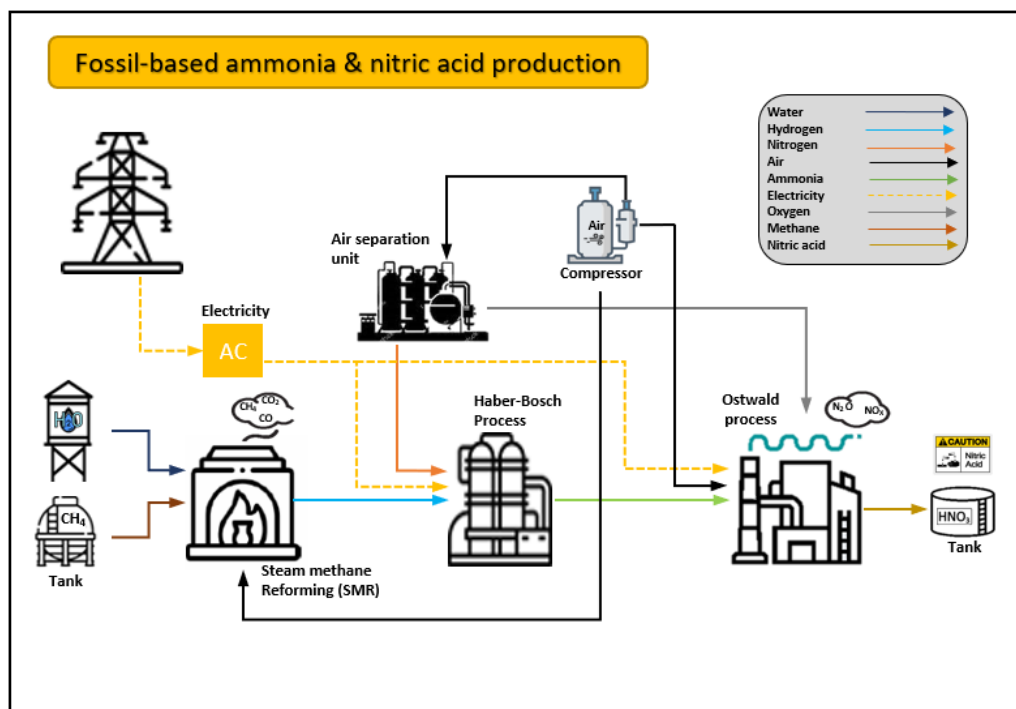


Figure 2.1: Flowsheet of a conventional ammonia and nitric acid production

2.1.1 Haber-Bosch process

The Haber-Bosch process gives its name in reference to the two chemists: Fritz Haber and Carl Bosch. They are known as the fathers of ammonia synthesis. This process was a revolution, removing the barriers that limited crop yield. Today's ammonia synthesis process has been truly improved, but Bosch and Haber were able to recognise and describe the main features of their invention. This work led to both of them being awarded in 1931 with the Nobel Prize in Chemistry for their work on ammonia synthesis [2].

Conventional ammonia is mainly produced from water, air and fossil fuels. In this case, the fuel source that provides the hydrogen is a hydrocarbon commercially called natural gas. The conventional ammonia synthesis process consists of 8 stages as can be seen in Figure 2.2. The first process is the desulphurisation of natural gas. The natural gas is a dry gas containing at most 40 ppm by weight of sulphur. This sulphur must be removed as it acts as a poison for the reforming catalyst. This sulphur is removed by treating natural gas with zinc oxide.

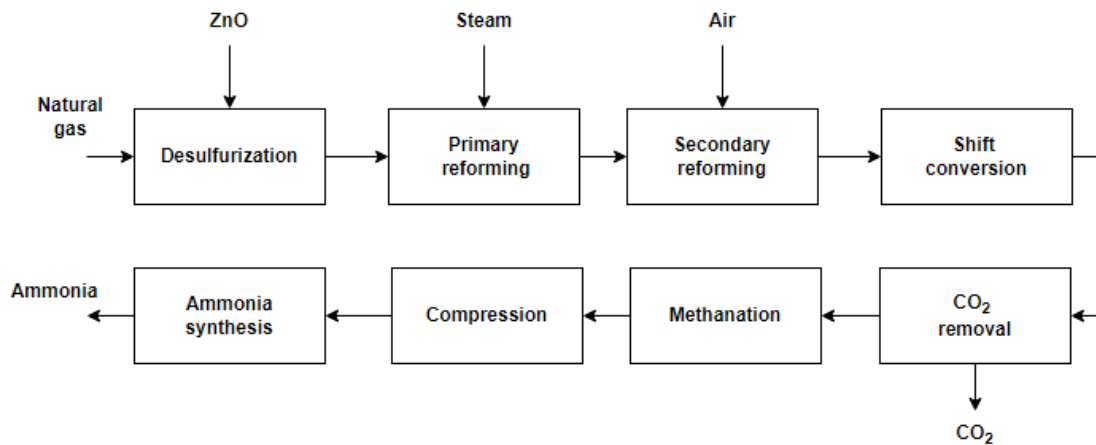
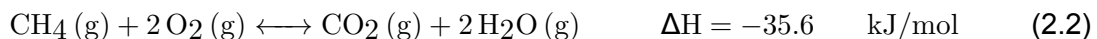
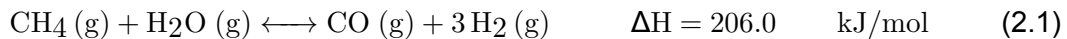
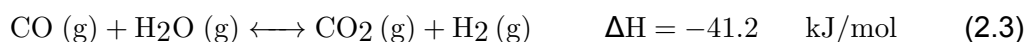


Figure 2.2: Block chart of Haber-Bosch process

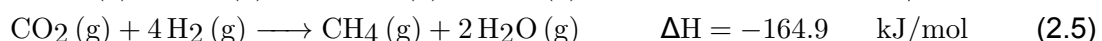
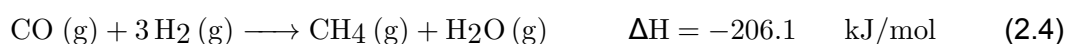
It absorbs the hydrogen sulphide and reduces the sulphur content to a maximum of 5 ppm. Once the sulphur is removed, the natural gas is ready to enter the two reforming sections.



In primary reforming, natural gas in the presence of steam is reformed into hydrogen and carbon monoxide (Equation 2.1). The gas leaving the primary reforming unit enters the secondary reforming section to be treated with hot air and obtain a methane content below 0.3 % by volume (Equation 2.2). The next step is the conversion of carbon monoxide into carbon dioxide. This process consists of two catalytic stages: the first at high temperature with Fe_3O_4 or CrO as catalysts and the second at low temperature with CuO , ZnO or Al_2O_3 as catalysts (Equation 2.3).



The carbon dioxide is then removed and captured with ammonia, producing ammonium hydrogen carbonate as by-product. The purified gas with a CO_2 content of 0.1 % by volume is called synthesis gas. As it is mentioned above with the presence of sulphur, small amounts of CO and CO_2 also lead to catalyst poisoning in the ammonia synthesis. For this reason, the CO and CO_2 content is reduced by reacting the synthesis gas in the presence of a nickel-based catalyst (Equation 2.4 & 2.5).



In this way, the carbon oxides composition is reduced to less than 10 ppm. Once the synthesis gas (74 vol% H₂, 24 vol% N₂, 0.8 vol% CH₄ and 0.3 vol% Ar) is free of impurities, it is compressed to the design pressure and fed into the converter to proceed with a strongly exothermic ammonia synthesis (Equation 2.6) [15].



According to the stoichiometry, the desired H₂/ N₂ molar ratio downstream the methanation process should be 3. (Equation 2.6) is energetically demanding and kinetically complex as it requires high temperatures (400 - 500°C) and pressures (100-200 atm) [10].

2.1.2 Ostwald process

The production of nitric acid is one of the oldest and most important chemical processes. It was developed by the German chemist Wilhelm Ostwald at the beginning of the 20th century. This process consists mainly of three steps as shown in Figure 2.3.

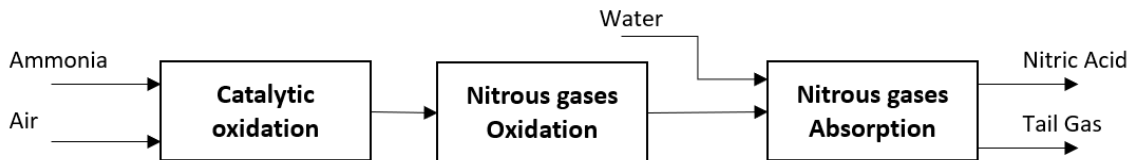
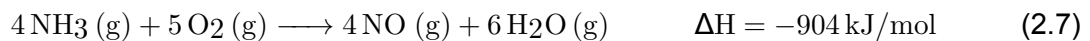
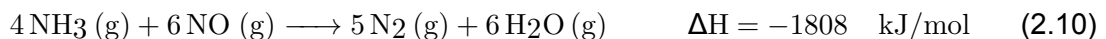
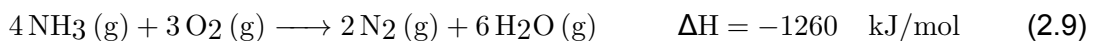
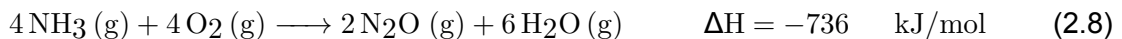


Figure 2.3: Block chart of the Ostwald Process

The catalytic oxidation of ammonia forms the basis of the nitric acid process. The oxidation occurs when anhydrous ammonia in contact with air passes over a platinum-rhodium gauze catalyst composed of 90% platinum and 10% rhodium. Under optimal temperature conditions and in the presence of a Pt-Rh based catalyst, the catalytic combustion efficiency of ammonia is quite high, around 93-98%. The ammonia diffuses through the gaseous film to the catalyst surface, where it reacts with adsorbed oxygen to form nitric oxide.[16] At the end of the combustion chamber, the gaseous mixture is promptly quenched with the aim of preventing the NO decomposition. This step is an extremely fast heterogeneous reaction, with a time of approximately 0.1 thousandths of a second [17].



Along with the main reaction 2.7, the following side reactions can take place:



All reactions are sufficiently exothermic to be self-sustaining. The equations 2.7, 2.8 and 2.9 take place directly and are practically irreversible. In fact, without the presence of a catalyst, only nitrogen would be formed. For that reason, the presence of a suitable catalyst (e.g. Pt-Rh) is essential to produce nitric oxide. Additionally, Equation 2.10 only takes place if the gas velocity is low enough for the already formed nitric oxide to diffuse towards the catalyst. This secondary reaction can easily be avoided by decreasing the contact time between a catalytic wire gauze and the vapor gases [6].

The second step is the oxidation of nitric oxide into nitrogen dioxide and dinitrogen trioxide. The remaining non-reacted oxygen from ammonia combustion starts to react with the nitric oxide formed to produce nitrogen dioxide. This reaction occurs while the exit gas is cooled to recover the heat released by the strongly exothermic reaction. At the same time, nitrogen dioxide can dimerise to form dinitrogen tetraoxide. Consequently, nitric oxide and nitrogen dioxide can react to form dinitrogen trioxide which is considered an undesirable reaction (Equation 2.13).



Finally, the last step is the reactive absorption of nitrogen dioxide and dinitrogen tetraoxide in water. NO_x absorption has been defined by many researchers as one of the most complex absorption mechanisms due to several reasons [18]:

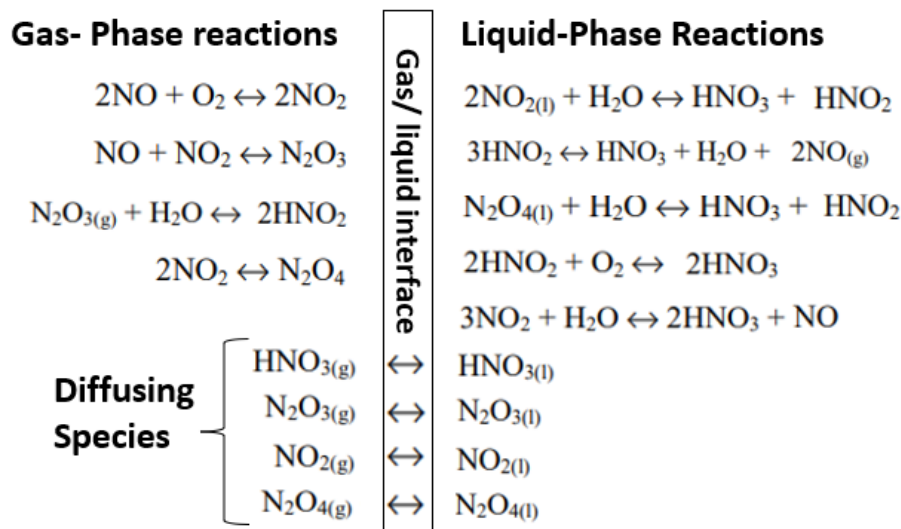


Figure 2.4: NO_x absorption mechanism in aqueous solution for mass transfer and gas-liquid phase reactions

- NO_x gas is a mixture of several nitrogen oxides (NO , NO_2 , N_2O_3 and N_2O_4). The absorption of these nitrogen oxides in water results in two oxyacids, nitric acid and nitrous acid.
- More than forty equilibrium reactions occur in both gas and liquid phases. The full NO_x mechanism is shown in Figure 2.4
- The absorption of NO , NO_2 , N_2O_3 , and N_2O_4 is accompanied by chemical reaction whereas the desorption of NO , NO_2 and HNO_2 is preceded by chemical reaction.
- Heterogeneous equilibrium prevail between gas-phase and liquid-phase components
- Limited or incomplete data of physical and chemical properties for the nitrogen oxides species involved

Absorption of NO_x gases in aqueous solution has been studied over the years since it plays a crucial role in many processes. A part from the manufacture of nitric acid, the

removal of NO_x from flue gases (e.g. exhaust-gases) have received high attention in the last decades with the increasing climate change the world is facing.

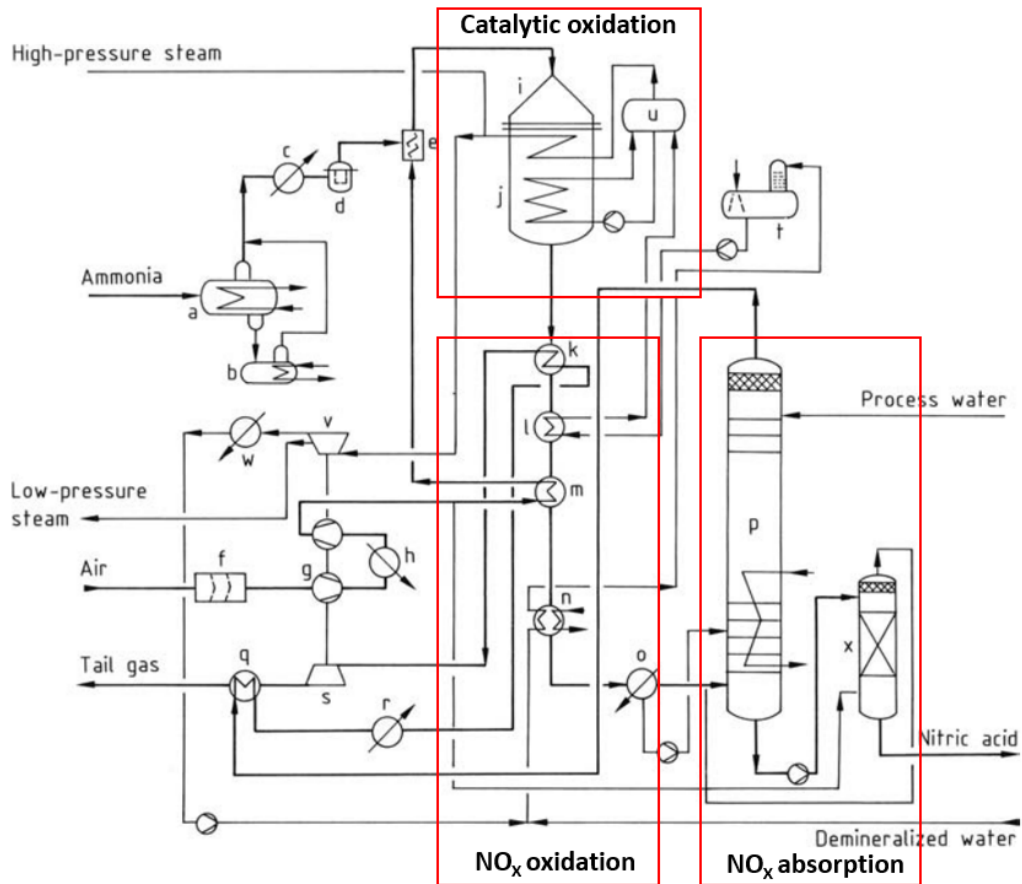


Figure 2.5: Simplified flowsheet of a medium-pressure process a) Ammonia evaporator; b) Ammonia stripper; c) Ammonia preheater; d) Ammonia gas filter; e) Ammonia – air mixer; f) Air filter; g) Air compressor; h) Interstage cooler; i) Reactor; j) Waste-heat boiler; k) Tail-gas preheater; l) Economizer; m) Air preheater; n) Feedwater and warm-water preheaters; o) Cooler – condenser; p) Absorption tower; q) Tail-gas preheater; r) Tail-gas preheater; s) Tail-gas expansion turbine; t) Feedwater tank with deaerator; u) Steam drum; v) Steam turbine; w) Steam turbine condenser; x) Bleacher [6]

The nitric acid production process has been implemented in industry with different configurations depending on the operating pressure of the process:

- **Monopressure plants:** The same pressure is maintained during the whole process. In monopressure processes two possibilities can be distinguished: medium-pressure and high pressure. For medium-monopressure plants the ammonia combustion and the NO_x absorption take place at a working pressure of 2.3-6 bar. Whereas, high-monopressure plants runs at 7-11 bar.
- **Dual-pressure plants:** For this case, the pressure is not maintained during the whole process. A lower pressure (4-6 bar) is considered in the catalytic oxidation of ammonia and a higher pressure (9-14 bar) for the absorption section.

The factors that influence the selection of a monopressure or dual-pressure process are: environmental impacts, energy costs, plant capacities and locations. In fact, monopres-

sure plants are more suitable in locations with lower energy costs and shorter depreciation periods. For that reason, high-monopressure plants predominate in North-America and dual-pressure plants in Europe due to the higher energy costs. Dual pressure processes are preferably used when large capacities are needed since it combines the favorable economics of medium pressure combustion with efficiency of high-pressure absorption [6].

For the production of fertilisers, such as ammonium nitrate, a nitric acid concentration of 50-70% by weight is required. Nevertheless, there are processes in the organic chemical industry that require nitric acid concentrations of 98-100 wt%, such as metal purification, explosives production, adhesive production, drug detection and laboratory practices, among others.

2.2 Solar-based ammonia and nitric acid production

In reference to ammonia synthesis, it is vital to mention the amount of energy (30.5 MJ/ kg NH_3) required in the process to achieve high temperatures (400-500 °C) and pressures (100-200 bar) [10]. From an environmental perspective, the conventional ammonia process accounts for 1.5% of total greenhouse gas emissions. In fact, 3-5% of natural gas production is used solely for ammonia production. With the growing concern about climate change, renewable technologies have been proposed in recent decades to produce ammonia in a more sustainable way [4].

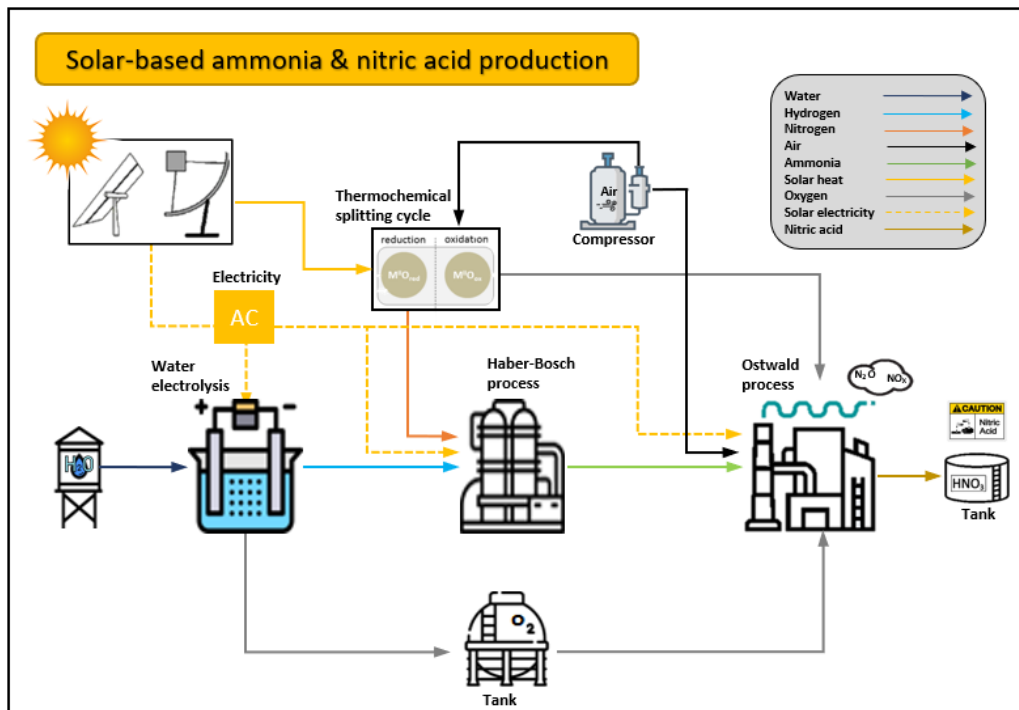


Figure 2.6: Pathways for a solar-based ammonia & nitric acid production.

One of the main research topics is the search of synergy between solar energy and ammonia production and their further implementation in the Ostwald process. The aim is to produce green ammonia using solar technologies for the required energy, as well as, the required hydrogen and nitrogen production (Figure 2.6).

2.2.1 Solar energy production

Solar energy technologies can be divided into active and passive systems. Passive systems collect directly the solar power without converting thermal or light energy, whereas active solar technologies mainly focus on the absorption of solar radiation [19].

There are two main passive solar technologies by which solar energy is harnessed: photovoltaic (PV), in which light is converted directly into electricity; and concentrated solar power (CSP), which produces energy using the heat released from the sun.

The main disadvantage of using PV panels is the storage of electricity. Currently available batteries are quite expensive and are not capable of storing large amounts of energy. As

a weather-dependent technology, their use as a sole source of energy is rather limited in industry. In contrast, this energy storage problem can be solved with CSP plants, as storing thermal energy is more feasible [20].

- **Concentrated solar power technology**

Concentrated solar power plants use mirrors to reflect the sun’s radiation and concentrate the energy onto receivers for further conversion into electricity (Figure 2.7). CSP technology has countless applications such as power generation, cooling, heating, material processing, process heat and chemical cycle. One of the main advantages compared to the PV technology is the possibility of storing thermal heat efficiently and economically, such as the use of molten salt as an energy storage and heat transfer medium[21].

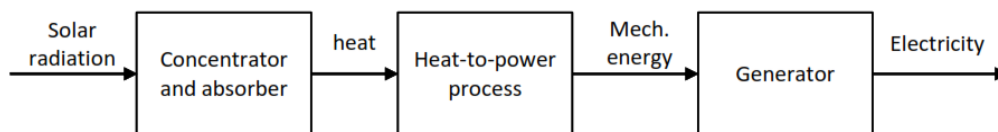


Figure 2.7: Schematic structure of the energy conversion in a CSP plant.

Different receivers can be distinguished as shown in Figure 2.8. Figure 2.9 shows a comparison of the most relevant parameters for the CSP technologies. The central receiver, also known as solar tower, results to be the most promising technology based on storage,

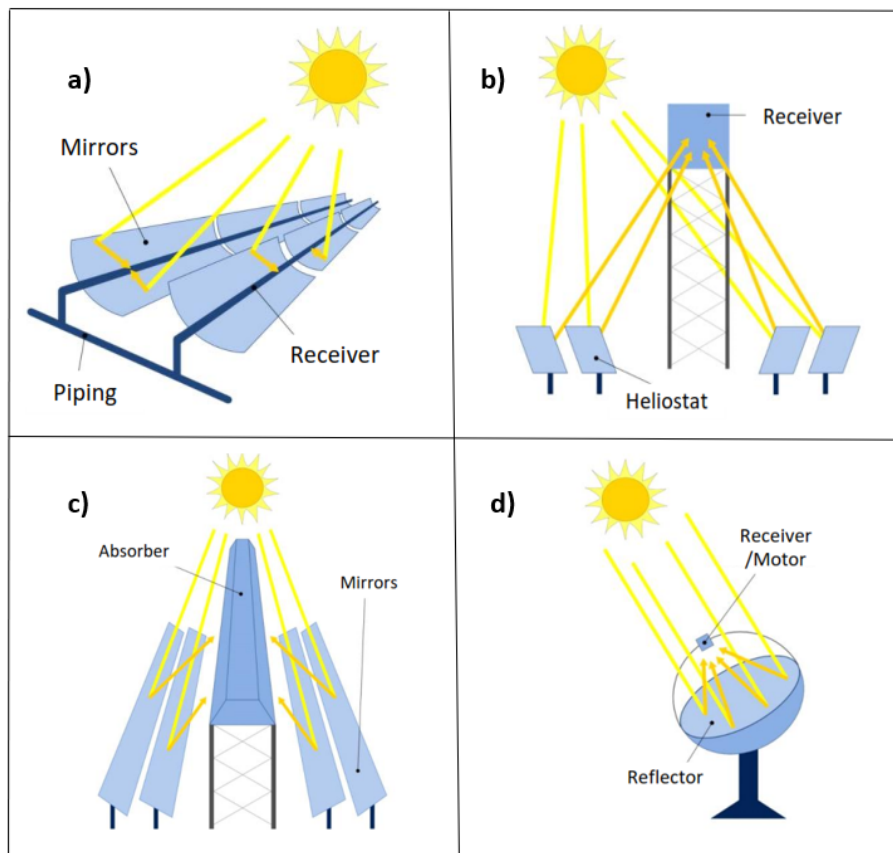


Figure 2.8: Types of receivers in CSP plants: a) Parabolic trough. b) Central receiver. c) Linear fresnel. d) Parabolic dish. [22]

conversion efficiency and cost [19]. Even if parabolic dishes can achieve higher temperatures (up to 1500 °C) and efficiencies (up to 30%) compared to the other receivers, the capital costs of dishes do not make it possible to compete with central receivers [23].

Figure 2.9: Comparison of core CSP technologies [19].

Parameters	Central receiver	Parabolic trough	Linear Fresnel	Parabolic dish
Concentration ratio	>1000	70–80	>60	>1300
Working temperature (°C)	300–1000	200–400	50–300	120–1500
Typical efficiency (%)	25–28	18	12	30
Recorded Peak efficiency of the plant (%)	23–35	14–20	18	30
Typical capacity (MW)	10–200	10–300	10–200	0.01–0.025
Development status	Commercial	Commercially proven	Pilot project	Demonstration stage

CSP technologies offer the possibility of producing carbon-free fuels such as hydrogen. Thermochemical solar hydrogen can be produced by thermolysis without any impact on the environment.

2.2.2 Solar hydrogen production

There is a growing awareness of the environmental impact of the conventional hydrogen production. Steam methane reforming releases 9.26 kg CO₂/ kg H₂ [24]. Over 79 % percent of global hydrogen production comes from fossil fuels. Accounting fossil-based hydrogen responsible of the 2 % of global CO₂ emissions in energy and industry in 2020 [25].

Fortunately, there are already technologies that are in the process of being scaled up for the production of green hydrogen. It is the case of water electrolysis, which is expected to be the main source of hydrogen production in the future, considerably reducing the steam methane reforming process.

- **Water electrolysis**

Water electrolysis is an electrochemical process that by using electricity is able to split the water molecule into hydrogen and oxygen. This process can be a much more environmentally-friendly option, if the source of the electricity is a renewable energy source. Therefore, solar energy can be implemented into the process of producing hydrogen from water electrolysis.

There are mainly 4 electrolyser technologies (Figure 2.10): alkaline, proton exchange membrane (PEM), solid oxide electrolysis cells (SOECs), and anion exchange membranes technologies. Alkaline electrolysers dominate with 61% of installed capacity in 2020, while PEMs have a 31% share. The remaining capacity is of unspecified electrolyser technology and SOECs [25].

Unfortunately, the cost per kg of hydrogen produced by means of electrolysis is significantly higher than the cost by means of SMR. It is hoped that a competitive price can be obtained by improving this technology and penalising the use of fossil fuels by 2030. The global awareness about climate change is notably accelerating the push for this technology and gradually reducing dependence on fossil fuels such as natural gas.

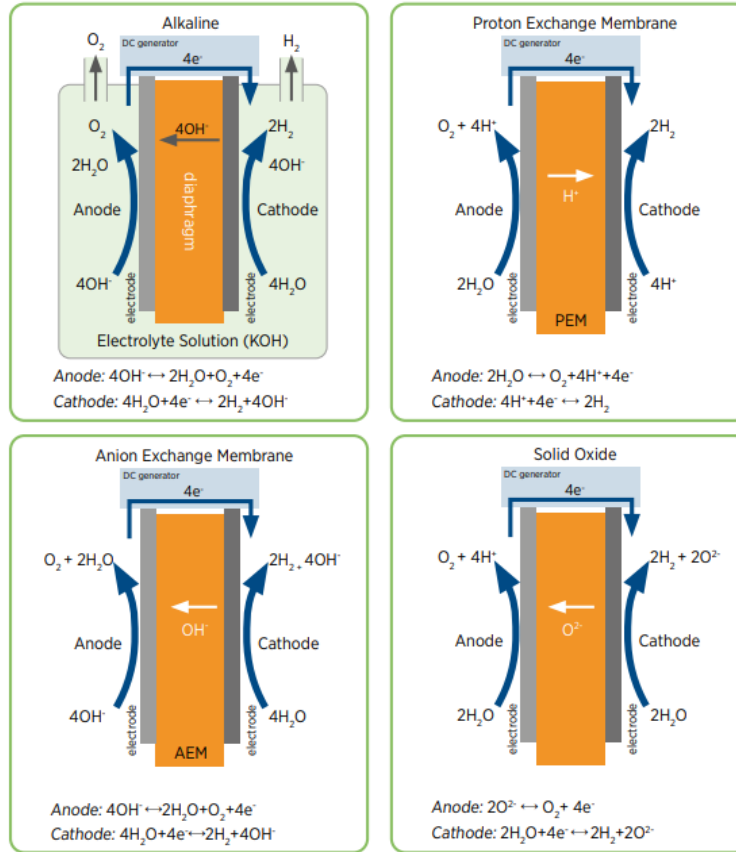
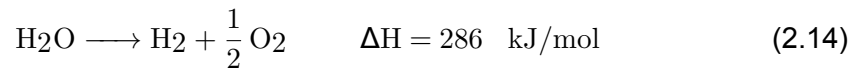


Figure 2.10: Overview of commercially available electrolyser technologies [13].

- **Thermochemical water splitting cycles**

The main advantage of thermochemical cycles is that the thermal energy from CSP plants can be directly utilised without the inert conversion losses from electricity generation. The inclusion of this method offers the possibility of using solar heat directly to obtain hydrogen for the ammonia synthesis process [26].

Thermolysis, and more specifically the thermochemical water splitting (TWS), is seen as a potential competitor to electrolysis in the near future [27]. It consists on applying extremely high temperatures (~2500 K) to breakdown the water molecule into hydrogen and oxygen base components (Equation 2.14).

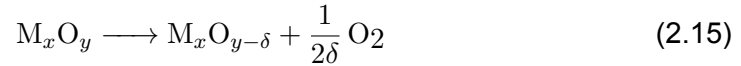


Unlike the electrodes used in electrolyzers, this technology does not use noble metals but metal oxides which are much more abundant and have less impact on the environment.

Thermochemical processes are based on redox materials such as multivalent metal oxides [28]. The process is a closed-loop, therefore, the metal oxides are fully recycled and the only raw materials consumed are water and solar energy [29].

TWS cycle consists of two steps (Figure 2.11):

- **Reduction step:** A first step in which an endothermic reaction takes place and in which the metal oxide is partially reduced at high temperature and/or lower oxygen partial pressure. (Equation 2.15).



- **Oxidation step:** A second step in which an exothermic reaction takes place. The oxygen affinity of the partial reduced oxide is increased by lowering temperature and/or by raising oxygen partial pressure. In that way, oxygen is captured from a gas stream. Then hydrogen, oxygen and the initial metal oxide are produced when the reduced valence metal oxide reacts with water (Equation 2.16).

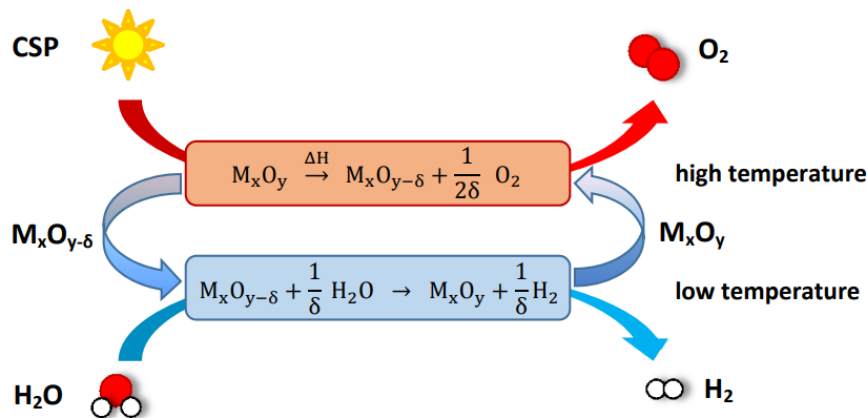
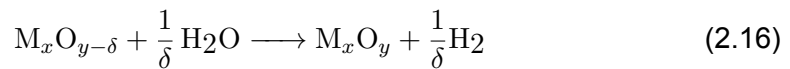


Figure 2.11: Solar thermochemical water-splitting cycle [30].

The solar heat collected by CSP technologies can also be used in thermochemical cycles to obtain purified nitrogen for the HaberBosch process.

2.2.3 Solar-driven air separation

Nitrogen and hydrogen constitute the two main feedstock for ammonia synthesis and their purity play a crucial role in the Haber-Bosch process. The presence of oxygen and water in Equation 2.6 leads to the main deactivation of the catalyst, resulting in a considerable increase in the operating costs of the reactor [31].

The process most commonly used in industry for the separation of nitrogen from air is known as the Hampson-Linde process [32]. This process is very energy intensive (12 kJ/mol N₂) as cryogenic temperatures are needed to obtain oxygen and nitrogen in a liquid state [33]. On the other hand, there are other techniques based on adsorption at high pressures that also requires a high energy consumption such as pressure swing adsorption (PSA) or at low temperatures such as temperature swing adsorption (TSA) [28].

The amount of energy consumed during PSA process depends on the product gas purity and it can be approximated by the following equation:

$$w_{sep} = \ln\left[\left(\frac{p_{O_2,in}}{p_{O_2,out}}\right)^2\right] \cdot 1000; \quad J/mol \quad (2.17)$$

Nitrogen purity with an oxygen concentration below 500 ppm requires more energy than cryogenic air separation [33]. For that reason, Haber-Bosch plants prefer to obtain nitrogen from the Hampson-Linde process over PSA.

Apart from these physical separation methods, there are thermochemical loops that can directly harness the solar heat from CSP plants to separate nitrogen and oxygen from air. Solar thermochemical air-separation cycle uses a similar approach to the thermal water splitting process described before. The only difference is that air is used as oxidant instead of using water [28].

2.2.4 Oxygen-enriched air into conventional nitric acid process

In both air separation and hydrogen production, pure oxygen is obtained as a by-product. This gave rise to the idea of studying the feasibility and integration of this pure oxygen into the conventional Ostwald process. This research is doubly valuable in the quest to decarbonise chemical processes by 2050. It is a study aiming to optimise a nitric acid plant by integrating renewable technologies and making fertiliser production more sustainable.

The implementation of oxygen-enriched air into the conventional nitric acid process is discussed in various patents. A summary of these works is compiled in Appendix C. This technique aims at optimising the nitric acid production process in several ways:

1. Maximising the catalytic combustion of ammonia conversion to generate an increase in nitric acid production
2. Increasing gaseous nitrous oxides conversion to reduce the final concentration of NO_x gases in the tail-gas
3. Boosting the bleaching process to increase the nitric acid strength and quality of the final product

3 Methodology

Over the years, different process design methodologies have been proposed as different ways to solve a problem such as incremental refinement, mathematical programming or systematic/heuristic approaches [34].

The aim of this section is to describe the methods used in the two main sections of the master thesis: process simulation and the economic analysis. The process design methodology used is known as task-based design. It consists on decomposing complex design problem (e.g. the design of a nitric acid plant) into simpler sub-problems which are solved successively [34].

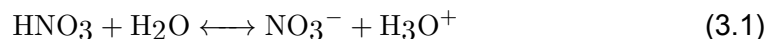
3.1 Process simulation

As mentioned in section 1.2, one of the core objectives is the simulation of the Ostwald process. Aspen Plus[®] V11, one of the most recognised and widely used commercial process simulators in the chemical industry, is used for this purpose.

The first step in process simulation is to establish the goals: the type of plant (Section 2.1.2), the capacity of the plant and the characteristic of the desired product. It is decided to perform a simulation of a medium-monopressure nitric acid plant in Aspen Plus[®]. The plant is designed to operate at 5.8 bar with a capacity fixed to 700 t/d of nitric acid (eq. 100%) which is equivalent to 1166.67 t/d of product at a concentration of 60 wt% in nitric acid.

3.1.1 Thermodynamic models

For the main part of the process, the electrolyte nonrandom two-liquid (ELECNRTL) model is used [35]. This thermodynamic model implemented in Aspen Plus[®] provides an accurate description of the aqueous nitric acid system. Nitric acid is a strong acid that in presence of water is dissociated into hydronium and nitrate ion (Equation 3.1). Therefore, the presence of ions in the liquid phase requires non-ideal solution thermodynamics as ELECNRTL.



On the other hand, many parts of the plant operate at high pressure and temperature where no liquid-phase is present. In that case, the NRTL-RK method is used. This model uses the Redlich-Kwong (RK) equation of state to describe the vapor phase and the non-random two-liquid model for the liquid phase (NRTL). For cooling water and steam, the STEAMNBS model is used since it counts with NBS/NRC equation of state for steam and liquid water properties [36].

Henry's law is used to model the vapor-liquid equilibria for NO, NO₂, O₂, N₂ and N₂O₄ in the aqueous phase. However, the Henry's law constants for NO₂ and N₂O₄ are not included in the Binary Data Bank in Aspen Plus[®]. The values at 25°C are 8.47·10⁶ and 7.25·10⁴ m³Pa/kmol respectively [37]. It was assumed that Henry's law constants for NO₂ and N₂O₄ have the same temperature dependency as that for SO₂ in water.

Table 3.1: Thermodynamic model for each section of the nitric acid plant

Species	Section	Thermodynamic model
Air, Water and Ammonia	Air compression/Gas mixing	NRTL-RK
Air, steam and Ammonia	Ammonia oxidation	NRTL-RK
NO _x gases, Air and Ammonia	Nitric oxides oxidation	NRTL-RK
NO _x gases, Air, Water and Nitric acid	Absorption	ELECNRTL
Cooling water and Steam	Utilities	STEAMNBS

3.1.2 Implemented kinetics

Within this section a distinction has to be made between three kinetic models used:

- **Model 1:** Catalytic oxidation of ammonia.
- **Model 2:** Oxidation of nitrogen oxides in reactive heat exchangers.
- **Model 3:** Absorption of nitrogen oxide gases with water.

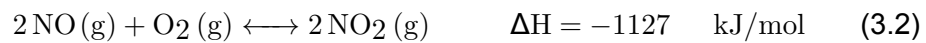
• Catalytic oxidation of ammonia

As already mentioned in Section 2.1.2, the selectivity towards NO (Equation 2.7) is around 93-98%. There are some undesirable byproducts formed during reactions (2.8-2.10).

The catalytic oxidation of ammonia is simulated in Aspen Plus® considering only equations 2.7 and 2.9. The conversion of ammonia towards reactions 2.8 and 2.10 is quite low. Therefore, those reactions are neglected in our model. The block used to simulate this unit is a stoichiometric reactor (R-101) considering a NH₃ conversion of 96% and 4% for equations 2.7 and 2.9 respectively.

• Oxidation of nitrogen oxides in reactive heat exchangers

During the heat recovery stage in the heat exchangers (E104 - E107) only three vapour phase reactions take place:



There are other intermediate by-products such as HNO₂ and N₂O₃ which are unstable species and are not considered in the simulation. These reactions are computed creating a Fortran user kinetic subroutine (Appendix A). The user subroutine named as HNO₃ is used to describe the kinetic model for several heat exchangers modelled as plug flow reactors (PFRs) in the nitric acid simulation.

The first equilibrium reaction corresponds to the oxidation of nitric oxide to nitrogen dioxide. This is a slow homogeneous reaction which is favourable at low temperatures and high pressures. At temperatures below 150°C and with sufficient residence time, almost all of the nitric oxide is converted to nitrogen dioxide [38].

$$r_{3.2f} = \frac{k_{3.2f}}{RT} P_{\text{NO}}^2 P_{\text{O}_2}; \quad \log k_{3.2f} = \left(-1.0366 + \frac{652.1}{T}\right) \quad \text{atm}^{-2} \text{s}^{-1} \quad (3.5)$$

$$r_{3.2b} = \frac{k_{3.2b}}{RT} P_{\text{NO}_2}^2; \quad k_{3.2b} = \frac{k_{3.2f}}{K_{eq}}; \quad \ln K_{eq} = \left(-17.9956 + \frac{13870.9}{T}\right) \quad \text{atm}^{-1} \quad (3.6)$$

The reverse reaction of 3.2 gains importance at low temperatures [38]. Therefore, the forward and backward reaction rates need to be considered (Rate 3.5 & 3.6).

The second equilibrium reaction (Equation 3.3) corresponds to the dimerisation of nitrogen dioxide. This reaction reaches rapidly the equilibrium state. As Le Chatelier's principle indicates, lower temperature and high pressure shift the equilibrium towards the production of dinitrogen tetroxide. Nevertheless, during the whole heat recovery unit only a small fraction of nitrogen dioxide is converted into dinitrogen tetroxide.

$$r_{3.3f} = \frac{k_{3.3f}}{RT} P_{NO}^2; \quad k_{3.3f} = 10 \cdot k_{3.2f} \quad atm^{-1} s^{-1} \quad (3.7)$$

$$r_{3.3b} = \frac{k_{3.3b}}{RT} P_{N_2O_4}; \quad k_{3.3b} = \frac{10 \cdot k_{3.2f}}{K_{eq}}; \quad \ln K_{eq} = \left(-21.244 + \frac{6891.6}{T}\right) \quad atm^{-1} \quad (3.8)$$

A rate constant of 10 times the NO oxidation reaction has been used for the forward reaction. This factor can be considered as an adjustable parameter in controlling the reaction rate for nitrogen dioxide dimerisation [39].

Finally, the last reaction is the formation of nitric acid from water and nitrogen dioxide (Equation 3.4). This reaction takes place really fast in gas-phase until it reaches equilibrium. The equilibrium constant used for this reaction comes from the Kuokolif and Marek investigation [17].

$$r_{3.4f} = \frac{k_{3.4f}}{RT} P_{NO_2}^3 P_{H_2O}; \quad k_{3.4f} = 8000 \cdot k_{3.2f} \quad atm^{-3} s^{-1} \quad (3.9)$$

$$r_{3.4b} = \frac{k_{3.4b}}{RT} P_{HNO_3}^2 P_{NO}; \quad k_{3.4b} = \frac{k_{3.4f}}{K_{eq}}; \quad \ln K_{eq} = \left(-19.7292 + \frac{4282.34}{T}\right) \quad atm^{-1} \quad (3.10)$$

The reaction rate constant for the forward reaction has been set to 8000 the basic NO oxidation rate constant. This factor is chosen to simulate effectively the equilibrium model [39].

- **Absorption of nitrogen oxide with water**

Over the years, new methods have been proposed to calculate the complex absorption of nitric oxide gases with aqueous solution. They can be classified into 3 groups depending on: the number of reactions considered, the factors included in the kinetic reactions and the different mathematical models used [6].

In Figure 2.4, the complete non-stoichiometric model for the absorption of nitrogen oxides in water is shown. However, it was decided to use a simpler model developed by Miller in 1987. This model has correlations to model the behaviour of absorption towers in the production of nitric acid [40].

As Figure 3.1 shows, this model considers two vapor-phase and one liquid-phase reaction. Firstly, the NO oxidation takes place to form NO₂ (Equation 3.2). In Miller's paper the kinetic rate considered is described in a different way than that of equations 3.7 and 3.8. Nevertheless, it is assumed to use the kinetic rate described by Bodenstein in 1922 [38].

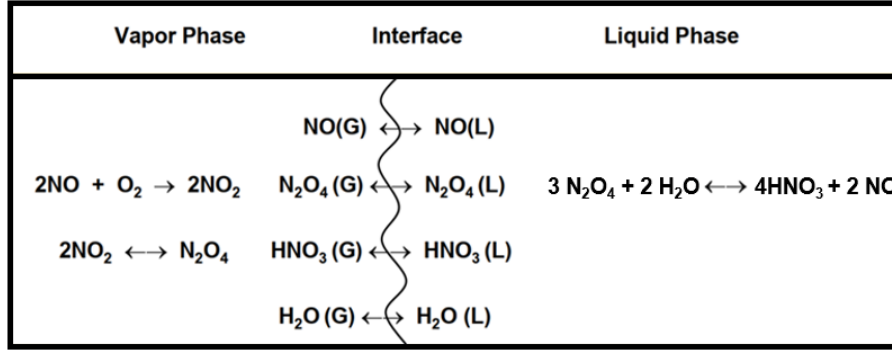
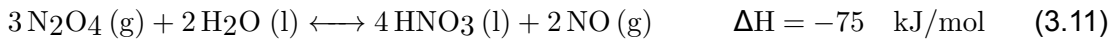


Figure 3.1: Simplified mechanism (Miller's approach) [40].

Secondly, the dimerisation of nitrogen dioxide takes place (Equation 3.3). This equilibrium equation has been modelled using the equilibrium capability in Radfrac.

Finally, the overall reaction for the production of nitric acid can be described (Equation 3.11). Miller stated that dinitrogen tetroxide first absorbs in the liquid phase as a mass-transfer limited reaction and then quickly reacts to form nitric acid.



This mass transfer effect is described with the following reaction rate:

$$r_{\text{N}_2\text{O}_4} = J_{\text{N}_2\text{O}_4} \cdot A \cdot P_{\text{N}_2\text{O}_4}; \quad \text{kmol/s} \quad (3.12)$$

This reaction rate is written as a function of the absorption rate ($J_{\text{N}_2\text{O}_4}$), the interfacial area (A) and the partial pressure of dinitrogen tetroxide ($P_{\text{N}_2\text{O}_4}$).

The interfacial area is a function of the superficial gas velocity (u_g), the bubble cap slot or sieve hole submergence (S) and the column diameter (d).

$$A = 325 \cdot u_g^{1/2} S^{-1/2} \pi \frac{d^2}{4}; \quad \text{m}^2 \quad (3.13)$$

Miller found different correlations for the absorption rate ($J_{\text{N}_2\text{O}_4}$) as a function of temperature (T) and mass fraction (W_{HNO_3}). The absorption rate was described depending on the type of tray:

- **Bubble-cap trays:**

$$J_{\text{N}_2\text{O}_4} = \exp \left(-\frac{1500}{T} - 4.3790 - 23.279W_{\text{HNO}_3} + 130.42W_{\text{HNO}_3}^2 - 370.87W_{\text{HNO}_3}^3 \right. \\ \left. + 486.94W_{\text{HNO}_3}^4 - 236.54W_{\text{HNO}_3}^5 \right); \quad \text{kmol m}^{-2}\text{kPa}^{-1} \text{ s}^{-1} \quad (3.14)$$

- **Sieve trays:**

For $W_{\text{HNO}_3} > 0.05$:

$$J_{\text{N}_2\text{O}_4} = \exp \left(-\frac{1500}{T} - 2.7648 - 39.614W_{\text{HNO}_3} + 181.98W_{\text{HNO}_3}^2 - 429.65W_{\text{HNO}_3}^3 \right. \\ \left. + 496.99W_{\text{HNO}_3}^4 - 223.24W_{\text{HNO}_3}^5 \right); \quad \text{kmol m}^{-2}\text{kPa}^{-1} \text{ s}^{-1} \quad (3.15)$$

For $W_{HNO_3} < 0.05$:

$$J_{N_2O_4} = \exp \left(-\frac{1500}{T} + 0.2548 - 315.73W_{HNO_3} + 9256.2W_{HNO_3}^2 - 95602W_{HNO_3}^3 \right); \quad \text{kmol m}^{-2}\text{kPa}^{-1} \text{ s}^{-1} \quad (3.16)$$

This model can only be implemented in Aspen Plus® through a user kinetic subroutine. The user subroutine called NOABS has been created by AspenTech®. It is implemented in a Radfrac block and it has one integer input variable and 4 real input variables [39]. An integer value of 1 correspond to a bubble-cap trays column and a value of 2 for a sieve trays column. The 4 real values correspond to: 1. Column diameter (m), 2. Bubble cap slot or sieve hole submergence (m), 3. Factor for equation 3.7, and 4. Factor for equation 3.11.

3.1.3 Pinch analysis

The goal of the pinch analysis is to decrease heating and cooling utilities by integrating the hot streams to heat the cold streams up and vice versa. This methodology pretends to minimise energy consumption of chemical processes. The first step is to calculate the pinch temperature. This metric represents the minimum temperature difference between the hot and cold composite curve. It is the point where the design is more constraint. It constitutes the first step, after that the energy requirements can be fulfilled using heat exchanger to recover heat between the cold and hot streams. Once this step is executed, the heat exchanger network synthesis (HENS) is defined. In that way, the integration of the heat exchangers and the required utility streams are properly designed.

- **Heat capacity calculation**

First of all, all the streams must be classified as hot or cold streams. If the inlet temperature is higher than the outlet, they are classified as hot streams and marked in red. On the contrary, they are classified as cold streams and marked in blue.

Heat duties, flowrates, temperature differences and heat capacities need to be known to perform this method. The heat capacity (C_p) is not directly given by Aspen Plus®. Nevertheless, it can be easily calculated dividing the heat duty by the flowrate (F) and the temperature difference (ΔT).

$$C_p = \frac{Q}{F \cdot \Delta T} \quad (3.17)$$

Once the heat capacity is known, it is multiplied by the flowrate to obtain, FC_p , which is defined as the amount of heat required to increase or decrease the flow temperature by 1K per second.

- **Pinch point analysis:**

There are mainly two different approaches: a graphical method and an algebraic method known as the problem table algorithm (PTA). This last one uses a tabular algorithm for calculating net heat flows represented by grand composite curves [41].

In this case, the graphical representation method based on the construction of composite curves is chosen. This procedure is based on the following steps [42]:

- Select the minimum difference of temperature between the cold and hot composite curves (ΔT_{min}). The decision is based on equipment and utility costs. Normally, the analysis is performed for different ΔT_{min} and is plotted against the operational and capital costs.
- Calculate the temperature intervals and tabulate the hot streams in one column and the cold streams in another one. Sort the values from lowest to highest.
- Missing interval temperatures are filled following this procedure; cold stream temperatures are shifted up by ΔT_{min} and hot stream temperatures are shifted down by ΔT_{min} .

$$T_{hot} = T_{cold} + \Delta T_{min}; \quad T_{cold} = T_{hot} - \Delta T_{min} \quad (3.18)$$

- Calculate the available heat for each temperature interval.

$$Q_k = (T_{k-1} - T_k) \left(\sum_{i=1}^{k-1} FC_{p_i} \right) \quad (3.19)$$

- Calculate the cascade heat for both hot and cold streams.

$$\sum_{i=1}^k Q_i = \sum_{i=1}^{k-1} FC_{p_i} (T_i - T_k) \quad (3.20)$$

- Plot the composite curves versus their actual temperature scale.
- Shift the composite curve to fulfill the minimum temperature difference established. The pinch point is the point in which the temperature difference between the hot and cold composite curves is exactly equal to ΔT_{min} .
- Calculate the minimum cold or hot heat duty required.

3.1.4 Optimised nitric acid plant

In subsection 2.2.4 was pointed out how the injection of oxygen-enriched air into nitric acid plants can boost production, increase acid strength and help to control nitric oxide emissions. Moreover, in section 2.2 was described how the main raw materials for ammonia production could be obtained using only solar energy as a source. In both air separation and hydrogen production, pure oxygen is obtained as a by-product. This gave rise to the idea of studying the feasibility and integration of this pure oxygen into the conventional Ostwald process.

For this purpose, the amount of pure surplus oxygen is calculated in relation to the amount of hydrogen is needed to produce the amount of green ammonia that our nitric acid plant consumes. In this case, the oxygen is considered to come from a PEM electrolyser.

Table 3.2: Summary of industry-approved patents.

Injection location	Primary feed air pipeline	Secondary feed air pipeline	Upstream bleaching column	Upstream cooler/condenser	Upstream absorption column	Upstream combustion chamber
EP0808797B1 [14]	C	C	C	C	C	C
US6165435 [43]	C	C	NC	NC	C	NC
EP0799794A1 [44]	NC	NC	NC	NC	C	C
US3927182 [45]	C	C	NC	NC	NC	NC
US4183906 [46]	NC	NC	C	NC	C	NC
US6649134B2 [47]	NC	NC	NC	NC	NC	NC

C = Considered
NC = Not considered

A detailed summary of several industry-approved patents considering enriched-oxygen air into existing nitric acid plants is given in Appendix C. In addition, Table 3.2 classifies the different works according to the location of the injection points considered. Based on this information, it is decided to study four different cases and simulate them in Aspen Plus® in order to determine the feasibility and functionality of pure oxygen integration (Appendix B):

1. **Case A:** Pure oxygen is uniquely injected upstream of the bleaching column, T-102 (Figure B.1b).
2. **Case B:** Pure oxygen is uniquely injected upstream of the cooler/condenser, E-108 (Figure B.1c).
3. **Case C:** Pure oxygen is uniquely injected upstream of the absorption tower, T-101 (Figure B.1d).
4. **Case D:** Pure oxygen is uniquely injected into the primary feed air (Figure B.1e).

3.2 Economic analysis

The goal of this section is to perform an economic evaluation of the simulated process. The process simulation results from Aspen Plus® are used as inputs to calculate the capital expenses (CapEx), operational expenses (OpEx) and the net production costs (NPC).

The methodology applied to develop this analysis is based on the *Peters, Timmerhaus, West's book* [48]. The association for the advancement of cost engineering (AACE) created a guideline to estimate the classification to project cost estimates. According to the level of project definition, this project is estimated to be part of a class 3 & 4 following the AACE international guide. These levels implies that a cost assessment accuracy is between $\pm 30\%$ [49].

3.2.1 Capital expenses (CapEx)

The fixed capital investment (FCI) costs are mainly the equipment costs (EC) and the necessary capital for equipment installation. Equation 3.21 is used to determine the equipment cost of each specific operation [49]. f_i represents the equipment-specific cost function for every equipment described in the simulation. $S_{i,k}$ corresponds to the equipment input variable needed to estimate the cost of the unit (e.g exchange area, volume or power among others). CEPCI is the Chemical Engineering Plant Cost Index which is a metric to adjust process plant cost from one period to another. CEPCI considers the inflation and temporal cost variations of equipment [50].

$$EC_{ref,i} = f_i(S_{i,1}; S_{i,2}; \dots; S_{i,k}) \cdot \frac{CEPCI}{CEPCI_{ref}} \cdot F_{pre,i} \cdot F_{mat,i}, \quad i, k \in N \quad (3.21)$$

$F_{pre,i}$ and $F_{mat,i}$ are additional equipment factors related to specific materials and operating conditions.

Reference data for equipment costs are limited or given for different years. For that reason, it is important to use cost calculation base year. The original cost data must be updated and corrected according to the cost calculation base year. Therefore, Equation 3.22 is used to size adaptation of the equipment.

$$EC_i = EC_{ref,i} \cdot \left(\frac{S_i}{S_{ref,i}} \right) \quad (3.22)$$

Fixed capital cost were estimated according to Equation 3.23. Ratio factors ($F_{ind,i,j}$) and typical values for fluid processing plants are shown in Table 3.3.

$$FCI = \sum_{i=1}^m \left(EC_i \cdot \left(1 + \sum_{j=1}^{10} F_{ind,i,j} \right) \cdot \left(1 + \sum_{j=11}^{12} F_{ind,i,j} \right) \right) \quad (3.23)$$

Finally, the total capital investment (TCI) is calculated assuming that 11 % of the FCI is required as working capital (WC).

$$TCI = \frac{FCI}{0.89} \quad (3.24)$$

Table 3.3: Estimation cost factor for a fluid processing plant [51]

Indirect cost items, $F_{ind,i,j}$	j	Basis	Typical value
<i>Total direct plant costs (D)</i>			
Equipment installation	1	EC	0.47
Instrumentation and control	2	EC	0.36
Electrical systems (installed)	3	EC	0.68
Piping (installed)	4	EC	0.11
Buildings (including services)	5	EC	0.18
Yard improvements	6	EC	0.1
Service facilities (installed)	7	EC	0.55
<i>Total indirect plant costs (I)</i>			
Engineering and supervision	8	EC	0.33
Construction expenses	9	EC	0.41
Legal expenses	10	EC	0.04
<i>As function of total direct and indirect costs (D + I)</i>			
Contractor's fee	11	D + I	0.05
Contingency	12	D + I	0.1

3.2.2 Operational expenses (OpEx)

Operational expenses are mainly based on two categories: Direct OpEx and indirect OpEx. Direct operational expenses are calculated based on results from the process simulations (subsection 3.2.5). The cost of raw material and utilities are part of the direct OpEx. However, the cost related to maintenance, insurances, labor and taxes are part of indirect OpEx.

Commodity price index (CPI) is used to update older market price data. These indices are extracted from the World Bank Commodity Price Data (The Pink Sheet) [52] and the Rogers International Commodity Index [53].

$$\sum OPEX_{dir} \left(\frac{\text{€}/\$}{\text{year}} \right) = \sum_{i=1}^m \dot{m}_{r\&B_i} \cdot c_{R\&B_i} \cdot \left(\frac{CPI_i}{CPI_{ref,i}} \right) \quad (3.25)$$

$$+ \sum_{j=1}^n E_{power_j} \cdot c_{power_j} + \sum_{k=1}^p \text{heat}_k \cdot c_{heat_k}$$

Indirect OpEx are mainly based on maintenance, labor and administration costs. Since exact costs prediction is difficult, the typical estimations are used based on historical data from the chemical process industry [49], which are summarized in Table 3.4.

Table 3.4: Ratio factors for estimating indirect OPEX [49]

Investment items	j	Basis	Typical value
Operating supervision	1	OL	0.15
Maintenance and repairs	2	FCI	0.06
Operating supplies	3	M ^a	0.15
Laboratory charges	4	FCI	0.15
Taxes (property)	5	FCI	0.02
Royalties	6	NPC	0.01
Insurance	7	FCI	0.01
Plant overhead, general	8	TLC ^b	0.6
Administration	9	PO	0.2
Distribution & selling	10	NPC	0.05
Research & Development	11	NPC	0.04

^a M = Maintenance labor & maintenance material.

^b TLC = Total labor costs consisting of operating labor, supervision and maintenance labor

3.2.3 Profitability metrics

The aim of this section is to describe the profitability metrics when performing cumulative cash flow analysis. These economic investment indicators help to evaluate the feasibility and profitability of the plant design projects. Different types of metrics can be distinguished:

- Metrics regardless of time value of money
- Metrics considering time value of money
- Sensitivity and uncertainty analysis of metrics

Return on investment (ROI)

The return on investment is defined as the ratio between the annual net profit and the total capital investment. The units of ROI are a fraction of total capital investment recovered each year over the investment period (or project life time) [49].

$$ROI(\%/year) = \frac{\text{Annual net profit}}{\text{Total capital investment (TCI)}} \quad (3.26)$$

ROI is then compared with minimum acceptable rate of return (m_{ar}), corresponding to different risk category of project. These levels of risk are tabulated in Table G.1 [49]. This threshold is company specific and used to decide for go or no-go decision.

Payback period (PBP)

The payback period can be defined as the minimum time to recover fixed capital invested, therefore the time when the cumulative cash flow is equal to zero [49].

$$PBP(year) = \frac{\text{Fixed capital investment}}{\text{Annual cash flow}} \quad (3.27)$$

The annual cash flows is defined as the sum of the net profits and the depreciation.

Net present value (NPV)

The net present value, also known as net present worth (NPW), is the total of the present worth of all cash flows minus the present worth of all capital investments [49].

$$NPV = \sum_{j=1}^N PWF_{cf,j} [(s_j - c_{oj} - d_j)(1 - \phi) + d_j] - \sum_{j=-b}^N PWF_{v,j} TCI_j \quad (3.28)$$

Where $PWF_{cf,j}$ is the present worth factor for the cash flow in year j , s_j sales in year j , c_{oj} total production cost in year j , d_j depreciation in year j , ϕ is income tax rate, $PWF_{v,j}$ present worth factor for investment in year j , b indicates the construction time year (2 or 3 years before start-up) and TCI is total investment in year j . The key feature here is the discount rate, i , used for evaluating the present worth factors:

$$PWF_{cf,j} = (1 + i)^{-j}; \quad PWF_{v,j} = (1 + i)^{-j} \quad (3.29)$$

The appropriate discount rate i used for discrete compounding is equal to minimum acceptable rate of return, m_{ar} used by company standards. The NPV metric is an indicator of the profitability for a given discount rate. The higher the NPV, the more favourable the investment.

Discounted cash flow rate of return (DCFR)

The discounted cash flow rate of return is the return obtained from an investment in which all investments and cash flows are discounted [49]. The DCFR is calculated by iterating i_{dcfr} until satisfies the equability constraint for Equation 3.28 being zero.

Minimum selling price of product (MSEP)

The MSEP is defined as the minimum product price that ensures a minimum investment target based on the DCFR and the m_{ar} . It must be solved by iterating until the product price, p satisfies the equality constrain for NPV being zero for a given minimum acceptable rate of return.

$$0 = \sum_{j=1}^N (1 + m_{ar})^{-j} [(F_j p - c_{oj} - d_j)(1 - \phi) + d_j] - \sum_{j=-b}^N (1 + m_{ar})^{-j} TCI_j \quad (3.30)$$

This metric is useful to estimate the final product price that is given to clients.

3.2.4 Sensitivity analysis

Product price, raw materials and utility prices are subject to fluctuation due to market forces and socioeconomic aspects. Therefore, sensitivity analysis is considered a useful practice to study the impacts of possible market fluctuations on your project design plant. Moreover, it has been considered to perform sensitivity analysis to FCI, profits, income taxes, m_{ar} and other inputs that affects the profitability metrics.

The method used to perform sensitivity analysis is known as as one factor at a time (OFAT). It considers that the sensitivity of a model response ($y = f(x)$) to a factor x corresponds to the rate of change of the response in the direction of increasing values of the factor x [54]. This rate of change is known as the slope and defined as:

$$\text{Absolute sensitivity: } s_a = \frac{\partial y}{\partial x} \quad (3.31)$$

$$\text{Relative sensitivity: } s_r = \frac{\partial y}{\partial x} \frac{x^\circ}{y^\circ} \quad (3.32)$$

The absolute sensitivity means the effect on y by perturbing x around its nominal value (x°). The relative sensitivity is the relative effect of y by perturbing x with a fixed fraction of its nominal value (x°). The interpretation of both functions are simple since a zero value would mean that the input value does not affect the output value.

Depending on the direction of perturbation, the sensitivity analysis can be approximated using:

$$\text{Forward perturbation: } \frac{\partial y}{\partial x} = \frac{f(x^\circ + \Delta x) - f(x^\circ)}{\Delta x} \quad (3.33)$$

$$\text{Backward perturbation: } \frac{\partial y}{\partial x} = \frac{f(x^\circ) - f(x^\circ - \Delta x)}{\Delta x} \quad (3.34)$$

$$\text{Central difference: } \frac{\partial y}{\partial x} = \frac{f(x^\circ + \Delta x) - f(x^\circ - \Delta x)}{2\Delta x} \quad (3.35)$$

3.2.5 Assumptions

The techno-economic analysis is performed for the current year 2022 and the currency used to express the results is the euro (€). The expected lifetime of the plant is assumed to be 15 years with a full load operating time of 8000 hours per year. These plants are assumed to be located in southern Spain, in the region of Andalusia.

The cost information about raw materials and utilities are shown in Table 3.5. All the market prices are updated to 2022. Due to the impossibility of obtaining market figures for nitric acid prices, the economic analysis is done based on the minimum selling price of nitric acid that meets a m_{ar} of 10 % (Equation 3.30).

The cash flow analysis is performed assuming a three years construction period in which 15% , 35% and 50% of the FCI is invested in the first, second and third year of the construction period respectively. The three years of the construction period are denoted as negative years in the cash flow analysis (see Appendix E).

Regarding the start-up cost, it is assumed a cost of 10 % of FCI in the first year and two-year ramp up to reach full capacity with 50 % production in the first year and 90%

production in the second year. Spain has an income tax rate around the 25% for large companies [55]. Depreciation is considered for the whole plant life time. The methodology chosen to calculate the annual depreciation is the accelerated cost recovery system (MACRS). Figure G.3 shows the depreciation rate percentage used considering a recovery period of 15 years [48]. On the other hand, land costs and inflation related to the cost of construction, the price of the product and the TPC are not considered in the cash flow analysis.

Table 3.5: Market prices for raw materials and utilities

	Market price (2022)	Units	Reference
<i>Raw materials and utilities</i>			
Ammonia	835.65	€/t	[12]
Pt-Rh Catalyst	544.12	€/g	[56]
Green ammonia (from electrolysis)	1160.00	€/t	[57]
Compressed air	0.05	€/m ³	[48]
Electricity (from grid)	0.13	€/kWh	[58]
Electricity (from CSP)	0.19	€/kWh	[59]
Cooling water	0.35	€/m ³	[49]
Process water	6.00	€/m ³	[60]
Medium pressure steam	16.66	€/kg	[48]

Three different types of nitric acid plants are considered in the economic evaluation. The first study is carried out on a conventional nitric acid plant (CON-NA), i.e Fossil-based ammonia price and electricity. The second nitric acid plant studied is considering solar-based ammonia. Therefore, hydrogen consumed in ammonia production comes from water electrolysis powered by solar energy and the remaining energy required in the ostwald process is assumed to be obtained from concentrated solar power technology. The last case evaluated is the optimised nitric acid plant (OXY-SOL-NA). It integrates the surplus oxygen from water electrolysis in the SOL-NA plant.

4 Results and discussion

This chapter contains the presentation and discussion of the results from the simulation in Aspen Plus and from the economic analysis. In addition, the discussion of the sensitivity analysis carried out on the two main cores of the project is presented.

4.1 Process simulation

The Aspen process flowsheet with the operating conditions (temperature and pressure) during the whole plant is shown in Figure 4.1. Liquid ammonia is first vaporized in E-101 and overheated in E-102 at 150 °C before being mixed with the air stream. Filtered atmospheric air passes through a three-stages compressor train (C-101) to remove air moisture and achieve the design pressure of 5.8 bar. This air-stream is splitted into two streams: a primary stream goes to the ammonia-air mixer and a secondary stream goes to the bleaching column (T-102). Ammonia-air mixture is preheated at 200 °C before the catalytic combustion chamber (R-101). Ammonia and air are combusted while crossing through a Pt-Rh catalytic gauze. The catalytic combustion of ammonia generates a gas stream composed of nitrogen oxides, nitrogen and oxygen.

The heat released by the series of exothermic reactions (Equation 2.7-2.10) is recovered in a series of heat exchangers called heat-recovery unit (Figure 4.2). During these heat recovery steps, nitric oxide is first oxidized to nitric dioxide (2.11) and secondly dimerised to form dinitrogen tetroxide (Equation 2.12). Then, this gas stream is partially condensed in a cooler-condenser (E-108) by cooling-water. A high quantity of weak nitric acid is formed at the bottom and sent to the lower-middle part of the absorption column (T-101). On the contrary, the remain gas stream is mixed with the air leaving the bleaching column (T-102) and sent to the bottom of the absorption column. Then, NO_x gas stream is put in counter-current contact with process water that enters at top of the column. This absorption process leads to obtain the require nitric acid strength at the bottom. Finally, this yellow acid liquid goes to the bleaching column to be bleached with secondary air.

The NO_x gases leaving at the top of the absorption column are sent to a series of gas-gas heat exchangers. After that, they are treated in a removal NO_x section before being vented at a concentration lower than 50 ppmv. As a result, 199.5 tons per day of ammonia, 3915.5 tons per day of air and 243.6 tons per day of process water are needed to produce 700 tons of nitric acid per day. The results of the mass and energy balances for every stream are shown in Table D.1 and D.2.

Catalytic oxidation of ammonia

The specification inputs in Aspen plus to model the combustion chamber is shown in Table 4.1. The catalytic combustion of ammonia is composed by a series of exothermic reactions. Therefore, the simulation results show that 63058.7 kW are liberated during this process. This energy will be later recovered by a series of heat exchangers.

One of the main important economic and design aspects of this unit is the loading amount of catalyst required. The amount of Pt-Rh catalyst needed and consumed during this process can only be obtained rigorously by performing a computational fluid dynamic simulation.

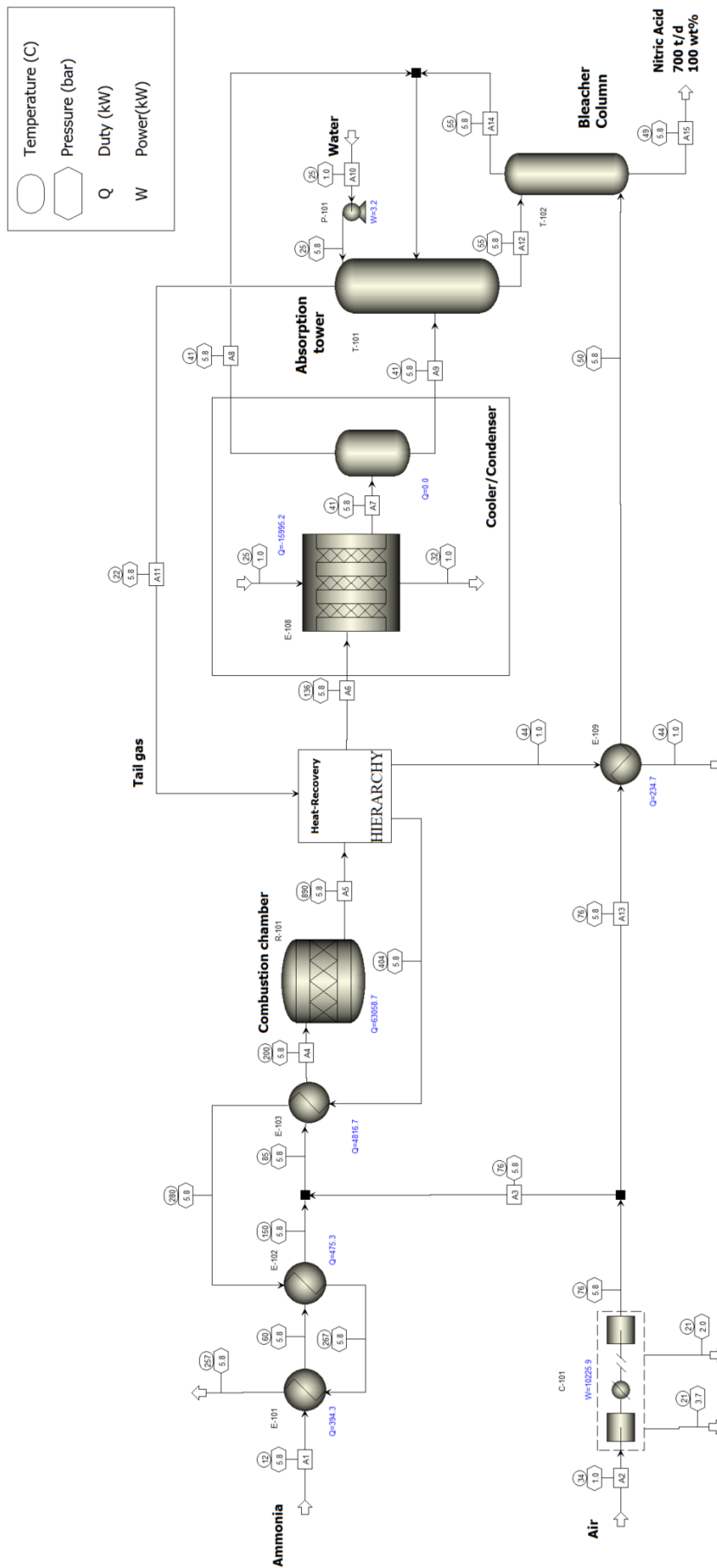


Figure 4.1: Conventional nitric acid plant flowsheet in Aspen Plus[®].

As it is out of the scope of this work, the consumption of catalyst is taken from literature (0.11 g/ton HNO_3) [61]. Assuming that the plant is running 8000 hours per year, 25.67 kg of catalyst would be lost every year. In Appendix F, all the design specifications are calculated based on the volumetric flowrates from the simulation. The amount of catalyst calculated is around 20.32 kg which is lower than the annual consumption of 25.67 kg. It clearly indicates that might be some features that are not being considered. According to literature, 52 kg of Pt-Rh catalyst are used to produce 450 t/d of nitric acid [62]. This number is finally used for the economical calculations.

Table 4.1: Ammonia combustion chamber specifications (R-101)

Operating parameters	Value	Ammonia Conversion ratio (%)	
Reactor type	RStoic	Equation 2.7	96
Reaction set	Model 1	Equation 2.9	4
Pressure drop (bar)	0		
Temperature ($^{\circ}\text{C}$)	890		

Nitrogen oxides oxidation

In the Aspen plus flowsheet (Figure 4.1) can be noticed the use of a hierarchy block . This functionality in Aspen plus allows to create a new flowsheet inside of the block. In this case, it has been used to simulate the heat recovery unit. This unit is composed of four reactive heat exchangers modelled as plug flow reactors and two pipes modelled as adiabatic reactors. More information about this decision is properly given in Appendix A.

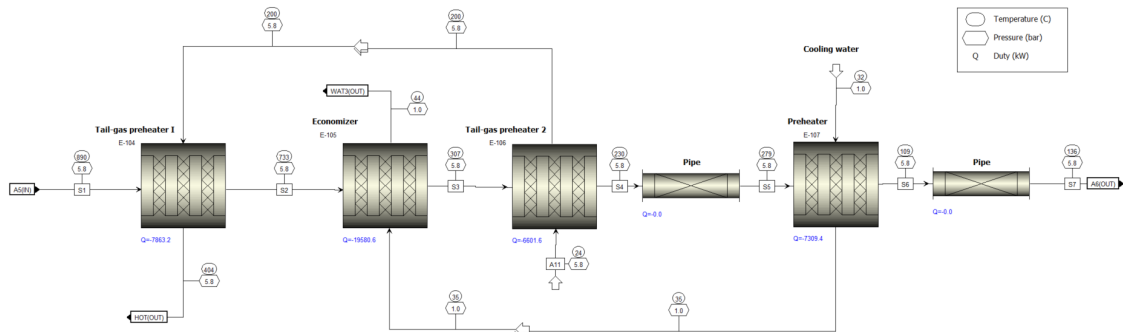


Figure 4.2: **Heat-recovery unit:** series of heat exchangers.

Figure 4.2 shows how the heat released from the catalytic combustion of ammonia (stream 5 at 890°C) is recovered by this heat-exchanger train (stream A6 at 136°C). The tail-gas leaving the absorption column (A11) is used as thermal fluid in unit E-104 and E-106. On the other hand, cooling water is used as thermal fluid in unit E-105, E-107 and E-108. The equipment specifications of this hierarchy block is described in Table 4.2.

Figure 4.3b shows the nitric oxide conversion along the heat-exchanger train. It can be noticed the effect of temperature on the oxidation of nitric oxide (Equation 3.2). In fact, above 250°C this reaction slightly favors the production of nitrogen dioxide. Two pipes are simulated as adiabatic reactors since reactions take place during the whole line. One

pipe is located between the E-106 and E-107 and the other between E-107 and E-108. Both pipes have an outlet temperature higher than the initial temperature due to equations 3.2, 3.3 & 3.4 are exothermic.

Table 4.2: Reactive heat exchangers specifications

Identification code	E-104	E-105	E-106	E-107	E-108
Operating parameters	Values				
Reactor type	RPlug (Reactor with counter-current thermal fluid)				
Reaction set	Model 2				
Heat transfer coefficient (kcal/h m ² C)	1100.6	175.69	162.89	200.7	1049.01
Thermal fluid outlet temperature (°C)	404	43.74	200	35.31	32.16
Number of tubes	-	643	1527	1527	1200
Length of tubes (m)	3.15	4.2	3	3	5.62
Diameter of tubes (m)	1.22	0.025	0.015	0.015	0.014

The goal of the cooler/condenser is to decrease the temperature in favour of the production of nitric acid. Figure 4.3b shows the profile of the liquid nitric acid composition along the cooler/condenser. A weak nitric acid concentration of 42 wt% is achieved downstream the unit E-108.

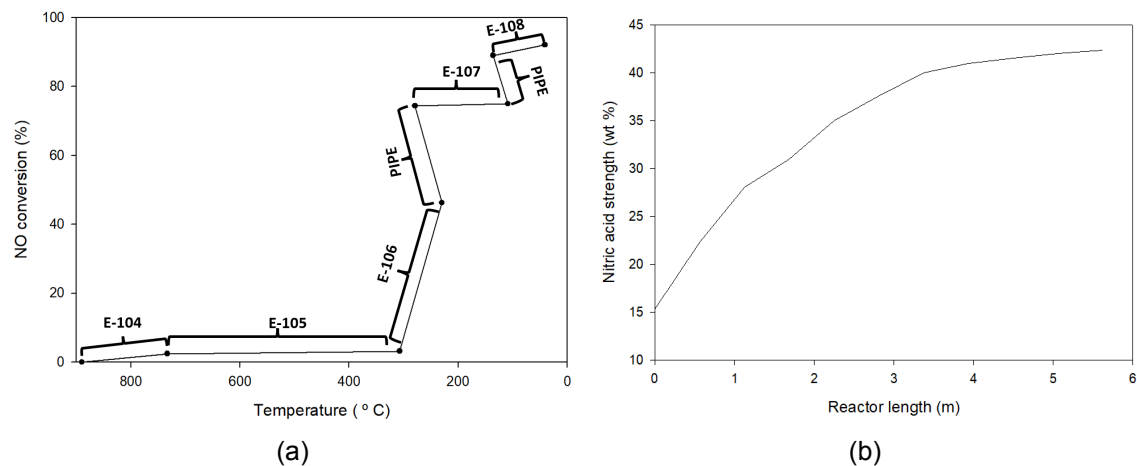


Figure 4.3: a) NO conversion along heat exchangers. b) Acid strength profile along the condenser.

Nitrogen oxides absorption

A special attention has been dedicated to simulate this complex NO_x absorption in aqueous solution. The design specifications for the absorption tower and the bleaching column are tabulated in Table 4.3. Both columns stages are numbered from top to bottom (tray 1: top plate; tray 35: bottom plate). To obtain a nitric acid strength of 60 wt%, 236.5 t/d of process water are put in counter-current with the NO_x gases leaving the bleaching column and the condenser. Cooling water is used to cool down every stage. The idea is to maintain the temperature profile in favour of the gases absorption.

In Figure 4.4a can be seen how the formation of nitric acid is increasing from top to bottom. At the top of the column, the acid formation is almost negligible due to small contact time between NO_x gases and the process water. The closer you get to the bottom of

the column, the higher the liquid holdup is. Therefore, the gas-liquid contact is superior leading to a higher acid production.

Table 4.3: Absorption and bleacher column specifications

Identification code	T-101	T-102
Operating parameters	Value	Value
Column type	RadFrac	RadFrac
Reaction set	Model 3	Model 3
Calculation type	Equilibrium	Equilibrium
Condenser	Partial	None
Reboiler	None	None
Convergence mode	Strongly non-ideal liquid	Strongly non-ideal liquid
Number of plates	35 (Sieve trays)	8 (Sieve trays)
Column diameter (m)	5.5	3.37
Holes diameter (m)	0.1	0.1
Pressure (bar)	5.8	5.8
Feed streams	A9 (plate 28), A10 (plate 1) & A14+A15 (plate 35)	A12 (plate 1) & A13 (plate 1)
Outlet streams	A11 (plate 1) & A12 (plate 35)	A14 (plate 1) & A15 (plate 8)
Bottom temperature (°C)	55	Not defined
Top temperature (°C)	22	Not defined

The profile of the nitric acid mass composition in the absorption column is shown in Figure 4.4b. The nitric acid strength increases similarly to the acid production over the absorption tower.

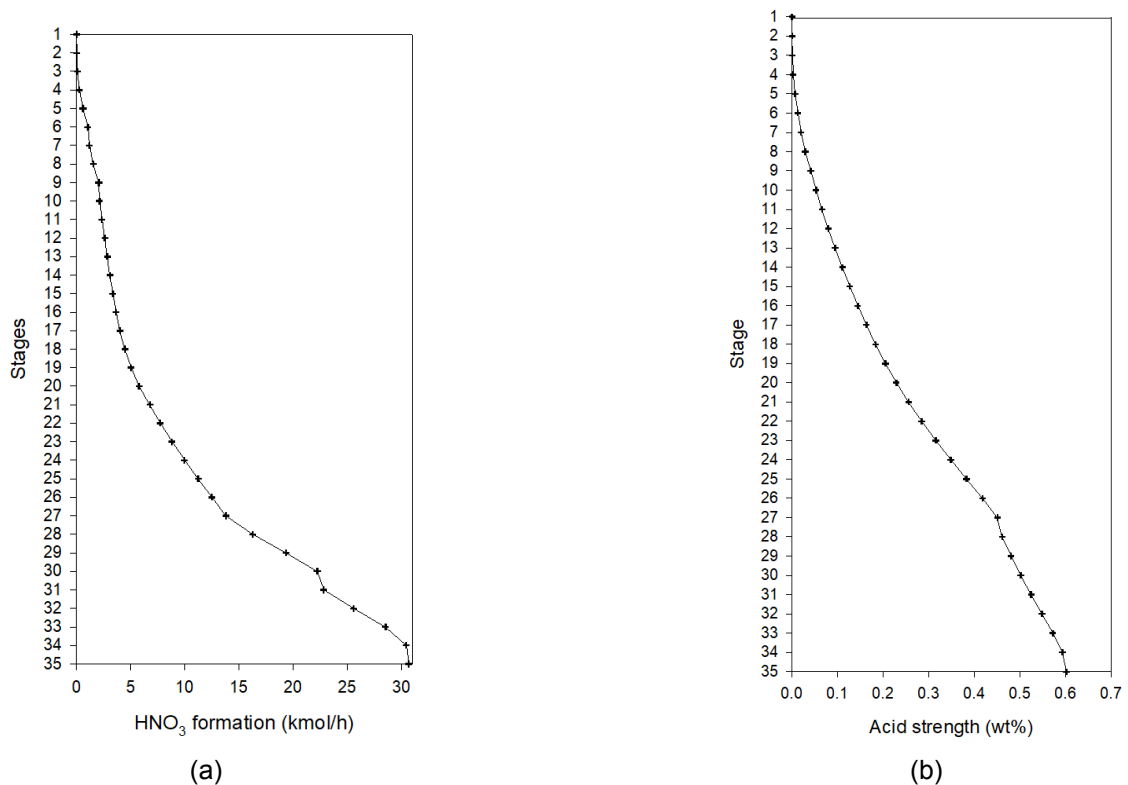


Figure 4.4: Profiles along the absorption tower. a) HNO₃ formation. b) acid strength.

Figure 4.4b shows the point in which the weak nitric acid stream from the condenser is fed into stage 28. In fact, the optimum feed stage for stream A9 is found looking at the behaviour of the absorption over the stages. Stream A9 is fed into stage 28 since it has a nitric acid composition of 42 wt% which is closely to the nitric acid strength in that stage.

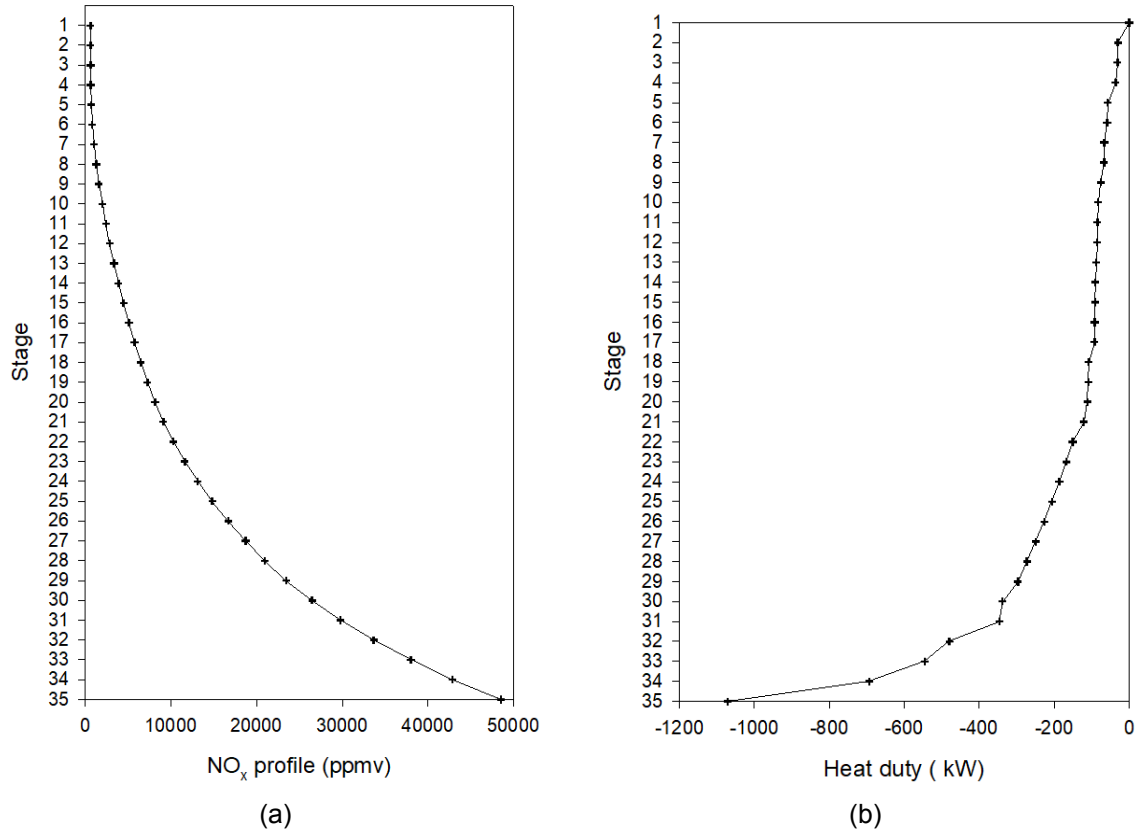


Figure 4.5: Profiles along the absorption tower. a) NO_x concentration. b) Heat duty.

The control of the NO_x emissions in a nitric acid plant is extremely important. Figure 4.5a shows the profile of the nitric oxides gases along the absorption column. The concentration is exponentially decreasing from bottom to top as the gas stream is reacting and being absorbed by the liquid phase along the column. The remaining gases leave the column at a NO_x concentration of 622 ppmv. They need to be further treated before being released to the atmosphere. According to the Industrial Emissions Directive 2010/75/EU of the European Commission, NO_x emissions levels in existing nitric acid plants must not contain a higher NO_x concentration of 150 ppmv [63].

4.1.1 Sensitivity analysis

The sensitivity analysis is focused on the absorption tower since it plays the most crucial role in nitric acid production. The idea of this analysis is to investigate the responsiveness of the column to certain design specifications. The column diameter, the plate type and the slot/hole of the trays are subject of study. The discussion is based on three important metrics: Nitric acid production, NO_x concentration and final nitric acid strength.

Figure 4.6a shows that as the diameter of the column increases, the production of nitric acid increases independently the type of plate used. It can also be noticed that sieve

trays lead to a higher production. For the same diameter, sieve trays are able to daily produce up to 0.72 % (3 t/d) more nitric acid per day compared to bubble cap trays. Additionally, the production of nitric acid is not favoured as the bubble cap slot or the sieve hole submergence increases.

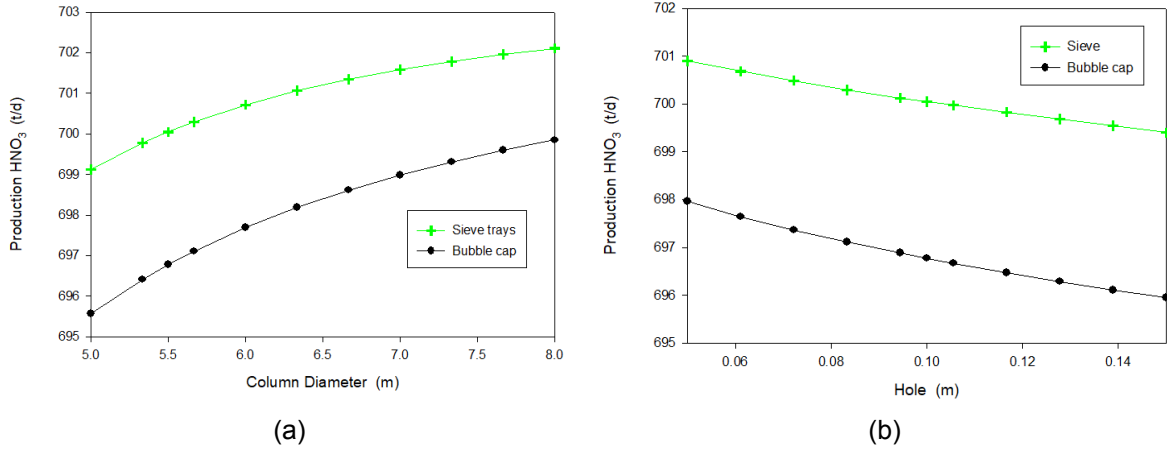


Figure 4.6: Effect on the production of nitric acid. a) Column diameter. b) Bubble cap slot/sieve hole submerge.

A similar behaviour is found in this case for the nitric acid mass composition (Figure 4.7a & 4.7b). The nitric acid strength increases as the column diameter is decreased and the bubble cap slot or sieve hole submerge is decreased. The differences between using a sieve or a bubble cap tray are almost the same as discussed for the effect on the production.

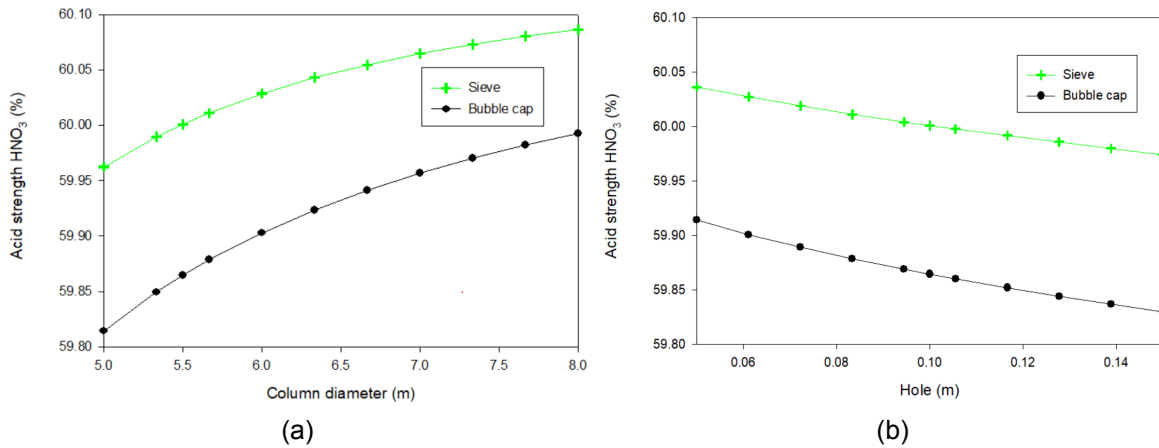


Figure 4.7: Effect on the acid strength. a) Column diameter. b) Bubble cap slot/sieve hole submerge.

Figure 4.8a shows that as the diameter increases there is a significant reduction of the NO_x concentration at top of the absorption column. Even if in this case the effect on the gas concentration between the sieve and the bubble tray is lower (around 9.6%) compared to effect on production, it is still noticeable. According to Figure 4.8b, a smaller bubble/sieve hole favours the reduction of nitrogen oxides.

Miller highlighted that bubble cap trays were less effective due to the less uniform gas-liquid distribution compared to sieve trays. Moreover, he mentioned that this effect is really significant on the final nitrogen oxides concentration at the top of the column [40].

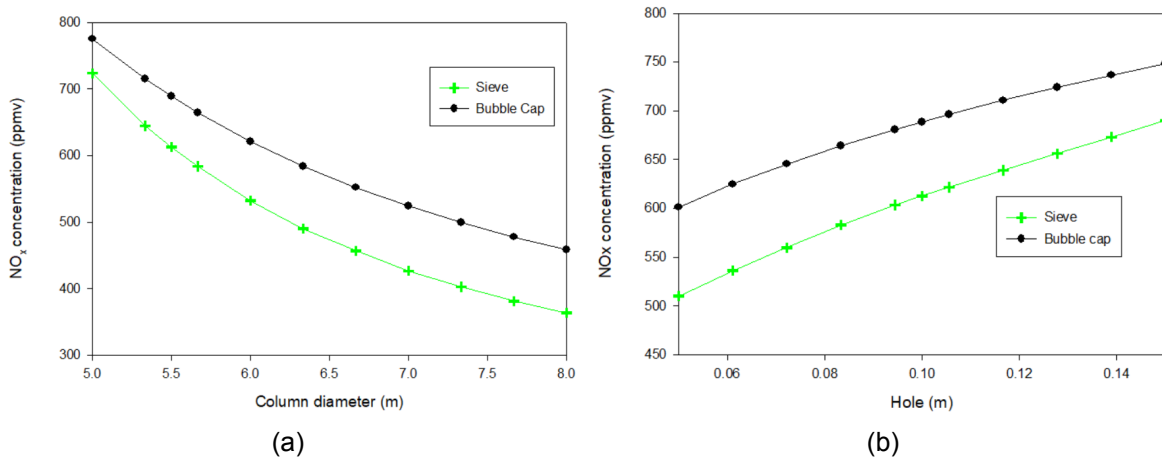


Figure 4.8: Effect on the NO_x composition. a) Column diameter. b) Bubble cap slot/ sieve hole submerge.

In fact, sieve trays are currently used over bubble cap trays. Bubble cap trays were replaced by sieve trays due to the superior performance and lower capital cost [64]. Thus, these results are in agreement with literature. Sieve trays show a better mass transfer performance than bubble caps for the evaluated metrics.

4.1.2 Pinch analysis

In this section, the pinch analysis is performed to find the pinch temperature and the minimum hot and cold utilities required to cover the energy plant demand.

The temperatures and heat duties for all plant streams are classified and summarised in Table 4.4. The hot streams are marked in red and the cold ones in blue. These streams are classified in intervals and the required and cumulative heat is calculated for a minimum temperature difference of 10 K (See Appendix E). With the information presented in Table E.1, the composite curves graph can be plotted by representing the cumulative heat in the abscissa axis and the hot scale temperature in the ordinate axis.

Table 4.4: Summary of stream temperatures and heat duties

Stream label	T_{in} [°C]	T_{out} [°C]	FC_p [kW/K]	Q [kW]
A1	12	60	13.61	653.52
A1A	60	150	5.16	464.63
A1B	85	200	41.50	4772.54
A6	133	42	41.98	16764.80
A13A	76	50	9.08	234.77
S1	890	734	49.43	7828.10
S2	733	310	48.08	19522.66
S3	310	230	43.75	7206.09
S5	279	110	43.31	7321.65

Figure 4.9 shows how the hot and cold composite curves intersect, violating the condition of minimum temperature difference. In order to calculate the pinch analysis and the minimum hot and cold utilities, the cold composite curve must be shifted until a minimum distance of 10 K between the two curves is met.

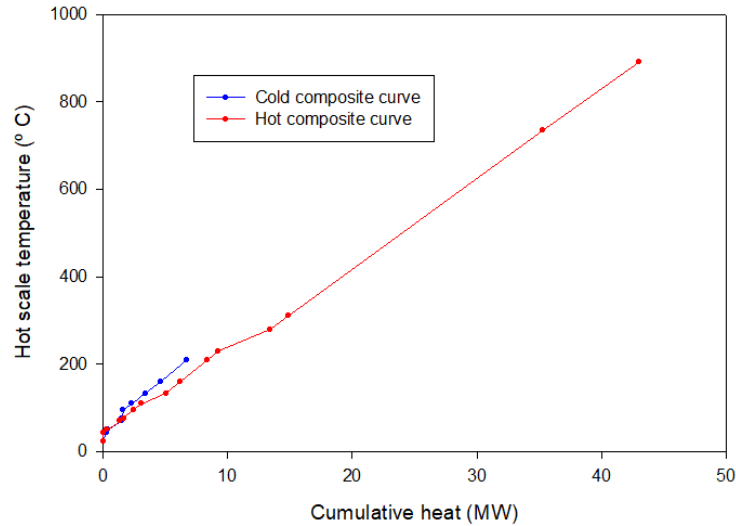


Figure 4.9: Composite curves for the hot scale temperature

The cold composite curve is shifted by 2.1 MW as it is shown in Figure 4.10. It is found that the pinch temperature is 220 °C for the hot scale and 210 °C for the cold scale. The minimum hot and cold utility required is -34.14 MW and 2.1 MW respectively.

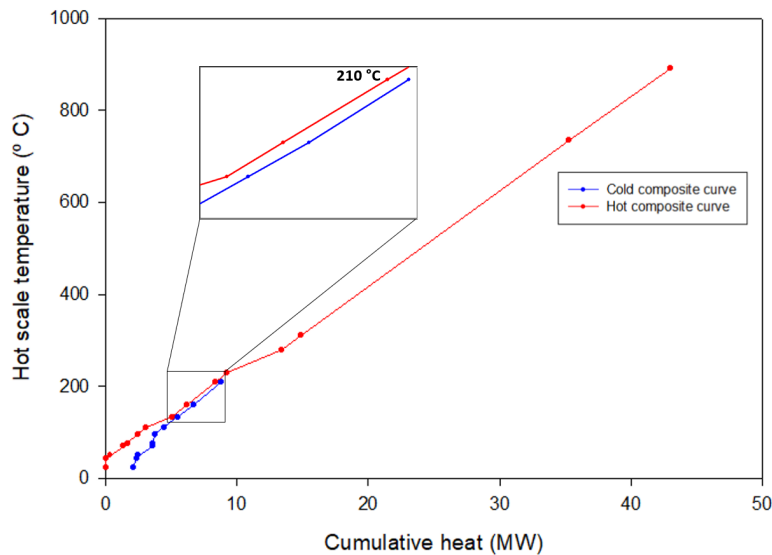


Figure 4.10: Shifted composite curves

The performed pinch analysis could be used as a basis for a detailed heat exchanger network synthesis (HENS), but this is out of scope of this thesis. Nevertheless, the heat integration between streams has been performed following the flowsheet proposed in *Ullmann's Encyclopedia of Industrial Chemistry* (Figure 2.5) [6]. Therefore, the outlet NO_x gases from stream A11 have been used as thermal fluid for the two tail-gas preheaters

(E-104 & E-106). On the other hand, cooling water is used as thermal fluid for equipment E-105, E-107, E-108 and E-109.

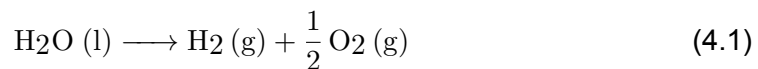
4.1.3 Optimised nitric acid plant through oxygen injections

In this section, it is intended to show the discussion of the results for the four different study cases:

1. **Case A:** Pure oxygen is uniquely injected upstream of the bleaching column, T-102 (Figure B.1b).
2. **Case B:** Pure oxygen is uniquely injected upstream of the cooler/condenser, E-108 (Figure B.1c).
3. **Case C:** Pure oxygen is uniquely injected upstream of the absorption tower, T-101 (Figure B.1d).
4. **Case D:** Pure oxygen is uniquely injected into the primary feed air (Figure B.1e).

The cases are compared based on three metrics: the strength of the final nitric acid, the acid production and the concentration of the leaving NO_x gases.

The amount of surplus oxygen available from electrolysis is calculated according to the amount of ammonia needed to produce the 700 daily tons of nitric acid. Theoretically, 3 moles of hydrogen and 1 mole of nitrogen are required to produce 2 moles of ammonia (Equation 2.6). Therefore, 177 kg of H_2 and 823 kg of N_2 are necessary to produce 1 ton of NH_3 . Since 199.5 daily tons of ammonia are needed to produce 700 tons of nitric acid, 35.31 daily tons of hydrogen are consumed.



Applying Equation 4.1, the surplus oxygen available is of 368 kmol per hour. The idea of this investigation is to find the best location for these injections and the influence of the amount of oxygen injected on the three metrics described before.

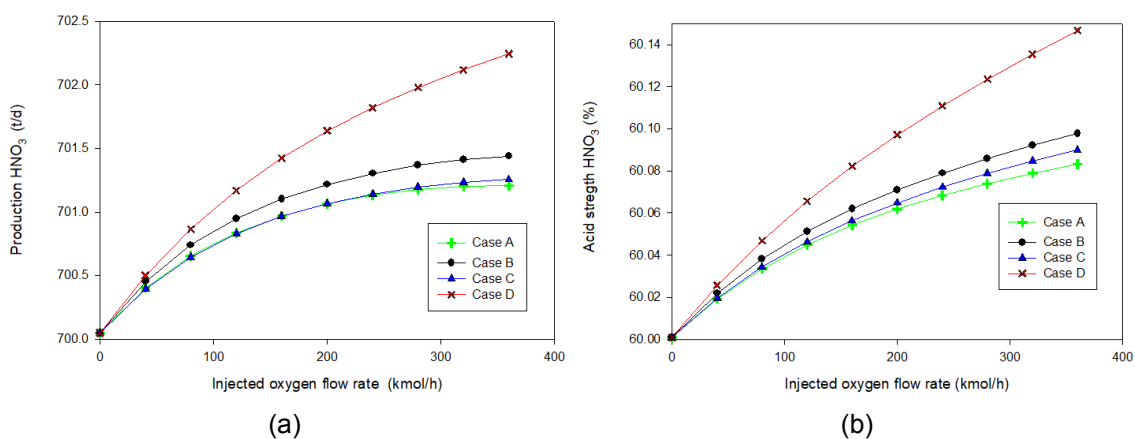


Figure 4.11: Effect of pure-oxygen injections. a) Nitric acid production. b) Nitric acid strength

Figure 4.11a shows that oxygen injection can boost the nitric acid production up to 2.2 daily tons. Comparing the different cases, increasing the oxygen content in the main air

pipeline (stream A2) leads to the higher nitric acid production and strength. The next highest production is obtained if oxygen injection occurs downstream the cooler/condenser. Finally, Case A and C show less promising results in terms of boosting the nitric acid production.

The nitric acid strength increases slightly as oxygen is injected (see Figure 4.11b). Up to a maximum increment of 0.14 wt% can be obtained for case D. Analogue to Figure 4.11b, it shows that there is a greater increase as soon as oxygen is injected into the plant, i.e. upstream the combustion chamber.

Injecting oxygen downstream the combustion chamber will maximise the residence time of oxygen and will favor the conversion of nitric oxide to nitrogen dioxide. A higher amount of nitrogen dioxide will be available for the absorption with water, resulting in a greater production of nitric acid. Nevertheless, there are other factors that play a crucial role such as catalyst losses and the flammability of ammonia in air. Increasing the residence time of oxygen in the burner will result in a higher catalyst loss due to rhodium and platinum react more easily to produce the corresponding oxides [14].

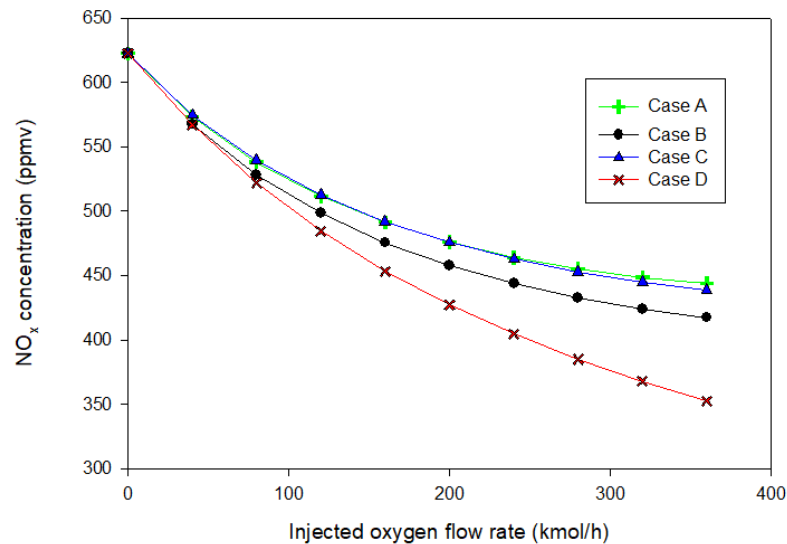


Figure 4.12: Effect of O₂ injection on the NO_x concentration leaving the absorption tower.

For safety reason, the ammonia concentration must be low to avoid the lower explosion limit of 13 vol% NH₃/air for medium-pressure systems [6]. The explosion limit also depends on the oxygen concentration, temperature, pressure, the flow velocity and the water content of the reaction mixture. For these reasons, case D may be undesirable due to increased loss of catalyst and safety concerns associated with ammonia combustion.

In Figure 4.12 shows how increasing the oxygen content in the conventional nitric acid plant will lead to a considerable decrease of the NO_x concentration in the tail-gas. A NO_x reduction of 28.66 %, 32.96 %, 29.56% and 43.6 % for case A, B, C and D respectively.

In conventional nitric acid plants primary air and the bleaching air are taken from the same compressor. Increasing oxygen content in the primary air stream reduces the load on the compressor and hence the power required. Figure 4.13b shows how the power required can be reduced up to 7 % by increasing the oxygen content in the primary air (Stream A2). Likewise, the cooling heat duty during compression stages decreases as oxygen content is increased, as it is shown in Figure 4.13a.

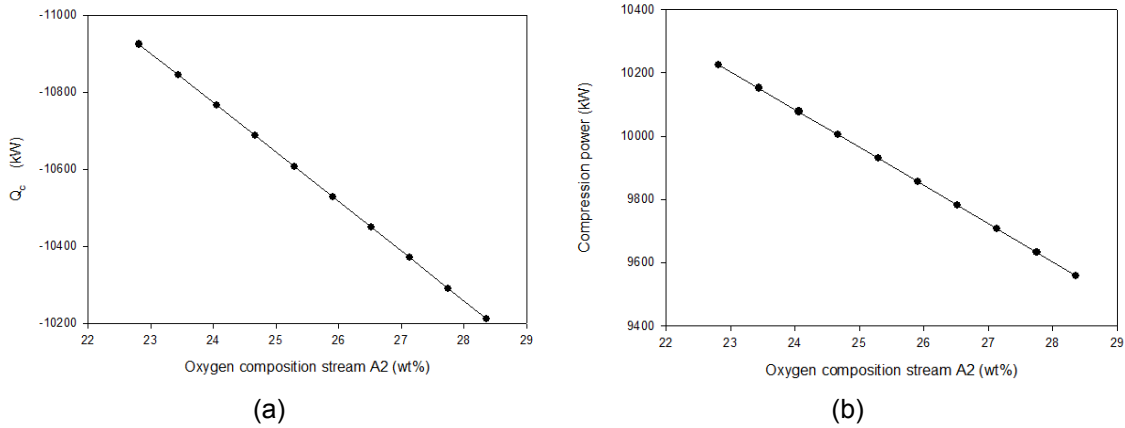


Figure 4.13: Compressor characteristic (C-101) for case D. a) Total heat duty stage/coolers. b) Compression power.

Table 4.5 shows the summary of the maximum percentage increase for all the cases evaluated. According to the results, the concentration of nitrogen oxides could be reduced by up to 43%. Therefore, the cleaning unit of the gas could be drastically reduced. Unfortunately, the simulation of this cleaning gas unit is out of the scope of the thesis which explains why no reference has been given to this reduction in economic and environmental terms.

Table 4.5: Summary of the maximum percentage increase for the four cases.

Case	Production (%)	Strength (%)	NO _x concentration (%)
A	0.17	0.14	-28.68
B	0.20	0.16	-32.96
C	0.17	0.15	-29.56
D	0.31	0.24	-43.6

The trends in the results are in line with the patents discussed in subsection 2.2.4. It can be concluded that injecting O₂ into conventional nitric acid plants can boost nitric acid production, reduce the final nitrogen oxides concentration in the tail-gas and increase the acid strength.

4.2 Economic analysis

The goal of this section is the discussion of the economic results for the three different types of nitric acid plants evaluated:

1. **Conventional nitric acid plant (CON-NA):** Considering ammonia and electricity prices of fossil-based production
2. **Solar-based nitric acid plant (SOL-NA):** Considering ammonia and electricity prices of solar-based production
3. **Optimised solar-based nitric acid plant (OXY-SOL-NA):** Integrating the surplus oxygen from water electrolysis in the SOL-NA plant.

The equipment costs for all the investigated scenarios are summarized in Table 4.6. The total equipments cost ascend to the sum of 20.33 M€ for CONV-NA and SOL-NA and 20.22M€ for OXY-SOL-NA. This 0.1 m€ saved is due to the lowest capacity of the compressor required for the last plant. In Figure G.7, it is shown how the 60 % of the total equipment costs correspond to the compressor cost. For that reason, FCI costs are 0.6% lower for the OXY-SOL-NA plant.

Table 4.6: Equipment costs results for the investigated plants

Equipment	Code	S _{ref}	Unit	EC ¹ ₂₀₂₂ (M€)	EC ² ₂₀₂₂ (M€)	Source
Ammonia evaporator	E-101	2.03	m ² (exchange area)	0.01	0.01	[48]
Ammonia preheater	E-102	3.38	m ² (exchange area)	0.01	0.01	[48]
Ammonia-air preheater	E-103	28.44	m ² (exchange area)	0.01	0.01	[48]
Tail-gas preheater I	E-104	12.07	m ² (exchange area)	0.01	0.01	[48]
Economizer	E-105	212.10	m ² (exchange area)	0.06	0.06	[48]
Tail-gas preheater II	E-106	215.87	m ² (exchange area)	0.06	0.06	[48]
Feedwater preheater	E-107	215.87	m ² (exchange area)	0.06	0.06	[48]
Cooler-Condenser	E-108	295.00	m ² (exchange area)	0.08	0.08	[48]
Bleacher preheater	E-109	17.49	m ² (exchange area)	0.01	0.01	[48]
Air compressor	C-101	10.23	MW (power consumption)	12.08	11.96	[48]
Combustion Chamber	R-101	12.50	m ³ (reactor volume)	0.17	0.17	[65]
Absorption Column	T-101	1021.14	m ³ (column volume)	6.55	6.55	[48]
Bleaching Column	T-102	178.48	m ³ (column volume)	1.23	1.23	[48]
Feedwater pump	P-101	3.20	kW (power consumption)	0.01	0.01	[48]
				TOTAL: 20.33 M€	TOTAL: 20.23 M€	

¹ CONV-NA & SOL-NA; ² OXY-SOL-NA

The results of the main economic metrics are tabulated in Table 4.7. CONV-NA and SOL-NA plants have a lower capacity compared to OXY-SOL-NA plant. In fact, in subsection 4.1.3 highlighted how oxygen-enriched air can increase nitric acid annual production by 0.55 %.

The capital expenses (CapEx) are practically the same for all the plants. Nevertheless, the operational expenses (OpEx) of the conventional plant are 17% lower compared to SOL-NA and OXY-SOL-NA plants. It is due to the ammonia price which is the main cost driver of the raw materials (Figure G.8). In fact, the cost of green ammonia is 38.81 % higher than the conventional ammonia (Table 3.5). And the cost of the raw materials constitute the 61-63% of the total OpExs, which fully explains the difference in operating costs between the plants (Figures G.11, G.11 & G.13).

Table 4.7: Summary economic results for the investigated plants.

Type of plant	CONV-NA	SOL-NA	OXY-SOL-NA
Plant capacity (10^3 t/y)	388.89	388.89	391.04
FCI (M€)	97.95	97.95	97.37
WC (M€)	19.90	19.90	19.78
CapEx (M€)	117.85	117.85	117.15
Direct OpEx (M€/y)	98.44	120.46	120.22
Indirect OpEx (M€/y)	20.73	22.94	22.85
OpEx (M€/y)	119.16	143.40	143.07

The cash flow analysis has been performed considering the minimum selling price (MSEP) of nitric acid that meets an annual ROI of the 10 %. The MSEP is calculated according to Equation 3.30 . This profitability metric for SOL-NA and OXY-SOL-NA plants is 13.9% and 14.5% respectively higher than the conventional plant (Table 4.8). Regardless of environmental considerations, a difference close to 15% of the final product plays a crucial role in deciding which supplier to choose.

Table 4.8: Feasibility metrics to ensure a $m_{ar} = 10$ %

Type of plant	CONV-NA	SOL-NA	OXY-SOL-NA
MSEP (€/t)	369.97	432.52	429.56
ROI (%/y)	10	10	10
PBP (y)	5.44	5.45	5.44
NPV (M€)	0.76	0.24	0.24
DCFR (%/y)	10.08	10.03	10.03

As the ROI is fixed to a 10 %, the payback period remains practically unchanged for all the plants. A higher NPV and DCFR is obtained for the conventional plant due to the lower operating annual expenses.

4.2.1 Sensitivity analysis

The sensitivity analysis has been performed for the three types of plant. Nonetheless, due to the difference between the results of the sensitivity analysis is practically identical to all the plants, it is decided to discuss the results for the OXY-SOL-NA plant. The sensitivity results for the CONV-NA and SOL-NA plants are shown in Appendix G.

The most sensitive cost drivers have been identified through the information provided by the pie charts in Appendix G. Figure G.8 shows that the cost of ammonia accounts for 80-85 % of the total cost of raw materials and the remaining percentage corresponds to catalyst cost. Regarding utility costs, cooling water constitutes 51% of the total (Figure G.9). Based on the above arguments, it is decided to vary the costs of ammonia, catalyst and cooling water within a range between -80% and +80% in order to observe the impact on the MSEP of nitric acid. In fact, the ammonia price from 2008 to 2021 has increased by 355 % as shown in the Figure G.10 [12].

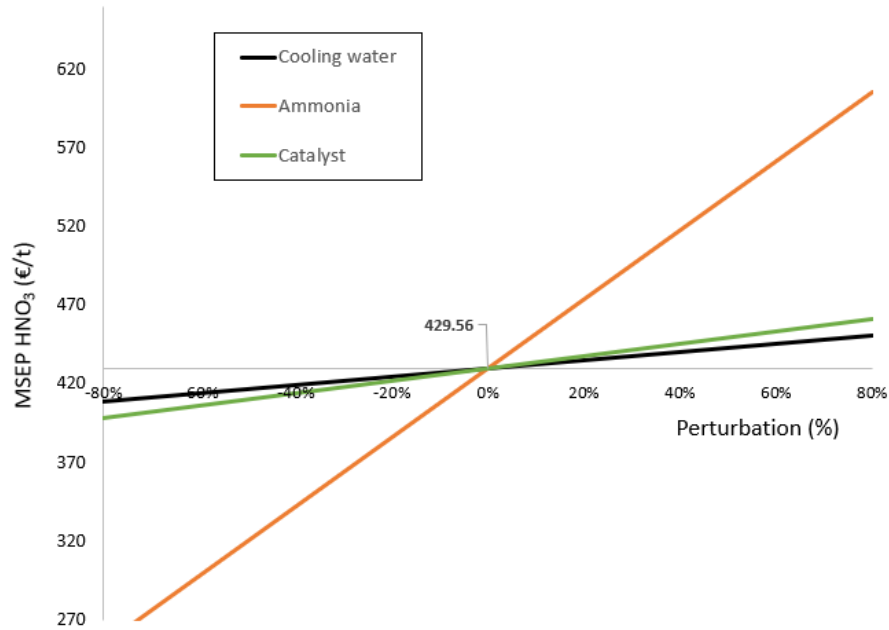


Figure 4.14: Sensitivity analysis on the three main cost drivers for the OXY-SOL-NA.

The sensitivity results of Figure 4.14 are aligned with the arguments described above. The slopes of the straight lines indicates the impact degree on the minimum selling price of nitric acid. It can be noticed that the ammonia cost is the most sensitive parameter for the MSEP of nitric acid. The price of nitric acid could be reduced by up to 41.86% if the cost of ammonia were reduced by 80%.

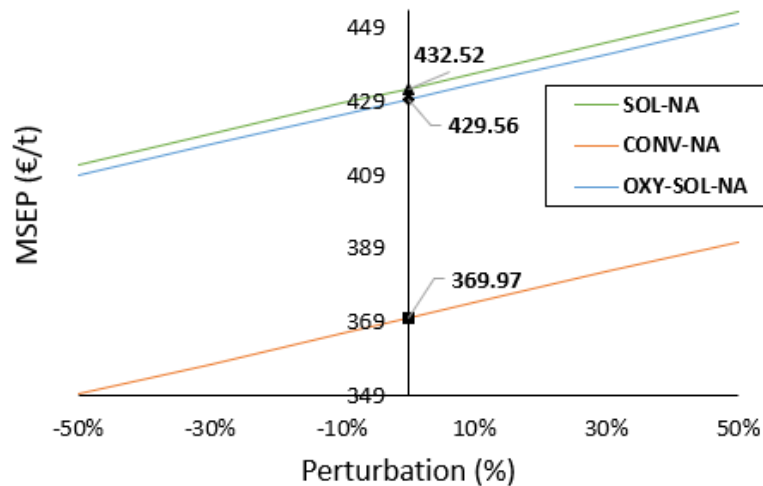


Figure 4.15: Response of the MSEP of nitric acid to changes in the m_{ar}

The minimum selling price of nitric acid has been evaluated in terms of the minimum return of investment. For this purpose, the minimum return of investment (m_{ar}) has been varied between a range of -50% and 50%. Figure 4.15 shows that the slope of the straight lines for the three types of plants is exactly the same. It means that the response of the MSEP to a change in the m_{ar} proceeds in the same way. The MSEP of nitric acid could increase or decrease by up to $\pm 5.7\%$ for a $\pm 50\%$ change in the m_{ar} .

In contrast, the sensitivity analysis is performed for the PBP, ROI, NPV and DCFR. In this case, the FCI, the profits and the income tax are varied within a range of $\pm 30\%$ to evaluate the impact on the main profitability metrics. In Figure 4.16 can be noticed that the direction of the slope for FCI and income tax is different from the direction for the profit due to the opposite signs in Equation 3.28.

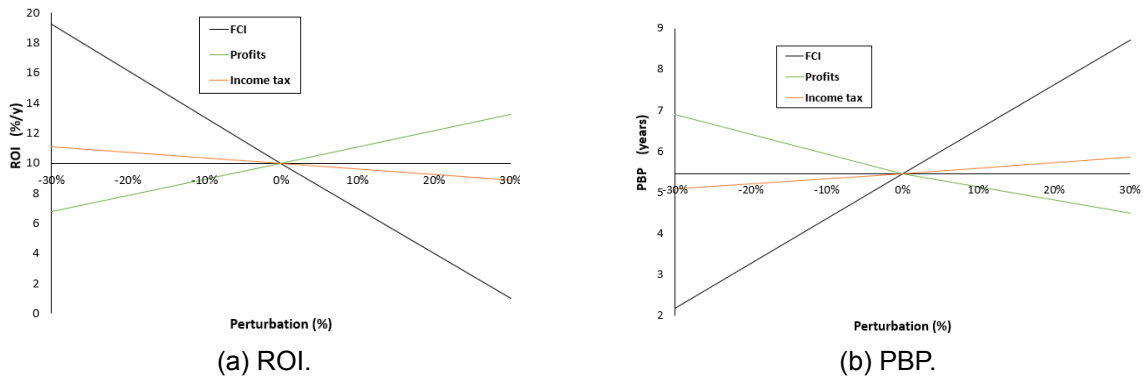


Figure 4.16: Sensitivity analysis on profitability metrics for OXY-SOL-NA

The FCI is the most sensitive parameter. In fact, while a 30% change in profits or income tax only changes the PBP by 21.2% and 7.8% respectively, the same change in the FCI causes a change by 60.1% (Figure 4.16b). Applying a 30% change in FCI and profits, a maximum increase of 90% and 24% in ROI respectively could be achieved. In contrast, the ROI would decrease by 11% for profits (Figure 4.16a).

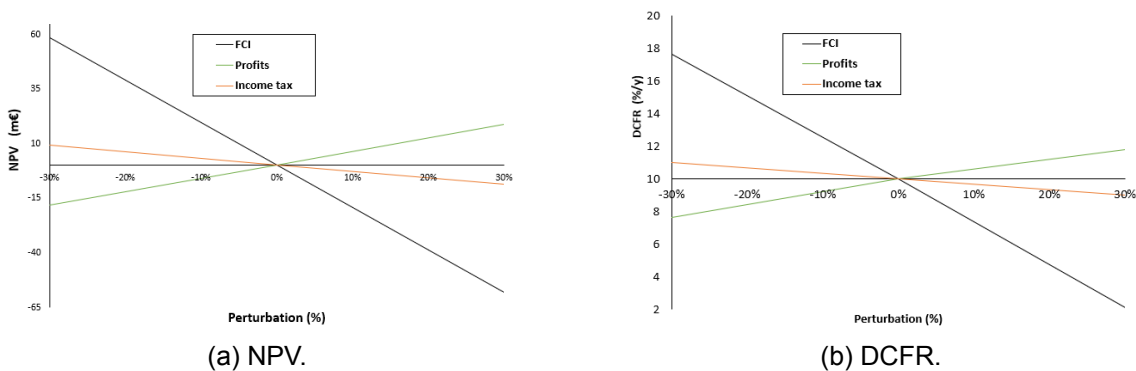


Figure 4.17: Sensitivity analysis on profitability metrics for OXY-SOL-NA

Comparing the sensitivity results of the four metrics, it can be seen that the greatest impact of a change in the FCI is on the NPV. With a change of 30% the NPV goes from 0.24 M€ to almost 60 m€ (Figure 4.17a). Alternatively, it can be obtained a maximum annual increase of 8% and 1% of the DCFR by decreasing the FCI and the income tax by 30% (Figure 4.17b). Similarly, the DCFR would be reduced by the same percentage if both parameters were increased (Figure 4.17b).

5 Conclusions

The results of the techno-economic analysis give a clear picture of the challenges and considerations when simulating and evaluating different types of nitric acid plants from an economic point of view.

The first and most fundamental step is to model and simulate the nitric acid plant in a rigorous way. The complexity of the simulation of the Ostwald process in Aspen Plus[®] lies in the implementation of the kinetic reactions during the heat exchangers and mainly in the absorption column. As a result of the simulation, it is obtained that 199.5 tons/day of ammonia, 3915.5 tons/day of air and 243.6 tons/day of process water are necessary to produce 700 tons/day of nitric acid (eq. 100 %) at a concentration of 60 wt% (Table D.1).

The feasibility of optimising nitric acid production and reducing the final NO_x concentration of the absorption column by injecting pure oxygen at different points of the plant is studied. The aim of this research is to find synergies between the remaining oxygen from green ammonia production and nitric acid production. The results indicate that the greatest benefits are obtained for case D. That is, by injecting oxygen into the main air line and increasing the oxygen content by 6.1 wt% (from 22.4 wt% to 28.5 wt%), the daily nitric acid production could be increased by 0.34 % and the nitrogen oxides content decreased by 43.6 % (Table 4.5). Nevertheless, it is mentioned that case D may be undesirable due to the higher loss of catalyst and safety issues associated with ammonia combustion.

The economic analysis is carried out on three different types of nitric acid plants to compare the main limitations and disadvantages of producing nitric acid in a more sustainable way compared to the conventional process.

The optimisation of the conventional process by oxygen injection (OXY-SOL-NA plant) is able to reduce the capital costs by 0.65 M€ compared to the CONV-NA and SOL-NA plants (Table 4.7). However, the operating costs end up being more relevant in the final cash flow analysis. The CONV-NA plant has 17 % lower operating costs compared to the two green ammonia plants which is explained by the fact that ammonia costs accounted for 52.65 % of the total operating costs (Figure G.13). Due to the above arguments, the conventional nitric acid plant could have a minimum end-product price 14 % lower than the SOL-NA and OXY-SOL-NA plants (Table 4.8). In addition to having a lower minimum price, it has a higher NPV and DCFR, which makes the economic feasibility and profitability of the project more certain. Regardless of environmental considerations, such a significant difference in the final price may make your product unable to compete with other potential competitors.

The results of the sensitivity analysis of the MSEP to changes in cooling water cost, ammonia cost and catalyst cost are consistent with the arguments mentioned above. In fact, it is found that the MSEP of nitric acid could decrease by almost 42 % with an 80 % decrease in the cost of ammonia. Similarly, the MSEP could escalate in the face of a similar increase in the cost of ammonia. In other words, the price of nitric acid will depend significantly on fluctuations in the ammonia market.

Finally, by performing sensitivity analysis on ROI, PBP, NPV and DCFR based on ±30% changes in FCI, profits and income tax, it is found that the most sensitive parameter is the FCI. The biggest impact is on NPV, as a 30% reduction in FCI increases the net present value by almost 60 euro. For the same change in the FCI, there is a 9.1% and 8% increase

in the ROI and DCFR respectively (Figures 4.16a & 4.17b) and a 3.4 year reduction in the PBP (Figure 4.16b).

Unfortunately, without an idea of the current market price of nitric acid, no conclusions can be drawn about the current feasibility of using green ammonia for nitric acid production from the economic analysis. What can be known, however, is the current feasibility of producing ammonia from renewable sources. Currently, green ammonia is mainly dependent on the price of green hydrogen production due to the high LCOE for solar energy and the lack of maturity of electrolyzers [66]. CO₂ pricing policies could make the implementation of green NH₃ in the nitric acid plant feasible in the near future [10].

Bibliography

- [1] K. Randive, T. Raut, and S. Jawadand. "An overview of the global fertilizer trends and India's position in 2020". In: *Mineral Economics* 34 (2021), pp. 371–384.
- [2] S.Vaclav. *Enriching the Earth: Fritz Haber, Carl Bosch, and the transformation of world food production*. Tech. rep. Massachusetts Institute of Technology, 2001.
- [3] *The fertiliser industry*. URL: <https://www.siyavula.com/read/science/grade-12/the-chemical-industry/14-the-chemical-industry-04>.
- [4] I. Rossetti. "Reactor design, modelling and process intensification for ammonia synthesis". In: *Green Energy and Technology* (2020).
- [5] I. Dincer and Y. Bicer. "2.1 Ammonia". In: *Comprehensive Energy Systems*. Vol. 2. 2018, pp. 1–39.
- [6] M.Thiemann, E. Scheibler, and K. Wiegand. "Nitric Acid, Nitrous Acid, and Nitrogen Oxides". In: *Ullmann's Encyclopedia of Industrial Chemistry*. Wiley-VCH Verlag GmbH & Co. KGaA, June 2000.
- [7] S. Budinis et al. *Ammonia Technology Roadmap. Towards more sustainable nitrogen fertiliser production*. Tech. rep. International Energy Agency, 2021, pp. 1–168.
- [8] *History of Climate Emergency Action by Councils*. 2020. URL: [CACEonline.org](https://www.caceonline.org).
- [9] IFA. "Fertilizers, Climate Change and Enhancing Agricultura Productivity Sustainably". In: *International Fertilizer Industry Association* (2009).
- [10] L. Wang et al. *Greening Ammonia toward the Solar Ammonia Refinery*. June 2018.
- [11] R. Lindsey. *Climate Change: Atmospheric Carbon Dioxide*. 2022.
- [12] E. Elkin. *Fertilizer Prices Rocket to All-Time High on Tightening Supplies*. 2021. URL: <https://www.bloomberg.com/news/articles/2021-11-12/fertilizer-prices-rocket-to-new-record-for-second-week?leadSource=verify%20wall>.
- [13] IRENA. *Green Hydrogen Cost Reduction: Scaling up Electrolysers to Meet the 1.5 °C Climate Goal*. Tech. rep. Abu Dhabi: International Renewable Energy Agency, 2020.
- [14] M. L. Wagner and W. Plains. *Direct oxygen injection in nitric acid production*. 2003.
- [15] M. Appl. "Ammonia, 2. Production Processes". In: *Ullmann's Encyclopedia of Industrial Chemistry*. Wiley-VCH Verlag GmbH & Co. KGaA, Oct. 2011.
- [16] N. I. Ilchenko. "Catalytic Oxidation of Ammonia". In: *Russian Chemical Reviews* 45.12 (Dec. 1976), pp. 1119–1134.
- [17] M. Koukolik and J. Marek. "Mathematical model of HNO₃ Oxidation-Absorption equipment". In: *Proc. Fourth European Symp. on Chem. Reaction Eng.* (1968).
- [18] N. J. Suchak and J. B. Joshi. *Simulation and Optimization of NO, Absorption System in Nitric Acid Manufacture*. Tech. rep.
- [19] M. Shahabuddin, M.A. Alim, and T. Alam. "A critical review on the development and challenges of concentrated solar power technologies". In: *Sustainable Energy Technologies and Assessments* 47 (2021).
- [20] R. Kistner. "Simulation of solar thermal power plants and their evaluation emphasising on energy economic issues and financing issues". PhD thesis. Berlin University of Technology, 2002.
- [21] A. Rosenstiel et al. "Electrochemical Hydrogen Production Powered by PV/CSP Hybrid Power Plants: A Modelling Approach for Cost Optimal System Design". In: *Energies* 2021, Vol. 14, Page 3437 14.12 (June 2021), p. 3437.
- [22] R. Pitz-Paal. "Concentrating Solar Power". In: *Future Energy* (2020), pp. 413–430.
- [23] Agency IE. *Technology roadmap solar thermal electricity*. Tech. rep. OECD, 2015.

- [24] P. Sun and A. Elgowainy. "Updates of hydrogen production from SMR Process in GREET 2019". In: (2019), pp. 1–7.
- [25] "Global Hydrogen Review 2021". In: *IEA Publications* (2021). URL: <http://www.iea.org/about/contact>.
- [26] K. Schultz. *Thermochemical Production of Hydrogen from Solar and Nuclear Energy*. 2003. URL: web.stanford.edu/group/gcep/pdfs/hydrogen_workshop/Schultz.pdf.
- [27] A. Borreti. "Which thermochemical water-splitting cycle is more suitable for high-temperature concentrated solar energy?" In: *International journal of hydrogen energy* 47 (2022), pp. 20462–20474.
- [28] J. Vieten et al. "Ammonia and Nitrogen-based Fertilizer Production by Solar thermochemical Processes". In: *AIP Conference Proceedings*. Vol. 2303. 2020.
- [29] A. Boretti, J. Nayfeh, and A. Al-Maaitah. "Hydrogen Production by Solar Thermochemical Water-Splitting Cycle via a Beam Down Concentrator". In: *Frontiers in Energy Research* (2021).
- [30] J. Vieten. "Perovskite oxides for application in thermochemical air separation and oxygen storage". In: *Journal of Materials Chemistry* 4.35 (2016), pp. 13652–13659.
- [31] A. A. Moghaddam and U. Krewer. "Poisoning of Ammonia Synthesis Catalyst Considering Off-Design Feed Compositions". In: *Catalysts* 10.1225 (2020), pp. 1–16.
- [32] R. Stokes. "A History of the International Industrial Gases Industry from the 19th to the 21st Centuries". In: *Cambridge University Press* (2015).
- [33] S. Li. "Thermodynamic Analyses of Fuel Production via Solar-Driven Metal Oxide Redox Cycling". In: *Energy & Fuels* 32.10 (2018), pp. 10848–10863.
- [34] L. T. Biegler, I. E. Grossmann, and A. W. Westerberg. *Systematic Methods of Chemical Process Design*. Prentice-Hall, 1997.
- [35] B. Mock, L. B. Evans, and C. C. Chen. "Thermodynamic representation of phase equilibria of mixed-solvent electrolyte systems". In: *AIChE Journal* 32.10 (1986), pp. 1655–1664.
- [36] L. Haar., J. S. Gallagher, and G. S. Kell. *NBS/NRC steam tables: thermodynamic and transport properties and computer program for vapor and liquid states of water in SI units*. Hemisphere Pub. Corp, 1984.
- [37] S.E. Schwartz and W. H. White. "Solubility equilibria of the nitrogen oxides and oxyacids in dilute aqueous solution". In: *Adv. Environ. Sci. Eng* (1981).
- [38] M. Bodenstein. "Bildung und Zersetzung der höheren Stickoxyde". In: *Z. Physik. Chem.* 100 (1922), pp. 68–123.
- [39] *Nitric Acid package*. Tech. rep. Aspen Technnology, Inc, 2004.
- [40] D.N. Miller. "Mass transfer in nitric acid absorption". In: *AIChE Journal* 33.8 (1987), pp. 1351–1358.
- [41] B. Linnhoff and J. R. Flower. "Synthesis of heat exchanger networks". In: *AIChE Journal* 24 (1978), pp. 633–642.
- [42] J. J. Klemes et al. *Process integration and intensification. Saving energy, water and resources*. DE GRUYTER, 2014.
- [43] S. Bhatia et al. *Oxygen injection in nitric acid production*. 1997.
- [44] D. F. Echegarary, A. M. Velloso, and M. L. Wagner. *Method and production of nitric acid*. 2000.
- [45] M. Gorywoda, D. F. Lupton, and J. Lund. *Method and apparatus for reducing nitrous oxide*. 2003.
- [46] J. B. Powell. *Process for making nitric acid by the ammonia oxidation-nitric oxide oxidation-water absorption method*. 1975.

- [47] M. Gorywoda, D. F. Lupton, and J. Lund. *Method and apparatus for reducing nitrous oxide*. 2003.
- [48] M. S. Peters, K. D. Timmerhaus, and R. E. West. *Plant Design and Economics for Chemical Engineers*. Fifth. McGrawHill, 2003.
- [49] P. Christensen et al. *Cost Estimate Classification System - As Applied in Engineering, Procurement, and Construction for the Process Industries*. Tech. rep. 2005.
- [50] W. M. Vatavuk. "Updating the CE Plant Cost index". In: *Chemical Engineering* (2002), pp. 62–70.
- [51] F. G. Albrecht et al. "A standardized methodology for the techno-economic evaluation of alternative fuels – A case study". In: *Fuel* 194 (2016), pp. 511–526.
- [52] *Beeland Management Company. Rogers International Commodity Index*. 2015. URL: <http://www.rogersrawmaterials.com/home.asp>.
- [53] "The World Bank. World Bank Commodity Price Data (The Pink Sheet)". In: (2016).
- [54] S. Razavi and H. V. Gupta. "What do we mean by sensitivity analysis? The need for comprehensive characterization of "global" sensitivity in Earth and Environmental systems models". In: *Water Resources Research* 51 (2015), pp. 3070–3092.
- [55] *Worldwide tax summaries*. URL: <https://taxsummaries.pwc.com/spain/corporate/withholding-taxes>.
- [56] Alfa Aesar. *Platinum Rhodium gauze, 80 mesh woven from 0.076mm*. 2022. URL: <https://www.alfa.com/en/catalog/012217/>.
- [57] N. Campion et al. "Techno-Economic Assessment of Green Ammonia Production with Different Wind and Solar Potentials". In: *SSRN* (2022).
- [58] Global petrol prices. *Spain electricity prices*. 2022. URL: https://www.globalpetrolprices.com/Spain/electricity_prices/#hl223.
- [59] J. Dersch et al. "LCOE reduction potential of parabolic trough and solar tower technology in G20 countries until 2030". In: *AIP Conference Proceedings*. Vol. 2303. American Institute of Physics Inc., Dec. 2020.
- [60] Selectra. *Precio de agua en España: Toda la información*. 2022. URL: <https://tarifasdeagua.es/info/precio>.
- [61] F. Sperner and W. Hohmann. "Rhodium-Platinum Gauzes for Ammonia Oxidation". In: *Platinum Metals Rev.* 20.1 (1976), pp. 12–20.
- [62] L. Xin, H. Yongqiang, and J. Husheng. "Pt-Rh-Pd Alloy Group Gauze Catalysts Used for Ammonia Oxidation". In: *Rare Metal Materials and Engineering* 46.2 (2017), pp. 339–343.
- [63] M. Kamphus. "Emission monitoring in nitric acid plants". In: *Nitrogen + Syngas* 328 (2014), pp. 48–53.
- [64] S. I. Clarke and W. J. Mazzafró. *Nitric Acid*. 2005.
- [65] A. U. Rehman et al. "Production of 140 MTPD Conc. Nitric Acid (98%) by Recycling and Rectification". PhD thesis. NFC Institute of Engineering & Fertilizer Research, 2007.
- [66] B. Lee et al. "Pathways to a Green Ammonia Future". In: *ACS Energy Letters* 7.9 (2022), pp. 3032–3038.
- [67] *Aspen Plus User models V10*. 2017.
- [68] R. W. W. Derby and P. G. Balkey. *Oxygen-enrichment columnar absorption process for making nitric acid*. 1980.
- [69] H. F. Rase. *Chemical reactor design for process plants*. Vol. 1. Wiley, 1977.

A User kinetic subroutines in Aspen Plus

There are different functionalities that cannot be directly introduced in Aspen Plus. This is the case for several kinetic equations that are not written in the conventional form. In that case, Aspen Plus® has created a developer user manual to allow the users to customize the simulator and adjust to their needs. One of the main functionalities is the so called "Fortran user models", subroutines are created by the user to perform several tasks as sizing and costing and unit operation models among others [67].

Kinetic forms in Aspen Plus

The power law expression (conventional form) has two possibilities:

- If T_0 is specified, then the general law expression will be:

$$r = k (T/T_0)^n e^{(-E/R) [\frac{1}{T} - \frac{1}{T_0}]} \prod_{i=1}^N C_i^{\alpha_i} \quad (\text{A.1})$$

- On the other hand if T_0 is not specified, the general law expression will reduce to

$$r = k(T)^n e^{(-E/R) [\frac{1}{T}]} \prod_{i=1}^N C_i^{\alpha_i} \quad (\text{A.2})$$

The rate is expressed in $kmol/(s \cdot \text{basis})$ where the basis is either m^3 for "Rate Basis: Reac (vol)", or kilogram catalyst for "Rate Basis: Cat (wt)".

Apart from the conventional forms, Aspen Plus offers different possibilities such as: Langmuir-Hinshelwood-Hougen-Watson (LHHW) reactions, equilibrium reactions, rate controlled reactions, salt precipitation reactions, crystallization reactions...etc

Nevertheless, the heat exchangers (From E-104 to E-108) were modelled as plug flow reactors (PFRs) since kinetic reactions cannot be included in the heat exchangers blocks in Aspen Plus®. The introduction of the kinetic in the conventional form led to problems during the simulation. Equilibrium reactions (2.12-2.13) must be simulated independently for PFRs: The forward reaction from one side and backward reaction from the other side. For that reason, all the kinetics were programmed in Fortran and introduced in Aspen Plus®.

Linking Aspen Plus with Microsoft Visual Studio and Intel Fortran Compiler

There are several steps to be done before writing and using any Fortran user model. Aspen tech software does not include Microsoft visual studio® (MVS) and Intel fortran compiler® (IFC) by default. Those programs are required for the code development, the compiling step and for the linkage of the files.

- **step 1:** Search in programs for "Set Compiler" in my case: "`C:\Program Files\AspenTech\AprSystem V11.0\Engine\Xeq\ApSetComp.exe`". Figure A.2 will appear in your desk.
- **step 2:** Check the compatibility versions for MVS and IFC and proceed to install the same versions. In my case, I have installed IFC 17/2017 with VS 2015 & IFC 18/2018 with VS 2015 (Figure A.2).

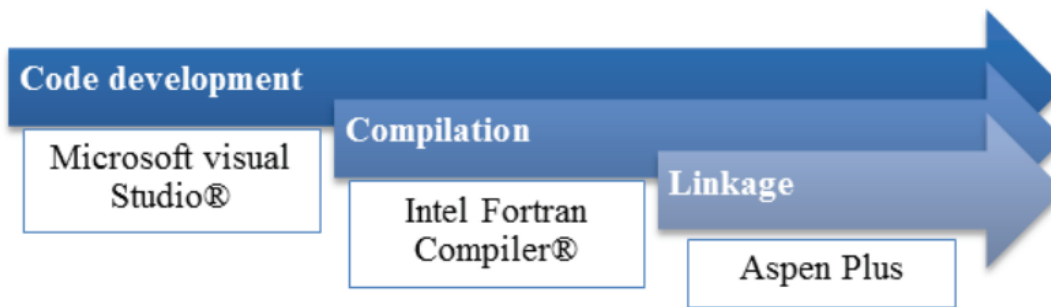


Figure A.1: Basic steps and required programs.

- **step 3:** Once both programs has being successfully installed “OK” message will appear instead of “ERROR” in the column state.
- **step 4:** Configure the compiler of Aspen Plus® for USER and MACHINE (see at the bottom of Figure A.2). Write the number of the row that your state column shows “OK” and click ENTER in your keyboard. Repeat the same for the machine option.

```

Set Compiler for V11
11 compiler sections in C:\Program Files\AspenTech\APrSystem V11.0\Engine\xeq\Compilers64.cfg
## Section      State Description
-----
1 IVF14_VS12    ERROR Intel Fortran 2013SP1 and Microsoft Visual Studio 12/2013
2 IVF15_VS12    ERROR Intel Fortran 15/2015 and Microsoft Visual Studio 12/2013
3 IVF16_VS12    ERROR Intel Fortran 16/2016 and Microsoft Visual Studio 12/2013
4 IVF16_VS14    ERROR Intel Fortran 16/2016 and VS 2015 WITH C++ (and express)
5 IVF17_VS14    OK     Intel Fortran 17/2017 and VS 2015 WITH C++ (and express)
6 IVF17_VS15    ERROR Intel Fortran 17/2017 and VS 2017 WITH C++ (and community)
7 IVF18_VS14    OK     Intel Fortran 18/2018 and VS 2015 WITH C++ (and express)
8 IVF18_VS15    ERROR Intel Fortran 18/2018 and VS 2017 WITH C++ (and community)
9 IVF19_VSB     ERROR Intel Fortran 19/2019 and Bundled VS 2015 shell and Win10 SDK
10 IVF19_VS14   ERROR Intel Fortran 19/2019 and VS 2015 WITH C++ (and express)
11 IVF19_VS15   ERROR Intel Fortran 19/2019 and VS 2017 WITH C++ (and community)

The current compiler option settings in order of searching
  IVF17_VS14 for current user in HKEY_CURRENT_USER registry
  Not set for current machine in HKEY_LOCAL_MACHINE registry
  IVF17_VS15 in file C:\Program Files\AspenTech\APrSystem V11.0\Engine\xeq\Compilers64.cfg

Enter option (1:11) for current USER, 0 to skip, -1 to delete:

```

Figure A.2: Set compiler window for Microsoft visual studio and Intel fortran versions.

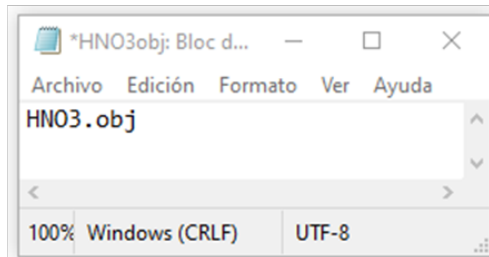
Code compilation and linkage with Aspen Plus

First of all, the Fortran code must be written following the Aspen User manual [67]. One of the easiest ways is to start using a default template available in the AspenTech folders (C:\Program Files\AspenTech\Aspen Plus V11.0\Engine\User).

Once the code is prepared and saved with the extension .f, it must be translated from the Visual Basic language to Fortran using IFC. it can be easily done following these steps:

- **step 1:** Open “*Customize Aspen Plus program*”. In my case: (“C:\Program Files\AspenTech\Aspen Plus V11.0\Engine\Xeq\aspsetup.bat”)

a.



b.

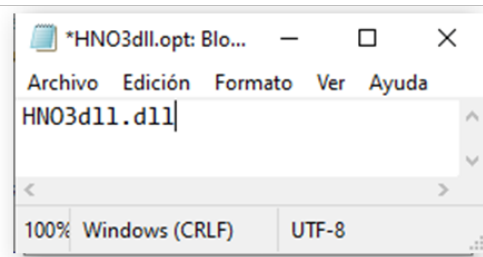


Figure A.3: .opt file creation in Notepad. a. Step 4 and b. Step 6.

- **step 2:** Open the location of your file. Type: **cd + “location of your fortran code file”** and click ENTER (see Figure A.4).
- **step 3:** Compile your fortran code. Write: **aspcomp + “the name of your fortran code file”.f** and click ENTER. This step creates an object file with an extension .obj (see Figure A.4).
- **step 4:** Create a file with the program Notepad and write down the name of the object file created (see Figure A.3). Then, save this file in the same location with the extension .opt.

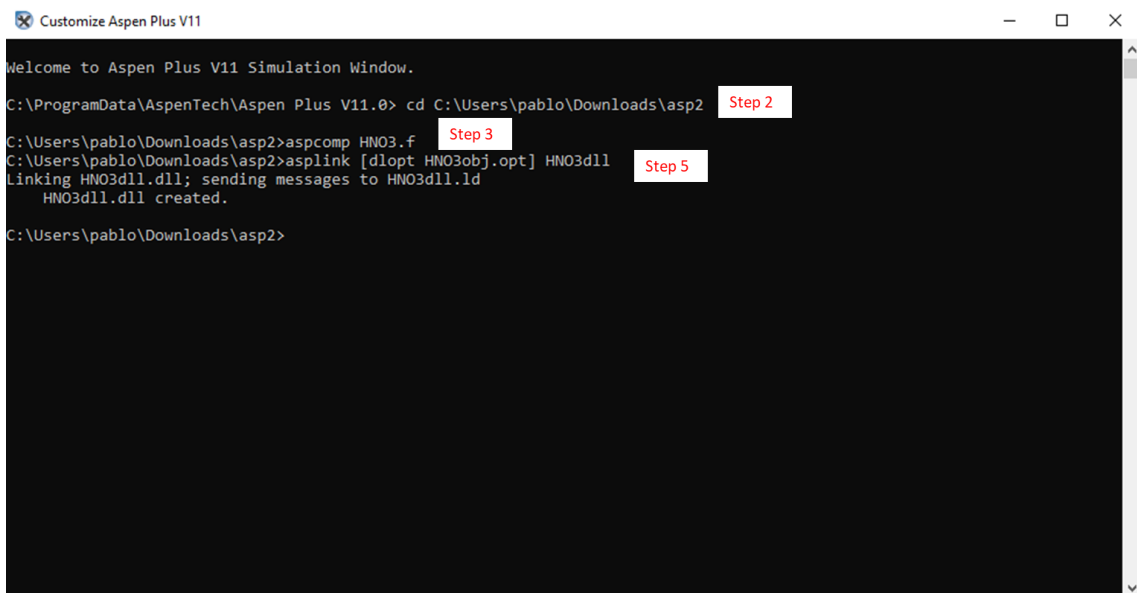


Figure A.4: Customize Aspen Plus window.

- **step 5:** Go back to Customize Aspen Plus® window and type: **asplink [dlopt “name of your object file”.opt] “type name of the file”**. This process generates a .dll, .ld and .lds file. However, we will just use the file with the extension .dll.
- **step 6:** Create a file with the program Notepad and write down the name of the dll file created (see Figure A.3). Then, save this file in the same location with the extension .opt.
- **step 7:** Go to Aspen Plus® simulation environment and click on: *Run* → *Settings* →

Engine Files → *Miscellaneous files* → *Linker options*. Select your final .opt file and your user subroutine would be ready to be used by Aspen (see Figure A.5)

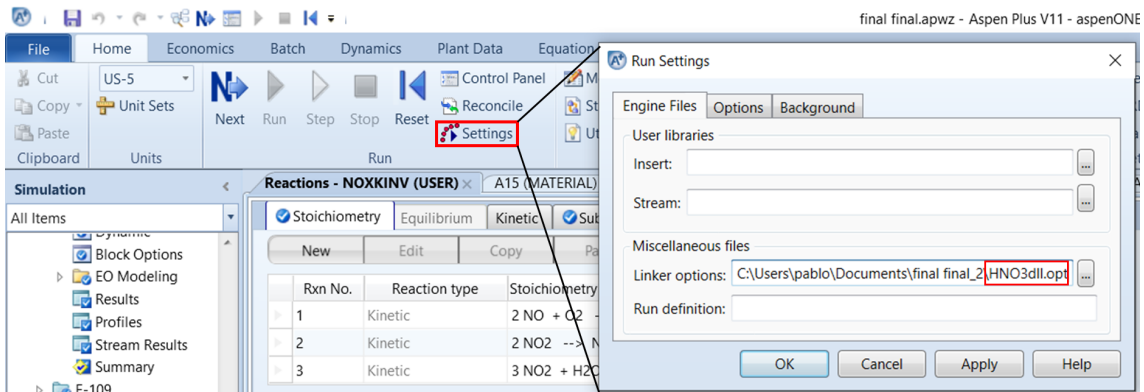


Figure A.5: Linking fortran code compiled with Aspen Plus®.

Fortran code

```

1
2 C
3 C   User Kinetics Subroutine for RPLUG
4
5 C
6 C   SUBROUTINE HNO3 (SOUT,   NSUBS,  IDXSUB,   ITYPE,   NINT,
7     2           INT,     NREAL,   REAL,     IDS,     NPO,
8     3           NBOPST, NIWORK,  IWORK,    NWORK,   WORK,
9     4           NC,      NR,      STOIC,    RATES,  FLUXM,
10    5           FLUXS,  XCURR,   NTCAT,    RATCAT, NTSSAT,
11    6           RATSSA, KCALL,   KFAIL,   KFLASH, NCOMP,
12    7           IDX,    Y,       X,        X1,     X2,
13    8           NRALL,  RATALL,  NUSERV,  USERV,  NINTR,
14    9           INTR,   NREALR,  REALR,   NIWR,   IWR,
15    *           NWR,   WR,      NRL,      RATEL,  NRV,
16    1           RATEV)
17 C
18 C   IMPLICIT NONE
19 C
20 C   DECLARE VARIABLES USED IN DIMENSIONING
21 C
22 C   INTEGER NSUBS, NINT, NPO, NIWORK,NWORK,
23 +         NC, NR, NTCAT, NTSSAT,NCOMP,
24 +         NRALL, NUSERV, NINTR, NREALR, NIWR,
25 +         NWR
26 C
27 #include "ppexec_user.cmn"
28 EQUIVALENCE (RMISS, USER_RUMISS)
29 EQUIVALENCE (IMISS, USER_IUMISS)
30 C
31 C
32 C
33 C.....RCSTR...
34 #include "rcst_rcstri.cmn"
35 #include "rxn_rcstrr.cmn"
36 C
37 C.....RPLUG...
38 #include "rplg_rplugi.cmn"
39 #include "rplg_rplugr.cmn"
40 EQUIVALENCE (XLEN, RPLUGR_UXLONG)

```

```

41     EQUIVALENCE (DIAM, RPLUGR_UDIAM)
42
43     EQUIVALENCE (ROCAT, RPLUGR_CAT_RHO)
44     EQUIVALENCE (FRACV, RPLUGR_BED_VOID)
45 C
46 C.....RBATCH...
47 #include "rbtc_rbati.cmn"
48 #include "rbtc_rbatr.cmn"
49 C
50 C.....PRES-RELIEF...
51 #include "prsr_presri.cmn"
52 #include "rbtc_presrr.cmn"
53 C
54 C.....RADFRAC/RATEFRAC
55 #include "rxn_disti.cmn"
56 #include "rxn_distr.cmn"
57 C
58 C.....REACTOR (OR PRES-RELIEF VESSEL OR STAGE) PROPERTIES...
59 #include "rxn_rprops.cmn"
60     EQUIVALENCE (TEMP, RPROPS_UTEMP)
61     EQUIVALENCE (PRES, RPROPS_UPRES)
62     EQUIVALENCE (VFRAC, RPROPS_UVFRAC)
63     EQUIVALENCE (BETA, RPROPS_UBETA)
64     EQUIVALENCE (VWAP, RPROPS_UVWAP)
65     EQUIVALENCE (VLIQ, RPROPS_UVLIQ)
66     EQUIVALENCE (VLIQS, RPROPS_UVLIQS)
67 C
68 C     INITIALIZE RATES
69 C
70 C
71 C     DECLARE ARGUMENTS
72 C
73     INTEGER IDXSUB(NSUBS), ITYPE(NSUBS), INT(NINT),
74 +     IDS(2), NBOPST(6,NPO), IWORK(NIWORK),
75 +     IDX(NCOMP), INTR(NINTR), IWR(NIWR),
76 +     NREAL, KCALL, KFAIL, KFLASH,NRL,
77 +     NRV, I
78     REAL*8 SOUT(1), WORK(NWORK),
79 +     STOIC(NC,NSUBS,NR), RATES(NC),
80 +     FLUXM(1), FLUXS(1), RATCAT(NTCAT),
81 +     RATSSA(NTSSAT), Y(NCOMP),
82 +     X(NCOMP), X1(NCOMP), X2(NCOMP)
83     REAL*8 RATALL(NRALL),USERV(NUSERV),
84 +     REALR(NREALR),WR(NWR), RATEL(1),
85 +     RATEV(1), XCURR
86 C
87 C     DECLARE LOCAL VARIABLES
88 C
89     INTEGER IMISS, J,
90 +     IDXP(5), NCP, KDIAG, KV, KER
91
92     REAL*8 REAL(3), RMISS,
93 +     XLEN, DIAM, TEMP,FACT4,
94 +     PRES, VFRAC, BETA, VWAP, VLIQ,
95 +     VLIQS, ROCAT, FRACV, KPEQ3,
96 +     KP1, Eac(4), Rg, FACT1, FACT2, FACT3,
97 +     VELOC(6), Cmolar(NC), XP(5), FLOW,
98 +     VMX, DVMX, K1, K2, KPEQ1, KP2, KP3,
99 +     Pasca, Ppar(NC), KPEQ2, K3, K4, K5, K6
100
101
102

```

```

103 C
104 C BEGIN EXECUTABLE CODE
105
106
107 FACT1 = REAL(1)
108 FACT2 = REAL(2)
109 FACT3 = REAL(3)
110 FACT4 = REAL(4)
111 C
112 Rg = 8314.7
113 Pasca = 101325.0
114 Eac = (/652.1, 13870.9, 6891.6, 4282.34/)
115 KP1 = (10.0**(Eac(1)/TEMP -1.0366))/(Pasca**2)
116 K1 = FACT1* KP1/(Rg*TEMP)
117 KPEQ1 = EXP (-17.9956 + (Eac(2)/TEMP))/Pasca
118 KPEQ2 = EXP (-21.244 + (Eac(3)/TEMP))/Pasca
119 KPEQ3 = EXP (-19.7292 + (Eac(4)/TEMP))/Pasca
120 K2 = (KP1/KPEQ1)/(Rg*TEMP)
121 KP2 = (10.0**(Eac(1)/TEMP -1.0366))/(Pasca)
122 K3 = (FACT2*KP1)/(Rg*TEMP)
123 K4 = ((0.0*KP1)/KPEQ2)/(Rg*TEMP)
124 KP3 = (10.0**(Eac(1)/TEMP -1.0366))/(Pasca**3)
125 K5 = (FACT3*KP1)/(Rg*TEMP)
126 K6 = ((FACT3*KP1)/KPEQ2)/(Rg*TEMP)
127
128 CALL SHS_CPACK ( SOUT(1:NC), NCP, IDXP, XP, FLOW)
129
130 KDIAG = 4
131 KV = 1
132 CALL PPMON_VOLV (TEMP, PRES, XP, NCP, IDXP, NBOPST, KDIAG, KV,
133 + VMX, DVMX, KER)
134
135
136 DO J=1, NC
137
138 Cmolar(J) = (SOUT(J)/SOUT(NC+1))/VMX
139 Ppar(J) = Cmolar(J)*Rg*TEMP
140
141 END DO
142
143
144 C RATE 1: 2 NO + O2 --> 2 NO2
145 C RATE 2: 2 NO2 --> 2 NO + O2
146 C RATE 3: 2 NO2 --> N2O4
147 C RATE 4: N2O4 --> 2 NO2
148 C RATE 5: 3 NO2 + H2O --> 2 HNO3 + NO
149 C RATE 6: 2 HNO3 + NO --> 3 NO2 + H2O
150
151 VELOC(1) = (WAP)*K1*Ppar(2)*Ppar(3)**2
152 VELOC(2) = WAP*K2*Ppar(4)**2
153 VELOC(3) = WAP*K3*Ppar(4)**2
154 VELOC(4) = WAP*K4*Ppar(8)
155 VELOC(5) = WAP*K5*Ppar(5)*Ppar(4)**2
156 VELOC(6) = FACT4*WAP*K6*Ppar(3)*Ppar(14)**2
157
158
159 RATES(3) = 2*(VELOC(2) - VELOC(1)) + VELOC(5) - VELOC(6)
160 RATES(2) = VELOC(2) - VELOC(1)
161 RATES(4) = 2*(VELOC(1) - VELOC(2) - VELOC(3) + VELOC(4))
162 + 3*(VELOC(6)-VELOC(5))
163 RATES(8) = VELOC(3) - VELOC(4)
164 RATES(14) = 2*(VELOC(5)-VELOC(6))

```



```
165      RATES(5) = VELOC(6)-VELOC(5)
166
167
168
169
170 C
171   RETURN
172   END
```

B Schematic configurations

The goal of this appendix is to show the schematic configurations for the cases studied in Aspen Plus[®]. The arrows represent the streams, and the blocks represent the main unit operations of the process flow diagram (PFD).

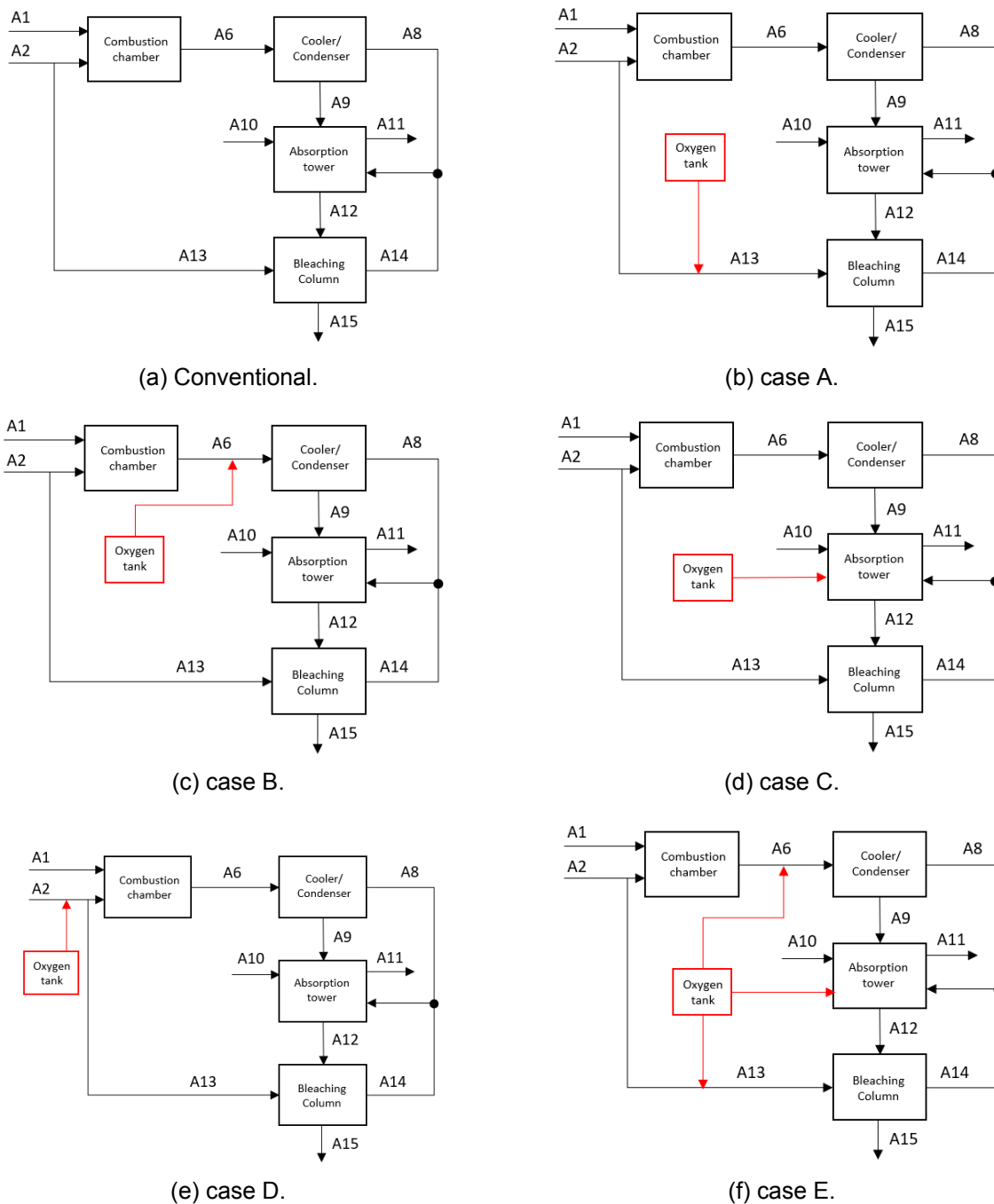


Figure B.1: Schematic configurations.

C Summary of the patents studied

A summary of literature research on this topic is presented below:

Direct oxygen injection in nitric acid production [14]

This patent aims to boost nitric acid production rate and strength by injecting oxygen-enriched air to existing plants. Five different embodiments of the invention are presented schematically:

- **Embodiment 1:** Two enriched-oxygen injections, one before the cooler-condenser and the other before the bleaching column. This configuration found that between 10% and 30% of the total oxygen should go directly to the cooler/condenser train. Injecting oxygen directly after the combustion chamber would be ideal, however it cannot be easily retrofitted in existing plants.
- **Embodiment 2:** Two enriched-oxygen injections, one before the catalytic combustion and the other before the bleaching column. This embodiment resulted in a higher catalyst losses due to more platinum and rhodium oxide is formed as the oxygen partial pressure increases. In addition, increasing the oxygen concentration could lead to safety risks if the explosive limit is exceeded.
- **Embodiment 3:** Three enriched-oxygen injections; before the cooler-condenser, the bleaching column and the absorption column. It was found that the acid strength could be increased by having a higher oxidation state of NO_x before the absorption column.
- **Embodiment 4:** Similar to embodiment 2 but the injection is performed directly into the secondary air line. This model confirmed the hypothesis that by increasing the oxidation state of NO_x gases, less oxygen would be needed in the secondary air pipeline.
- **Embodiment 5:** Similar to embodiment 3 but the injection in the absorption tower is studied in three points; at the base, at the middle and at the air pipeline. This approach was highlighted as less attractive due to the difficulties of being this configuration implemented.

This patent concluded that the cost of retrofitting existing plants to integrate oxygen-enriched air is justified by the increase of nitric acid production and the control of NO_x emissions.

Method and production of nitric acid [44]

This American patent aims to facilitate the removal of impurities from the liquid phase by injecting supplemental oxygen into the nitric acid process. The idea is to form gas bubble/liquid mixture in the stream. This bubble should be dispersed with a diameter less than 0.1 mm of diameter for the bubbles.

The invention embodiment is focused on injecting the oxygen via an in-line gas dispersion device that is capable of forming bubbles of less than 0.1 mm. This patent also studies different injection configurations in existing nitric acid plants. This method concluded that the uniform gas bubble/liquid mixtures increases the interfacial surface between the gas

bubbles and the nitric acid. It increases the mass transfer between the gas and liquid phases of the process boosting the nitric acid production and maintaining NO_x emissions.

Oxygen injection in nitric acid production [43]

The present invention provides a description of oxygen injections downstream the combustion chamber, but upstream the absorption column. This patent suggests an improved multi-step oxidation process for the production of nitric acid whereby improvements are realized with regard to an increase in the capacity of production, improvement in the strength of the acid product (%wtd HNO_3) and a reduction in the NO_x emissions.

Process for making nitric acid by the ammonia oxidation-nitric oxide oxidation-water absorption method [46]

This patent was one of the first to state that increasing the concentration of pure oxygen and recirculating the tail gas stream produced a considerable decrease in nitric oxide emissions.

This embodiment employs a high oxygen content gas for the process wherein the total amount of molecular oxygen available for oxidation is up to about 20 vol.% in excess of the amount required for complete oxidation of the ammonia to nitric acid on a stoichiometric basis, and recycling at least about 40 vol. % of the tail gas. This invention led to the following results:

- Substantial decrease in the amount of nitrogen oxides vented to the atmosphere. This amounts to less than 0.2% of the tail gas stream. The remaining portion of over 99.8% can be recycled, thus almost totally eliminating the discharge of nitrogen oxides to the atmosphere.
- Using tail gas recycle increases absorption efficiency for nitrogen oxides from 98 % to 100 % (99.95%).

Oxygen-enrichment columnar absorption process for making nitric acid [68]

The present invention comprises an improved nitric acid process through oxygen-enriched air in the absorption tower in regions of zones wherein the absorption reaction is from 50% to 90% complete. Moreover, this patent also contemplates the enrichment of the bleaching air feed, then less secondary air is needed.

The embodiment invention highlights the great advantage of enriching the secondary air upstream of the bleaching column. It allows to select a rate of feeding secondary air into the absorption zone or zones which can give favourable residence times (or gas velocities) and oxygen partial pressures at the bottom of the column. A higher residence times means a higher conversion of nitric oxides into nitric acid, therefore, a boost in nitric acid production and a decrease of NO_x gases.

D Simulation results

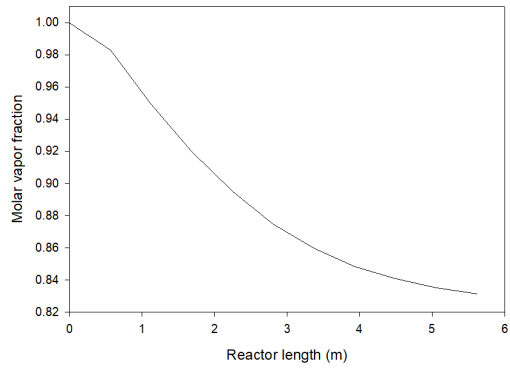
In this part of the appendix, the aim is to show the summary of the streams results for the CONV-NA plant.

Table D.1: Stream results of a monopressure nitric acid plant in Aspen Plus (1)

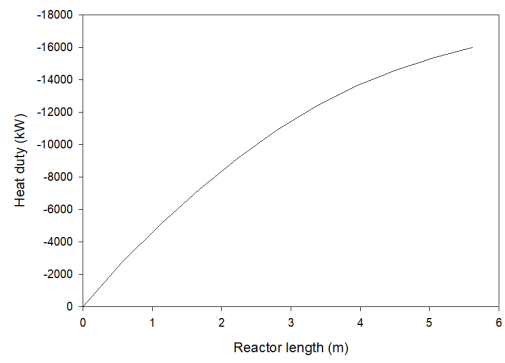
Stream Name	A1	A2	A3	A4	A5	A6	A7
Temperature (°C)	12.00	34.00	75.85	200.00	890.00	133.06	42.20
Pressure (bar)	7.00	1.00	5.80	5.80	5.80	5.80	5.80
Mass Flow (t/d)	199.50	3915.50	3061.14	3260.64	3260.64	3260.64	3260.64
Mole flow (kmol/h)	487.96	5749.35	4434.67	4922.63	5044.04	4830.07	4682.52
Species	Mass Fractions						
NO	0	0	0	0	0.102971	0.010782	6.74E-03
O2	0	0.223	0.228191	0.214229	0.073536	0.024028	1.34E-02
NO2	0	0	0	0	0	0.138793	0.075558
N2O4	0	0	0	0	0	5.28E-04	0.021325
HNO3	0	0	0	0	0	2.77E-03	0.069378
H2O	0.0050	0.0270	0.0044	0.0044	0.1010	0.1006	0.0911
N2	0	0.75	0.767459	0.720502	0.722505	0.722505	0.722505
NH3	0.995	0	0	0.060878	0	0	0
Species	Mole Fractions						
NO	0	0	0	0	0.092431	0.010107	0.006521
O2	0	0.197755	0.205104	0.184773	0.061898	0.021122	0.012168
NO2	0	0	0	0	0	0.084859	0.047652
N2O4	0	0	0	0	0	1.61E-04	6.72E-03
HNO3	0	0	0	0	0	0.001237	0.031945
H2O	4.73E-03	0.042528	6.95E-03	6.73E-03	0.150988	0.157058	0.146672
N2	0	0.759716	0.78795	0.709844	0.694683	0.725456	0.748317
NH3	0.995272	0	0	0.098657	0	0	0

Table D.2: Stream results of a monopressure nitric acid plant in Aspen Plus (2)

Stream Name	A8	A9	A10	A11	A12	A13	A14	A15
Temperature (°C)	42.20	42.20	25.00	22.16	54.20	75.85	54.14	49.76
Pressure (bar)	5.80	5.80	1.00	5.30	5.30	5.80	5.30	5.80
Mass Flow (t/d)	2760.12	500.52	243.60	3102.79	1179.51	765.28	778.07	1166.73
Mole flow (kmol/h)	3887.97	794.55	563.41	4595.33	1555.57	1108.67	1122.10	1542.13
Species	Mass Fractions							
NO	7.97E-03	8.68E-07	0	7.59E-04	1.72E-07	0	5.83E-10	4.71E-27
O2	0.015852	2.98E-06	0	0.047593	1.94E-05	0.2282	0.224302	7.75E-05
NO2	0.08925	5.32E-05	0	1.98E-05	2.26E-05	0	0.000188	1.46E-30
N2O4	0.025044	8.13E-04	0	2.34E-08	5.03E-04	0	0.000304	2.43E-17
HNO3	2.49E-03	0.438223	0	1.81E-12	0.601236	0	0.012136	0.600009
H2O	0.0059	0.5609	1	0.0031	0.3982	0.0044	0.0082	0.3999
N2	0.853516	4.06E-05	0	0.948534	4.43E-05	0.767459	0.754855	4.14E-05
NH3	0	0	0	0	0	0	0	0
Species	Mole Fractions							
NO	0.007854	7.59E-07	0	7.12E-04	1.81E-07	0	5.61E-10	4.95E-27
O2	0.014654	2.44E-06	0	0.041844	1.92E-05	0.205104	0.202523	7.64E-05
NO2	0.057384	3.04E-05	0	1.21E-05	1.55E-05	0	0.000118	1.00E-30
N2O4	8.05E-03	2.32E-04	0	7.17E-09	1.73E-04	0	9.53E-05	8.33E-18
HNO3	0.00117	0.182538	0	8.09E-13	0.301452	0	5.56E-03	0.300169
H2O	9.65E-03	0.817158	1	0.004832	0.69829	0.006946	0.013176	0.699708
N2	0.901236	3.80E-05	0	0.9526	5.00E-05	0.78795	0.778524	4.65E-05
NH3	0	0	0	0	0	0	0	0



(a) Molar vapor fraction.



(b) Heat duty.

Figure D.1: Profiles along the cooler/condenser (E-107)

E Pinch analysis calculations

Table E.1 shows the results of the calculations for the pinch analysis considering $\Delta T_{min} = 10$ K. The hot temperatures are highlighted in red and the cold ones in blue.

Table E.1: Summary of the pinch calculations ($\Delta T_{min} = 10$ K)

Cumulative heat [kW]	Available heat (kW)	Hot scale temperature [°C]	Interval	Cold scale temperature [°C]	Required Heat [kW]	Cumulative heat [kW]
-	-	22.00		12.00		0.00
0.00	-	42.00	1	32.00	272.30	272.30
335.86	335.86	50.00	2	40.00	108.92	381.22
1357.13	1021.27	70.00	3	60.00	1111.95	1493.16
1655.99	298.86	75.85	4	65.85	30.22	1523.38
2459.70	803.72	95.00	5	85.00	98.83	1622.21
3089.57	629.86	110.00	6	100.00	700.07	2322.28
5051.24	1961.67	133.00	7	123.00	1073.22	3395.50
6220.55	1169.31	160.00	8	150.00	1259.87	4655.37
8385.93	2165.38	210.00	9	200.00	2074.96	6730.33
9252.09	866.15	230.00	10	220.00	-	-
13514.02	4261.93	278.96	11	268.96	-	-
14872.07	1358.05	310.00	12	300.00	-	-
35259.00	20386.93	734.00	13	724.00	-	-
42970.71	7711.71	890.00	14	880.00	-	-

F Design of the combustion chamber (R-101)

One of the most important parts of equipment cost estimation is the proper and realistic design of the operational units. In this case, for the design of the ammonia catalytic combustion chamber it is really important to define correctly the measurements to ensure a correct flow distribution. An incorrect flow distribution would result in catalyst losses that could have a significant impact on nitric acid production costs.

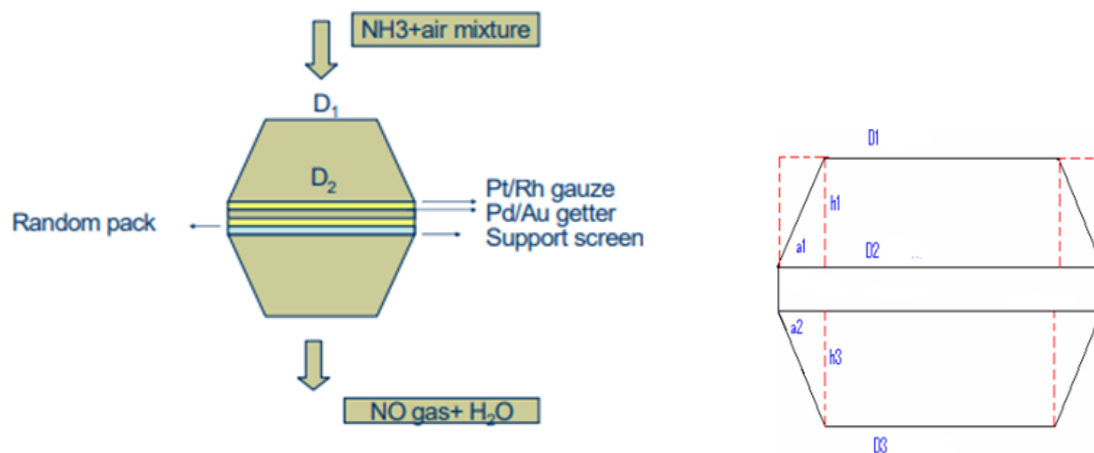


Figure F.1: Sketch combustion chamber.

The volume of catalyst needed can be calculated if the contact time and the volumetric flow rate is known. The contact time is reported to be 0.03 s from Pak-Arab fertilizer [65].

$$V_{catalyst} = \dot{Q} \cdot t \quad (F.1)$$

The amount of catalyst needed can be obtained if the free space gauge (x_{space}), the density of the catalyst ($\rho_{catalyst}$) and the safety factor (s_f) are known. A 20% of over-designed is assumed, i.e the safety factor is considered to be 1.2.

$$m_{catalyst} = s_f \cdot \rho_{catalyst} \cdot (1 - x_{space}) \cdot V_{catalyst} \quad (F.2)$$

Figure F.1 shows the sketch of the R-101 unit. The calculation of the inlet (D_1) and outlet (D_2) pipe diameters can be calculated applying the following equation [48]:

$$D_{i,opt} = 0.363 \cdot \dot{Q}^{0.45} \cdot \rho_{fluid}^{0.13} \quad (F.3)$$

As free space in gauze is 69.8% [65], the diameter of the combustion chamber can be calculated as:

$$D = \frac{D_{i,opt}}{0.698} \quad (F.4)$$

The catalyst screen depth (L) can be calculated considering the ratio L/D ($6.25 \cdot 10^{-3}$) proposed in the *Chemical Reactor design for Process plants* [69]. In addition, following

Figure F.1, a_1 , a_2 , h_1 and h_3 should be calculated:

$$a_1 = \frac{D_2 - D_1}{2} \quad \& \quad h_1 = a_1 \cdot \tan(\theta) \quad \text{where: } \theta = 70^\circ \quad (\text{F.5})$$

Similarly, a_2 and h_3 are described as:

$$a_2 = \frac{D_2 - D_3}{2} \quad \& \quad h_3 = a_2 \cdot \tan(\theta) \quad \text{where: } \theta = 70^\circ \quad (\text{F.6})$$

Therefore, the total height of the chamber (h):

$$h = h_1 + h_3 + L \quad (\text{F.7})$$

The total volume of the chamber is defined as:

$$V_{TOT} = V_1 + V_3 + \frac{\Delta V}{2} + \frac{\Delta V'}{2} + v_{catalyst} \quad (\text{F.8})$$

where:

$$V_1 = \pi \cdot R_1^2 \cdot h_1, \quad V_2 = \pi \cdot R_2^2 \cdot h_2, \quad V_3 = \pi \cdot R_3^2 \cdot h_3, \quad \Delta V = V_2 - V_1 \quad \text{and} \quad \Delta V' = V_2 - V_3$$

The results are tabulated in Figure F.2.

Identification:	Item Item No.	Reactor R-101	Date: 03/11/2022
Function:	To convert NH ₃ – air mixture to nitric oxide mixture.		
Operation :	Continuous		
Materials handled:			
	NH₃-air mixture	NO gas	
Quantity	9.28 m ³ /s	23.39 m ³ /s	
Pressure	5.8 bar	5.8 bar	
Temperature	200°C	870°C	
Design Data:	Catalyst	90% Pt, 10% Rh	
	Weight of catalyst	20.32 kg	
	Diameter of converter	2.29 m	
	Height of converter	2.09 m	
	Material of construction	Inconel 601	
	Inlet pipe diameter	1.18 m	
Controls:	Ammonia air ratio control		

Figure F.2: R-101 specification sheet.

G Economic analysis

The idea of this appendix section is to gather all the relevant information used to performed the economic analysis. In addition, this appendix contains the results that complement the work such as the pie charts, sensitivity graphs and cash flow analyses for the three types of nitric acid plants.

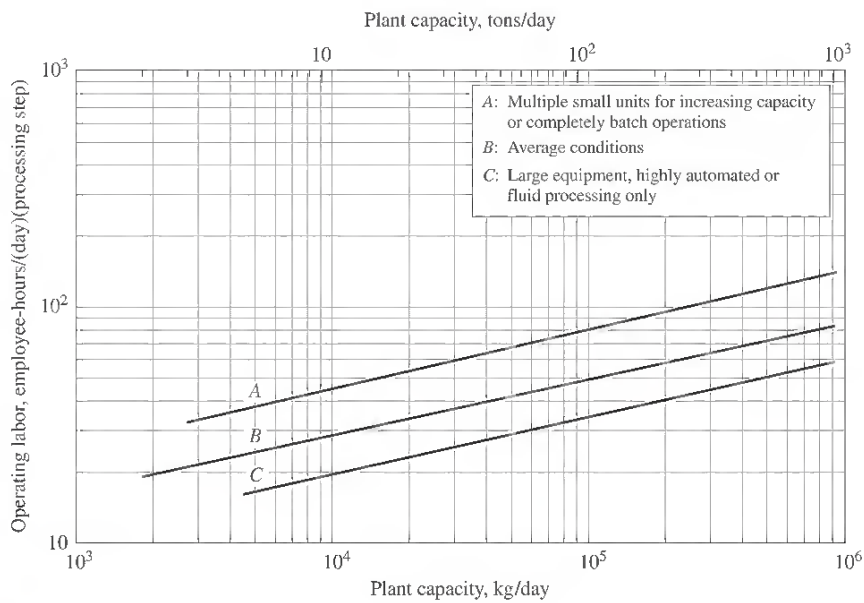


Figure G.1: Operating labor requirements in the chemical process industry [48]

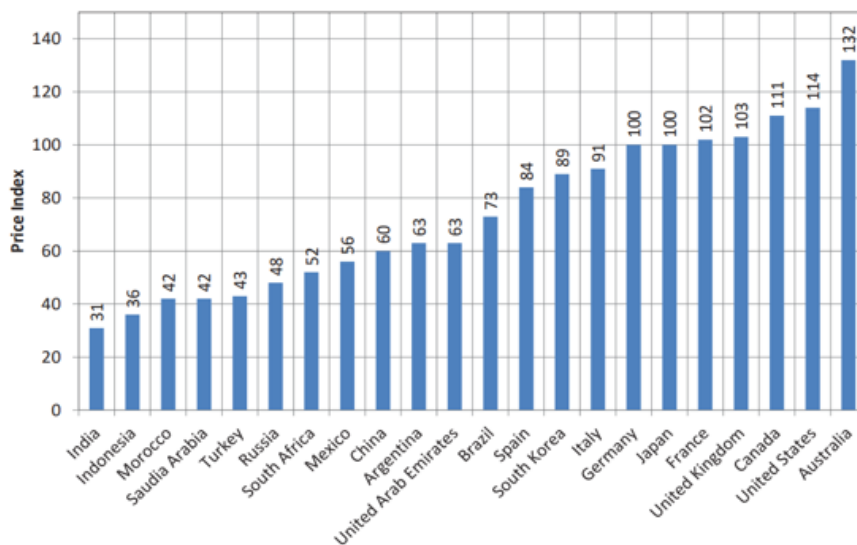


Figure G.2: Price index of all countries assessed [59]

Recovery year	Recovery period					
	3-year	5-year	7-year	10-year	15-year	20-year
Depreciation rate, %						
1	33.33	20.00	14.29	10.00	5.00	3.750
2	44.45	32.00	24.49	18.00	9.50	7.219
3	14.81	19.20	17.49	14.40	8.55	6.677
4	7.41	11.52	12.49	11.52	7.70	6.177
5		11.52	8.93	9.22	6.93	5.713
6		5.76	8.92	7.37	6.23	5.285
7			8.93	6.55	5.90	4.888
8			4.46	6.55	5.90	4.522
9				6.56	5.91	4.462
10				6.55	5.90	4.461
11				3.28	5.91	4.462
12					5.90	4.461
13					5.91	4.462
14					5.90	4.461
15					5.91	4.462
16					2.95	4.461
17						4.462
18						4.461
19						4.462
20						4.461
21						2.231

Figure G.3: MACRS depreciation rates [48]

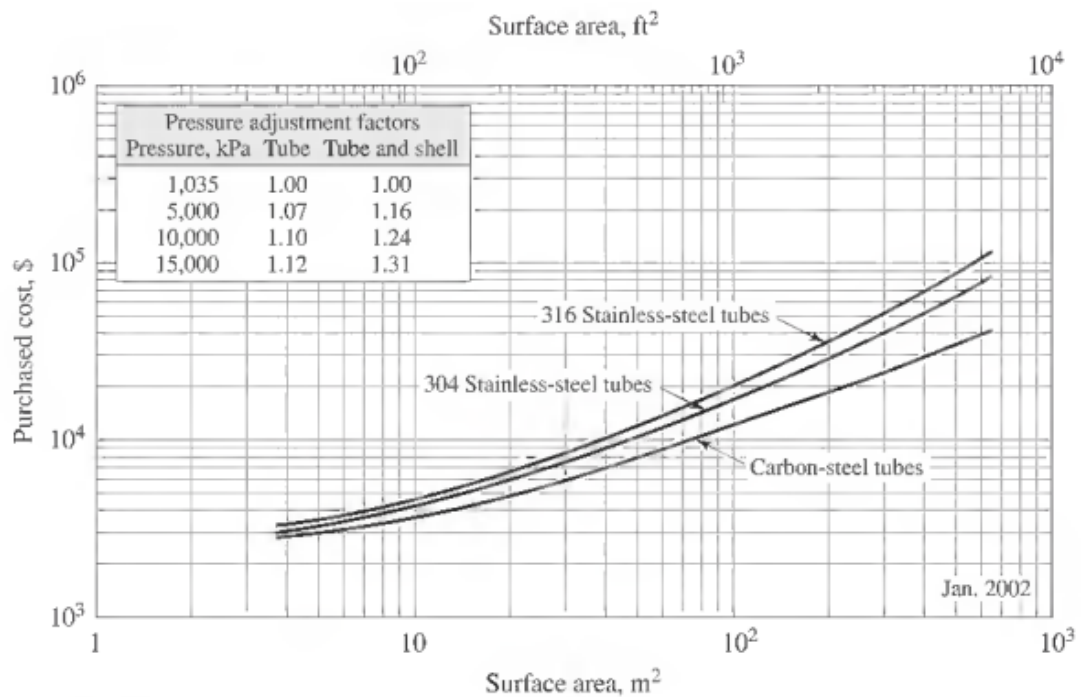


Figure G.4: Purchased cost of fixed-tube sheet heat exchangers with 0.019 m (3/4 in.) OD x 0.025-m (1-in) square pitch and 4.88- or 6.10 m (16 or 20 ft) bundles and carbon-steel shell operating at 1035 kPa (150 psia) [48]

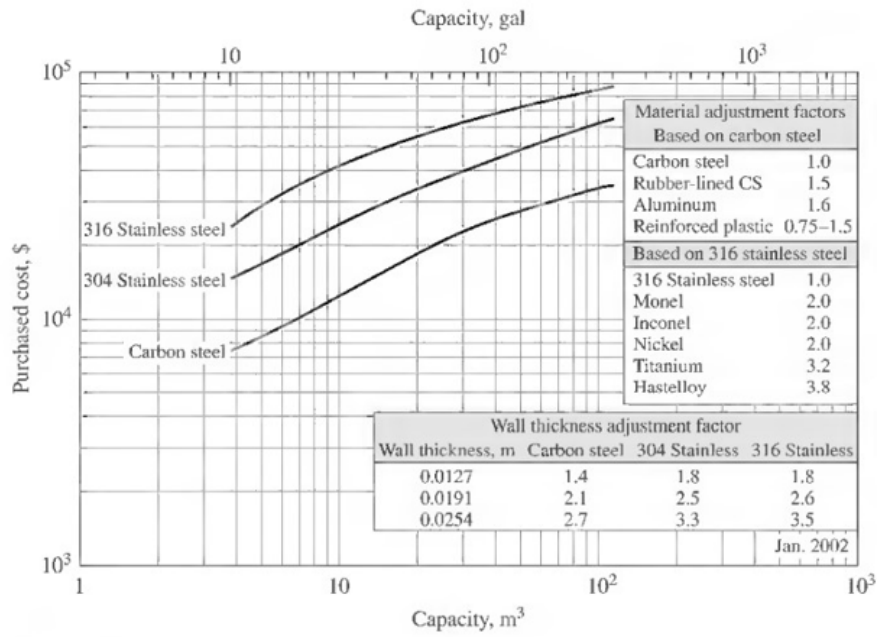


Figure G.5: Purchased cost of shop-fabricated tanks with a wall thickness of 6.35×10^{-3} m. For tanks requiring walls, use the wall thickness adjustment factor. [48]

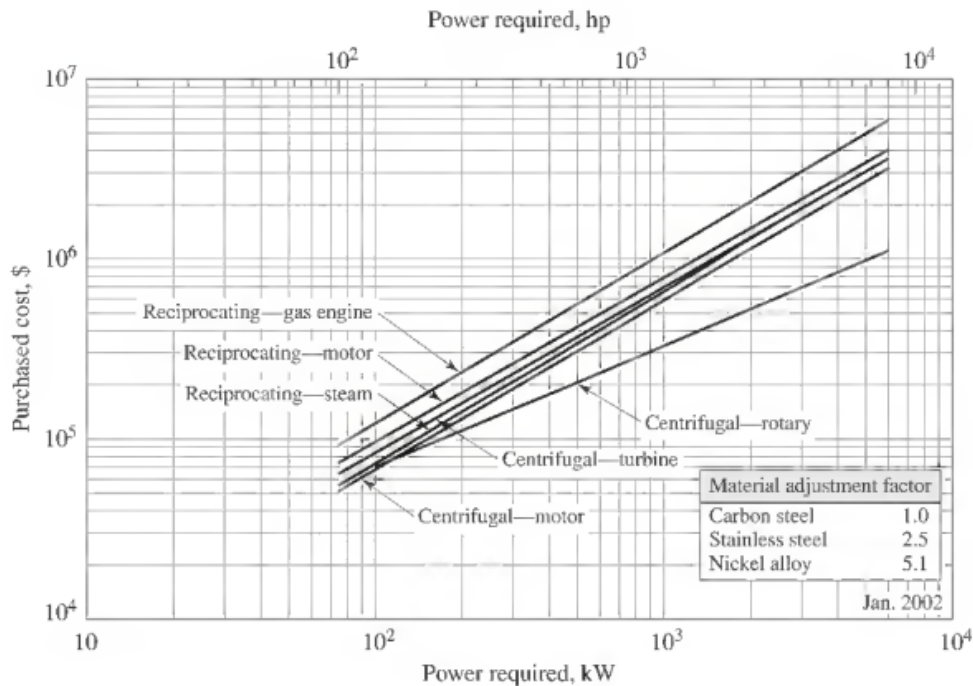


Figure G.6: Purchased cost of compressors. Price includes drive, gear mounting, base-plate, and normal auxiliary equipment; operating pressure to 7000 kPa (1000 psig). [48]

Table G.1: Suggested values for risk and minimum acceptable return on investment [48]

Investment description	Level of risk	Minimum acceptable return m_{ar} (after income taxes), percent/year
<i>Basis:</i> Safe corporate investment opportunities or cost of capital	Safe	4–8
New capacity with established corporate market position	Low	8–16
New product entering into established market, or new process technology	Medium	16–24
New product or process in a new application	High	24–32
Everything new, high R&D and marketing effort	Very high	32–48+

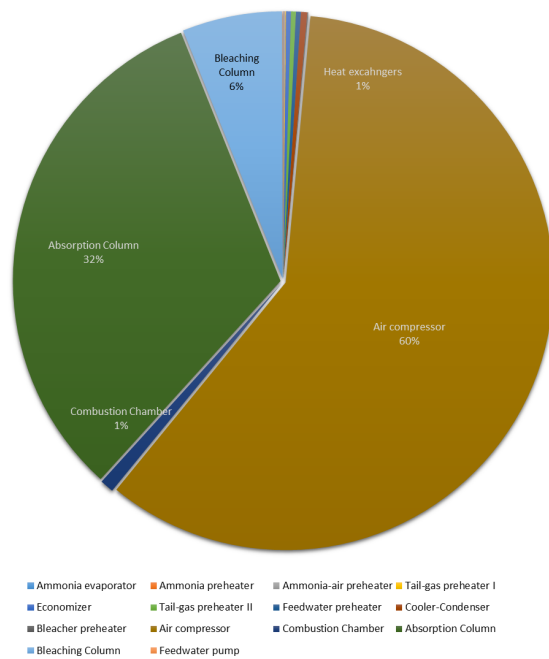


Figure G.7: Pie chart of the percentage of equipment cost unities

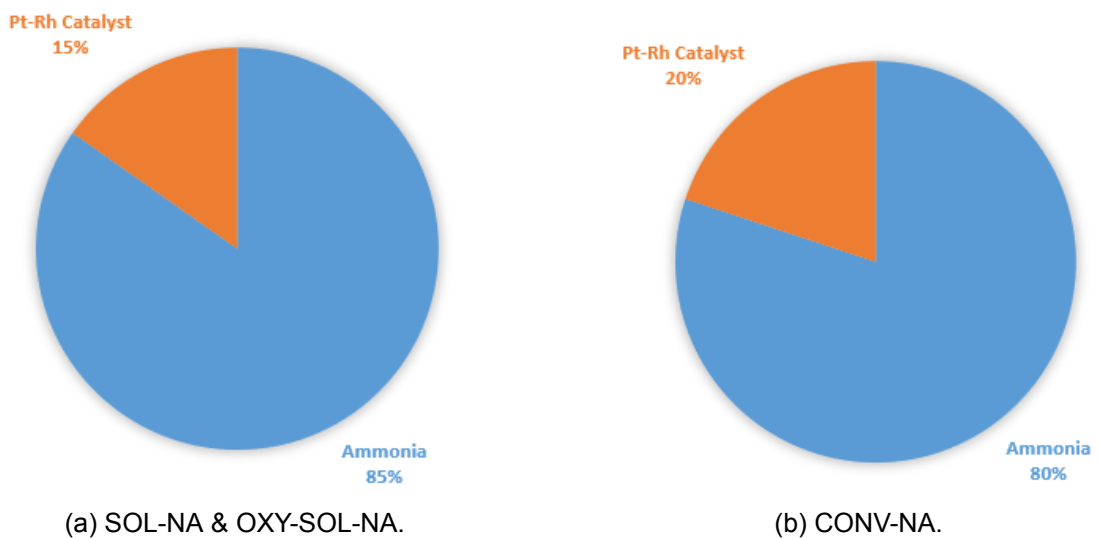


Figure G.8: Pie chart of the percentage of raw materials.

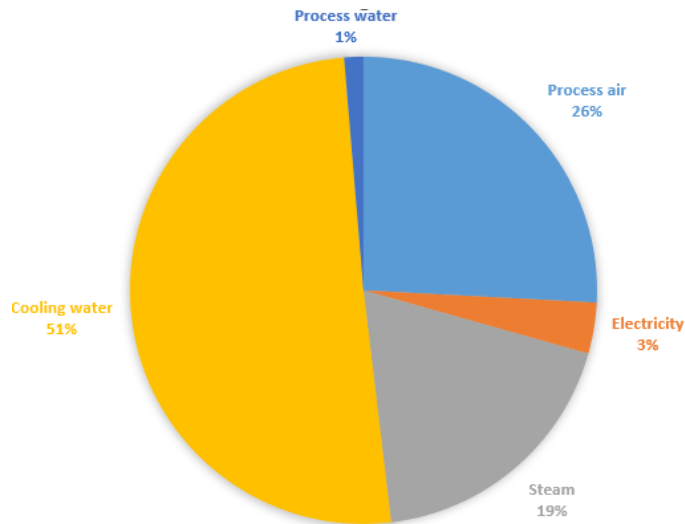


Figure G.9: Pie chart of the percentage of utilities for all the plants.

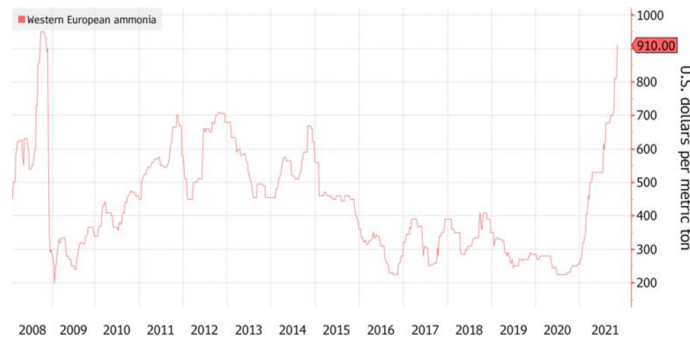


Figure G.10: Ammonia price for Western Europe in the last decade [12].

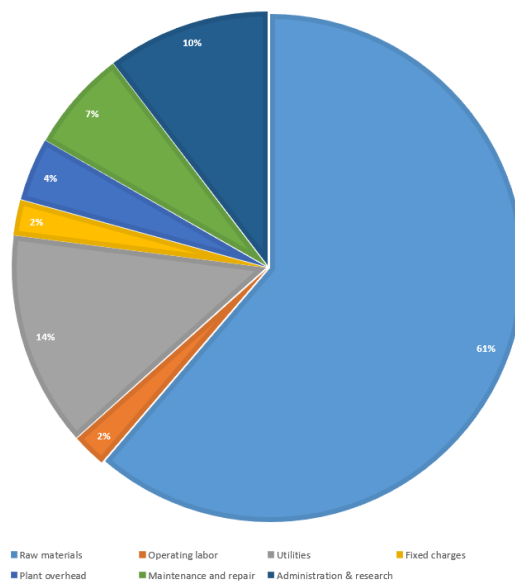


Figure G.11: Pie chart of the percentage of OpEx for CONV-NA plant.

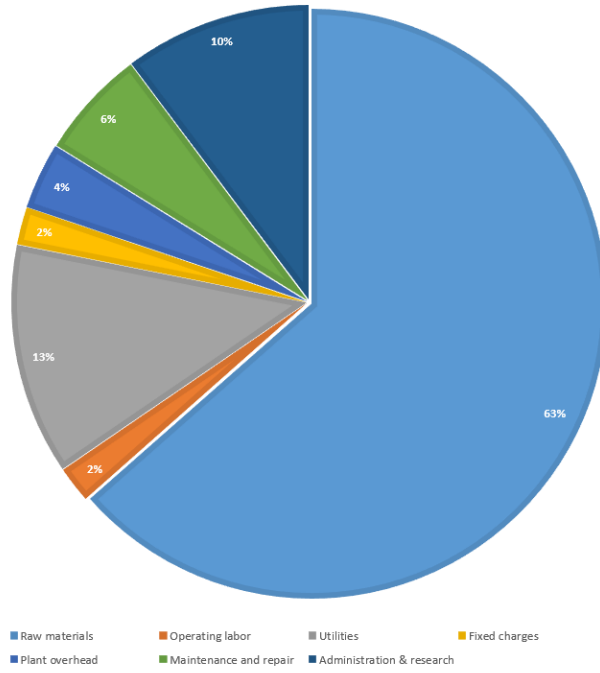


Figure G.12: Pie chart of the percentage of OpEx for SOL-NA plant.

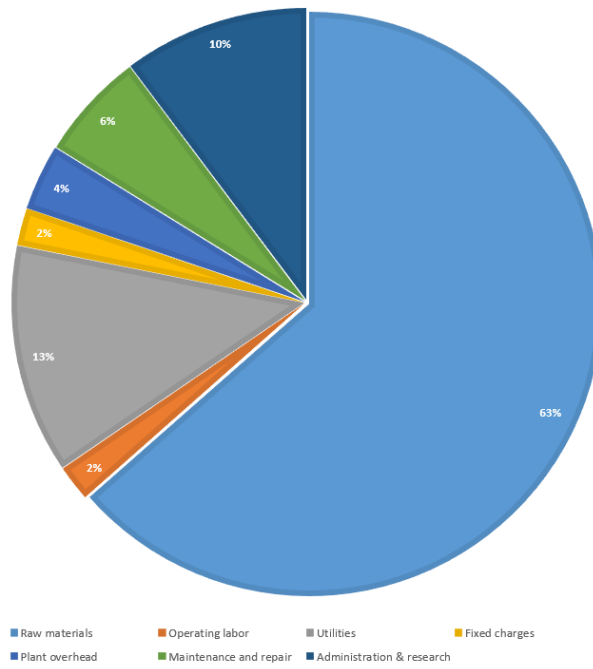


Figure G.13: Pie chart of the percentage of OpEx for OXY-SOL-NA plant.

Year ending at time	-2	-1	0	1	2	3	4	5	6	7	8	9	10	11	12	13	14	15 Row Sum	
1. Land, 10 ⁵ € (see notes)																			
2. Fixed Capital Investment, 10 ⁵ €	-14.69	-34.28	-48.97																
3. Working Capital, 10 ⁵ € (see notes)		-19.90																	19.90
4. Salvage Value, 10 ⁵ €																			0.00
5. Total Capital Investment, 10 ⁵ €	-14.69	-34.28	-68.88																-117.85
6. Annual Investment, 10 ⁵ €				0.00	0.00	0.00	0.00	0.00	0.00	0.00	0.00	0.00	0.00	0.00	0.00	0.00	0.00	0.00	0.00
7. Start-up cost, 10 ⁵ €				-9.79															
8. Operating rate, fraction of capacity				0.50	0.90	1.00	1.00	1.00	1.00	1.00	1.00	1.00	1.00	1.00	1.00	1.00	1.00	1.00	1.00
9. Annual sales, 10 ⁵ €				71.97	129.54	143.93	143.93	143.93	143.93	143.93	143.93	143.93	143.93	143.93	143.93	143.93	143.93	143.93	143.93
10. Annual Total Product Cost, depreciation not included, 10 ⁵ €				-69.94	-109.32	-119.16	-119.16	-119.16	-119.16	-119.16	-119.16	-119.16	-119.16	-119.16	-119.16	-119.16	-119.16	-119.16	-119.16
11. Annual depreciation factor, 1/y				0.050	0.095	0.086	0.077	0.069	0.062	0.059	0.059	0.059	0.059	0.059	0.059	0.059	0.059	0.059	0.030
12. Annual depreciation, 10 ⁵ €/y				9.31	8.37	7.54	6.79	6.10	5.78	5.78	5.78	5.78	5.78	5.78	5.78	5.78	5.78	5.78	2.89
13. Annual Gross Profit, 10 ⁵ €				-17.08	11.85	17.23	17.98	18.67	18.99	18.99	18.99	18.99	18.99	18.99	18.99	18.99	18.99	18.99	21.88
14. Annual Net Profit, 10 ⁵ €				-17.08	8.88	12.92	13.49	14.00	14.24	14.24	14.24	14.24	14.24	14.24	14.24	14.24	14.24	14.24	16.41
15. Annual operating cash flow, 10 ⁵ €				-7.77	17.26	20.46	20.27	20.10	20.02	20.02	20.02	20.02	20.02	20.02	20.02	20.02	20.02	20.02	19.30
16. Total annual cash flow, 10 ⁵ €				-68.88	-7.77	17.26	20.46	20.27	20.10	20.02	20.02	20.02	20.02	20.02	20.02	20.02	20.02	20.02	19.30
17. Cumulative cash position, 10 ⁵ €				-117.85	-125.62	-108.36	-87.90	-67.63	-47.52	-27.50	-7.48	12.54	32.57	52.59	72.61	92.64	112.66	132.69	151.99
Profitability measures, time value of money NOI included:																			
18. Return on investment, ave. %/y																			10.00
19. Payback period, y																			5.44
20. Net return, 10 ⁵ €																			0.00 at m _{ar} = 10.0 %/y
Profitability measures including time value of money, with ANNUAL END-OF-YEAR cash flows and discounting																			
21. Present worth factor	1.00	1.21	1.10	1.00	0.91	0.83	0.75	0.68	0.62	0.56	0.51	0.47	0.42	0.39	0.35	0.32	0.29	0.26	0.24
22. Present worth of annual cash flows, 10 ⁵ €	0.00	-17.78	-37.71	-68.88	-7.07	14.26	15.37	13.85	12.48	11.30	10.27	9.34	8.49	7.72	7.02	6.38	5.80	5.27	4.62
23. Net present worth, 10 ⁵ € =																			0.76
24. Discounted cash flow rate of return, DCFR, %/y =																			10.08
Iterated discount rate																			0.101
25. Present worth factor	1.00	1.21	1.10	1.00	0.91	0.83	0.75	0.68	0.62	0.56	0.51	0.46	0.42	0.38	0.35	0.32	0.29	0.26	0.24
26. Present worth of annual cash flows, 10 ⁵ €	0.00	-17.80	-37.74	-68.88	-7.06	14.24	15.34	13.81	12.43	11.25	10.22	9.28	8.43	7.66	6.96	6.32	5.74	5.22	4.57
27. Net present worth, 10 ⁵ €																			0.00

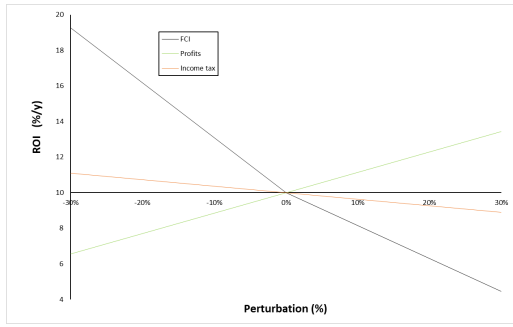
Figure G.14: Profitability evaluation for CONV-NA.

Year ending at time	-2	-1	0	1	2	3	4	5	6	7	8	9	10	11	12	13	14	15 Rew Sum	
1. Land, 10 ⁵ € (see notes)																			
2. Fixed Capital Investment, 10 ⁵ €	-14.69	-34.28	-48.97																-97.95
3. Working Capital, 10 ⁵ € (see notes)			-19.90																19.90
4. Salvage Value, 10 ⁵ €																			0.00
5. Total Capital Investment, 10 ⁵ €	-14.69	-34.28	-68.88																-117.85
6. Annual Investment, 10 ⁵ €				0.00	0.00	0.00	0.00	0.00	0.00	0.00	0.00	0.00	0.00	0.00	0.00	0.00	0.00	0.00	0.00
7. Start-up cost, 10 ⁵ €				-9.79															
8. Operating rate, fraction of capacity				0.50	0.90	1.00	1.00	1.00	1.00	1.00	1.00	1.00	1.00	1.00	1.00	1.00	1.00	1.00	1.00
9. Annual sales, 10 ⁵ €				84.13	151.44	168.27	168.27	168.27	168.27	168.27	168.27	168.27	168.27	168.27	168.27	168.27	168.27	168.27	168.27
10. Annual Total Product Cost, depreciation not included, 10 ⁵ €				-83.15	-131.34	-143.38	-143.38	-143.38	-143.38	-143.38	-143.38	-143.38	-143.38	-143.38	-143.38	-143.38	-143.38	-143.38	-143.38
11. Annual depreciation factor, 1/y				0.095	0.086	0.077	0.069	0.062	0.059	0.059	0.059	0.059	0.059	0.059	0.059	0.059	0.059	0.059	0.030
12. Annual depreciation, 10 ⁵ €/y				9.31	8.37	7.54	6.79	6.10	5.78	5.78	5.78	5.78	5.78	5.78	5.78	5.78	5.78	5.78	2.89
13. Annual Gross Profit, 10 ⁵ €				-18.12	11.73	17.34	18.10	18.78	19.11	19.11	19.11	19.11	19.10	19.10	19.10	19.10	19.10	19.10	22.00
14. Annual Net Profit, 10 ⁵ €				-18.12	8.80	13.01	13.57	14.09	14.33	14.33	14.33	14.33	14.32	14.32	14.33	14.33	14.32	14.32	16.50
15. Annual operating cash flow, 10 ⁵ €				-8.81	17.17	20.55	20.36	20.19	20.11	20.11	20.11	20.11	20.11	20.11	20.11	20.11	20.11	20.11	19.39
16. Total annual cash flow, 10 ⁵ €				-14.69	-34.28	-68.88	-8.81	17.17	20.55	20.36	20.19	20.11	20.11	20.11	20.11	20.11	20.11	20.11	19.39
17. Cumulative cash position, 10 ⁵ €				-14.69	-48.97	-117.85	-48.97	-8.81	-28.29	-8.18	11.93	32.04	52.15	72.26	92.37	112.48	132.59	151.98	-2.26
Profitability measures, time value of money, NOI included:																			
18. Return on investment, ave. %/y																			10.00
19. Payback period, y																			5.45
20. Net return, 10 ⁵ €																			0.00 at m _{br} = 10.0 %/y
Profitability measures including time value of money, with ANNUAL END-OF-YEAR cash flows and discounting																			
21. Present worth factor	1.00	1.21	1.10	1.00	0.91	0.83	0.75	0.68	0.62	0.56	0.51	0.47	0.42	0.39	0.35	0.32	0.29	0.26	0.24
22. Present worth of annual cash flows, 10 ⁵ €	0.00	-17.78	-37.71	-68.88	-8.01	14.19	15.44	13.91	12.54	11.35	10.32	9.38	8.53	7.75	7.05	6.41	5.82	5.30	4.64
23. Net present worth, 10 ⁵ € =																			0.24
24. Discounted cash flow rate of return, DCFR, %/y = iterated discount rate																			10.03
25. Present worth factor	1.00	1.21	1.10	1.00	0.91	0.83	0.75	0.68	0.62	0.56	0.51	0.47	0.42	0.38	0.35	0.32	0.29	0.26	0.24
26. Present worth of annual cash flows, 10 ⁵ €	0.00	-17.79	-37.72	-68.88	-8.01	14.18	15.43	13.89	12.52	11.33	10.30	9.36	8.51	7.73	7.03	6.39	5.81	5.28	4.62

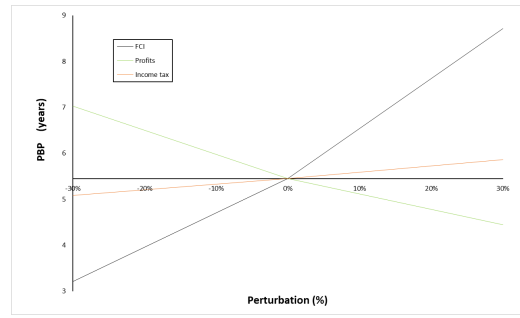
Figure G.15: Profitability evaluation for SOL-NA.

Year ending at time	-2	-1	0	1	2	3	4	5	6	7	8	9	10	11	12	13	14	15 Row Sum	
1. Land, 10 ⁶ € (see notes)																			
2. Fixed Capital Investment, 10 ⁶ €	-14.60	-34.08	-48.68																-97.37
3. Working Capital, 10 ⁶ € (see notes)		-19.78																	19.78
4. Salvage Value, 10 ⁶ €																			0.00
5. Total Capital Investment, 10 ⁶ €	-14.60	-34.08	-68.47																-117.15
6. Annual Investment, 10 ⁶ €				0.00	0.00	0.00	0.00	0.00	0.00	0.00	0.00	0.00	0.00	0.00	0.00	0.00	0.00	0.00	0.00
7. Start-up cost, 10 ⁶ €				-9.74															
8. Operating rate, fraction of capacity				0.50	0.90	1.00	1.00	1.00	1.00	1.00	1.00	1.00	1.00	1.00	1.00	1.00	1.00	1.00	1.00
9. Annual sales, 10 ⁶ €				83.91	151.03	167.81	167.81	167.81	167.81	167.81	167.81	167.81	167.81	167.81	167.81	167.81	167.81	167.81	167.81
10. Annual Total Product Cost, depreciation not included, 10 ⁶ €				-82.96	-131.05	-143.07	-143.07	-143.07	-143.07	-143.07	-143.07	-143.07	-143.07	-143.07	-143.07	-143.07	-143.07	-143.07	-143.07
11. Annual depreciation factor, 1/y				0.050	0.095	0.086	0.077	0.069	0.062	0.059	0.059	0.059	0.059	0.059	0.059	0.059	0.059	0.059	0.030
12. Annual depreciation, 10 ⁶ €/y				9.25	8.32	7.50	6.75	6.07	5.74	5.74	5.74	5.74	5.74	5.74	5.74	5.74	5.74	5.74	2.87
13. Annual Gross Profit, 10 ⁶ €				-18.04	11.66	17.24	17.99	18.68	19.00	19.00	19.00	19.00	19.00	19.00	19.00	19.00	19.00	19.00	21.87
14. Annual Net Profit, 10 ⁶ €				-18.04	8.74	12.93	13.50	14.01	14.25	14.25	14.24	14.25	14.24	14.25	14.24	14.25	14.24	14.24	16.40
15. Annual operating cash flow, 10 ⁶ €				-8.79	17.07	20.43	20.24	20.07	19.99	19.99	19.99	19.99	19.99	19.99	19.99	19.99	19.99	19.99	19.27
16. Total annual cash flow, 10 ⁶ €				-14.60	-34.08	-68.47	-68.47	-68.47	-68.47	-68.47	-68.47	-68.47	-68.47	-68.47	-68.47	-68.47	-68.47	-68.47	151.08
17. Cumulative cash position, 10 ⁶ €				-14.60	-48.68	-117.15	-125.94	-108.88	-88.45	-68.20	-48.13	-28.14	-8.15	11.85	31.84	51.83	71.83	91.82	111.81
Profitability measures, time value of money NOT included:																			
18. Return on investment, ave. %/y																			10.00
19. Payback period, y																			5.44
20. Net return, 10 ⁵ €																			0.00 at m _{ar} = 10.0 %/y
Profitability measures including time value of money, with ANNUAL END-OF-YEAR cash flows and discounting																			
21. Present worth factor	1.00	1.21	1.10	1.00	0.91	0.83	0.75	0.68	0.62	0.56	0.51	0.47	0.42	0.39	0.35	0.32	0.29	0.26	0.24
22. Present worth of annual cash flows, 10 ⁵ €	0.00	-17.67	-37.49	-68.47	-7.99	14.11	15.35	13.83	12.46	11.28	10.26	9.33	8.48	7.71	7.01	6.37	5.79	5.27	4.61
23. Net present worth, 10 ⁶ € =																			0.23
24. Discounted cash flow rate of return, DCFR, %/y =																			10.03
Iterated discount rate 0.100																			
25. Present worth factor	1.00	1.21	1.10	1.00	0.91	0.83	0.75	0.68	0.62	0.56	0.51	0.47	0.42	0.38	0.35	0.32	0.29	0.26	0.24
26. Present worth of annual cash flows, 10 ⁵ €	0.00	-17.68	-37.49	-68.47	-7.99	14.10	15.34	13.81	12.45	11.27	10.24	9.31	8.46	7.69	6.99	6.35	5.77	5.25	4.60

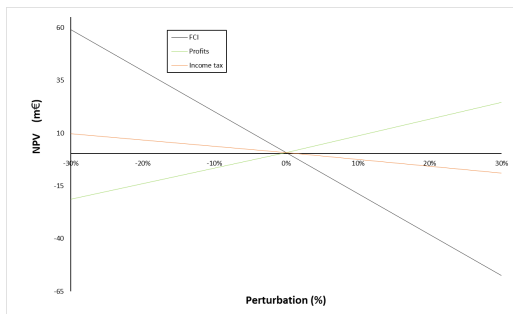
Figure G. 16: Profitability evaluation for OXY-SOL-NA.



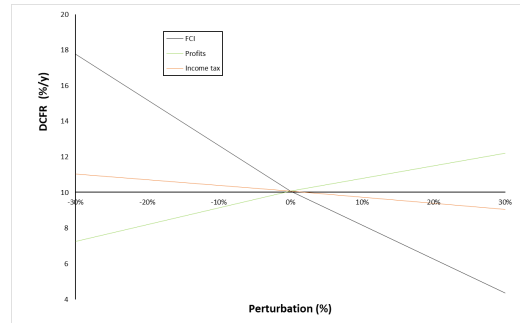
(a) ROI.



(b) PBP.

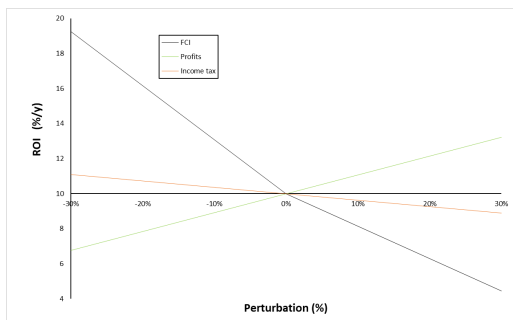


(c) NPV.

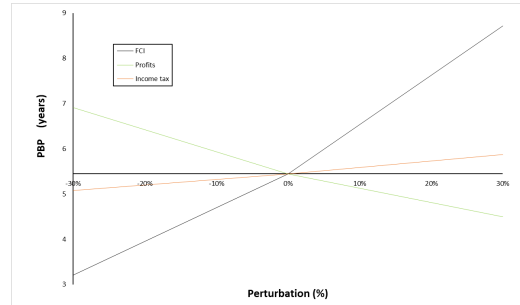


(d) DCFR.

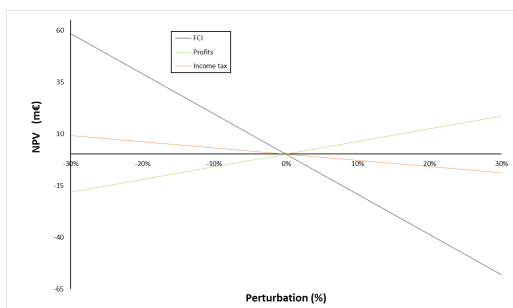
Figure G.17: Sensitivity results CONV-NA.



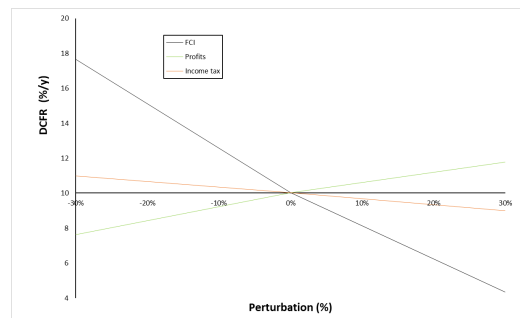
(a) ROI.



(b) PBP.



(c) NPV.



(d) DCFR.

Figure G.18: Sensitivity results SOL-NA.

